arXiv:2405.20926v3 [hep-ex] 11 Dec 2024

Search for a resonance decaying into a scalar particle and a Higgs boson in the final state with two bottom quarks and two photons in proton–proton collisions at $\sqrt{s}$=13 TeV with the ATLAS detector

The ATLAS Collaboration

A search for the resonant production of a heavy scalar X decaying into a Higgs boson and a new lighter scalar S, through the process $X \rightarrow S(\rightarrow b\bar{b})H(\rightarrow\gamma\gamma)$, where the two photons are consistent with the Higgs boson decay, is performed. The search is conducted using an integrated luminosity of 140 fb^{-1} of proton-proton collision data at a centre-of-mass energy of 13 TeV recorded with the ATLAS detector at the Large Hadron Collider. The search is performed over the mass range $170 \leq m_X \leq 1000$ GeV and $15 \leq m_S \leq 500$ GeV. Parameterised neural networks are used to enhance the signal purity and to achieve continuous sensitivity in a domain of the (m_X, m_S) plane. No significant excess above the expected background is found and 95% CL upper limits are set on the cross section times branching ratio, ranging from 39 fb to 0.09 fb. The largest deviation from the background-only expectation occurs for $(m_X, m_S) = (575, 200)$ GeV with a local (global) significance of 3.5 (2.0) standard deviations.
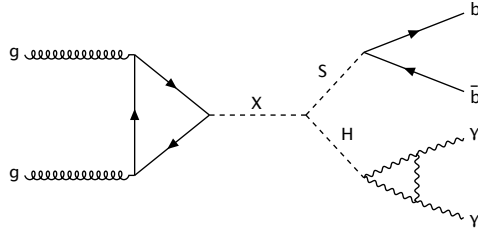
Figure 1: Example of a Feynman diagram showing gluon–gluon fusion production of a scalar X decaying into a scalar S and a Standard Model Higgs boson, which in turn decay into a pair of b-quarks and a pair of photons.

1 Introduction

The properties of the Higgs boson (H) discovered in 2012 [1, 2] by the ATLAS and CMS experiments at the Large Hadron Collider (LHC) are consistent with the Standard Model (SM) predictions [3, 4]. However the current experimental precision does not exclude that H may have a small mixing with additional scalar bosons, and may be part of an extended Higgs sector. Many Beyond the Standard Model (BSM) theories predict such an extended Higgs sector, where one of the physical Higgs boson states could correspond to the spin-0 boson observed with a mass of 125 GeV, while additional scalars remain to be discovered [5].

In this paper, the complete proton-proton dataset collected by the ATLAS experiment during Run 2 of the LHC is used to search for two additional scalar bosons X and S. Under the condition $m_X > m_S + m_H$, the decay $X \rightarrow SH$ is kinematically allowed. This phenomenology may arise in models where the SM Higgs sector is extended with either a complex singlet [6] or two real singlets [7], and in models such as the complex two-Higgs-doublet model (2HDM) [8], the 2HDM extended by a real scalar singlet [9, 10] or the Next-to-Minimal Supersymmetric Standard Model [11, 12].

The sensitivity of the LHC to the decay $X \rightarrow SH$ has been explored in several benchmark scenarios [7, 13, 14]. The decay of the scalar S is model- and mass-dependent. The CMS Collaboration has performed searches for $X \rightarrow S(\rightarrow b\bar{b})H(\rightarrow b\bar{b})$, $X \rightarrow S(\rightarrow b\bar{b})H(\rightarrow \tau\bar{\tau})$ and $X \rightarrow S(\rightarrow b\bar{b})H(\rightarrow \gamma\gamma)$ using Run 2 data [15–17]. In the $X \rightarrow S(\rightarrow b\bar{b})H(\rightarrow \gamma\gamma)$ final state, CMS observed a deviation from the background-only hypothesis with a local (global) significance of 3.8 (2.8) standard deviations at $m_X = 650$ GeV and $m_S = 90$ GeV. ATLAS published results on the search for $X \rightarrow S(\rightarrow VV)H(\rightarrow \tau\bar{\tau})$, where V denotes a W or Z boson [18].

This paper is focused on the search for $X \rightarrow S(\rightarrow b\bar{b})H(\rightarrow \gamma\gamma)$ and uses the same Run 2 dataset already exploited by ATLAS to search for Higgs boson pair production [19]. A di-photon mass peak arises from $H \rightarrow \gamma\gamma$, while the two b-tagged jets arise from the $S \rightarrow b\bar{b}$ decay, thus leading to a characteristic signal with three resonant mass peaks from $H \rightarrow \gamma\gamma$, $S \rightarrow b\bar{b}$ and $X \rightarrow b\bar{b}\gamma\gamma$. The natural widths of the new bosons are assumed to be much smaller than the experimental resolutions. In the particular scenario where the scalar S has couplings similar to those of the SM Higgs boson, $S \rightarrow b\bar{b}$ is the predominant decay for $m_S < 130$ GeV. The Feynman diagram for the main production mode of this process is illustrated in Figure 1.

The rate of production for the scalar X, and the decay branching ratios $BR(X \rightarrow SH)$ and $BR(S \rightarrow b\bar{b})$, are strongly dependent on which model is realised, and on the specific values of the parameters of the extended Higgs sector. Therefore, the results are expressed as 95% confidence level (CL) upper limits on $\sigma(pp \rightarrow X) \times BR(X \rightarrow SH) \times BR(S \rightarrow b\bar{b}) \times BR(H \rightarrow \gamma\gamma)$, denoted $\sigma(X \rightarrow SH \rightarrow b\bar{b}\gamma\gamma)$, rather

than on specific models, probing the m_X range between 170 and 1000 GeV and the m_S range between 15 and 500 GeV.

This article is structured as follows. Section 2 briefly introduces the ATLAS detector. Data and simulated event samples are given in Section 3. Object definitions are introduced in Section 4 while the event selection is described in Section 5. The strategy for background estimation is explained in Section 6. Section 7 is devoted to the description of the systematic uncertainties. Statistical modelling, validation of the background calculations and results are presented in Section 8. Finally the conclusions are given in Section 9.

2 ATLAS detector

The ATLAS detector [20] at the LHC covers nearly the entire solid angle around the collision point.[1] It consists of an inner tracking detector surrounded by a thin superconducting solenoid, electromagnetic and hadronic calorimeters, and a muon spectrometer incorporating three large superconducting air-core toroidal magnets.

The inner-detector system (ID) is immersed in a 2 T axial magnetic field and provides charged-particle tracking in the range $|\eta| < 2.5$. The high-granularity silicon pixel detector covers the vertex region and typically provides four measurements per track, the first hit generally being in the insertable B-layer (IBL) installed before Run 2 [21, 22]. It is followed by the SemiConductor Tracker (SCT), which usually provides eight measurements per track. These silicon detectors are complemented by the transition radiation tracker (TRT), which enables radially extended track reconstruction up to $|\eta| = 2.0$. The TRT also provides electron identification information based on the fraction of hits (typically 30 in total) above a higher energy-deposit threshold corresponding to transition radiation.

The calorimeter system covers the pseudorapidity range $|\eta| < 4.9$. Within the region $|\eta| < 3.2$, electromagnetic calorimetry is provided by a lead/liquid-argon (LAr) sampling calorimeter with accordion geometry. It is divided into a barrel section covering $|\eta| < 1.475$ and two endcap sections covering $1.375 < |\eta| < 3.2$. For $|\eta| < 2.5$, it is divided into three layers in depth, which are finely segmented in η and ϕ. An additional thin LAr presampler layer covering $|\eta| < 1.8$ is used to correct for energy loss in material upstream of the calorimeters. Hadronic calorimetry is provided by the steel/scintillator-tile calorimeter, segmented into three barrel structures within $|\eta| < 1.7$, and two copper/LAr hadronic endcap calorimeters. The solid angle coverage is completed with forward copper/LAr and tungsten/LAr calorimeter modules optimised for electromagnetic and hadronic energy measurements respectively.

The muon spectrometer (MS) comprises separate trigger and high-precision tracking chambers measuring the deflection of muons in a magnetic field generated by the superconducting air-core toroidal magnets. The field integral of the toroids ranges between 2.0 and 6.0 T m across most of the detector. Three layers of precision chambers, each consisting of layers of monitored drift tubes, cover the region $|\eta| < 2.7$, complemented by cathode-strip chambers in the forward region, where the background is highest. The

---

[1] ATLAS uses a right-handed coordinate system with its origin at the nominal interaction point (IP) in the centre of the detector and the z-axis along the beam pipe. The x-axis points from the IP to the centre of the LHC ring, and the y-axis points upwards. Polar coordinates (r, ϕ) are used in the transverse plane, ϕ being the azimuthal angle around the z-axis. The pseudorapidity is defined in terms of the polar angle θ as $\eta = -\ln\tan(\theta/2)$ and is equal to the rapidity $y = \frac{1}{2}\ln\left(\frac{E+p_z c}{E-p_z c}\right)$ in the relativistic limit. Angular distance is measured in units of $\Delta R \equiv \sqrt{(\Delta y)^2 + (\Delta \phi)^2}$.

muon trigger system covers the range $|\eta| < 2.4$ with resistive-plate chambers in the barrel, and thin-gap chambers in the endcap regions.

The luminosity is measured mainly by the LUCID–2 [23] detector that records Cherenkov light produced in the quartz windows of photomultipliers located close to the beampipe.

Events are selected by the first-level trigger system implemented in custom hardware, followed by selections made by algorithms implemented in software in the high-level trigger [24]. The first-level trigger accepts events from the 40 MHz bunch crossings at a rate below 100 kHz, which the high-level trigger further reduces in order to record complete events to disk at about 1 kHz.

A software suite [25] is used in data simulation, in the reconstruction and analysis of real and simulated data, in detector operations, and in the trigger and data acquisition systems of the experiment.

3 Data and simulated event samples

The data used in this search were collected by the ATLAS experiment between 2015 and 2018, from proton-proton collisions at $\sqrt{s}$ = 13 TeV at the LHC. After data quality requirements [26], this corresponds to an integrated luminosity of 140 fb^{-1}. The uncertainty in the combined 2015–2018 integrated luminosity is 0.83% [27], obtained using the LUCID-2 detector [23] for primary luminosity measurements, complemented by measurements using the inner detector and calorimeters.

Events are recorded using diphoton triggers that require two reconstructed photon candidates with minimum transverse energies of 35 GeV and 25 GeV [28]. The triggers used in 2015 and 2016 require both the photons to satisfy the *Loose* photon identification criterion defined in Ref. [29], while the *Medium* criterion [29] is used for 2017–2018 to cope with the increased pp interaction rate.

The Monte Carlo (MC) simulated event samples used in the analysis are listed in Table 1, along with the generator used in the simulation, the parton distribution function (PDF) set, the showering model and the set of tuned parameters (tune). The $X \rightarrow SH$ signal process is simulated at leading-order (LO) in QCD with Pythia 8.2 [30]. The Higgs boson is forced to decay into two photons, while the scalar S is forced to decay into two b-quarks. The X and S scalar decays are generated in the narrow-width approximation. A total of 161 signal mass points are generated in the range $170 \leq m_X \leq 1000$ GeV and $15 \leq m_S \leq 500$ GeV.

The backgrounds can be divided into three categories. The largest background category consists of events with two photon candidates featuring a smoothly falling, non-resonant diphoton mass spectrum. This population arises from processes with two prompt photons or from jet processes where one or both the photon candidates are misidentified jets via instrumental effects. The processes $Z(\rightarrow q\bar{q})\gamma\gamma$ and $t\bar{t}\gamma\gamma$ are also included in this category. All these backgrounds together are referred to as 'non-resonant diphoton background', the category is denoted $\gamma\gamma$+jets for short but does include γ+jets and dijet processes. Due to the significant contribution from instrumental background in the $\gamma\gamma$+jets category, its normalisation is constrained with data using dedicated control regions detailed in Section 6.1.

The processes $\gamma\gamma$+jets and $Z(\rightarrow q\bar{q})\gamma\gamma$, with two real photons, are simulated with Sherpa 2.2.4 and Sherpa 2.2.11 [33] respectively. Matrix elements at next-to-leading-order (NLO) in QCD for up to one parton and at LO for up to three partons are calculated with the Comix [52] and OpenLoops [53–55] libraries. An alternative $\gamma\gamma$+jets MC sample generated with MadGraph5_aMC@NLO [35] including production of up to two jets at NLO is considered for evaluation of systematic uncertainties. The $t\bar{t}\gamma\gamma$ process is generated with MadGraph5_aMC@NLO.

4

Table 1: Summary of the main signal and background samples, split by production mode: signal samples, continuum background samples, single Higgs boson processes and Higgs-boson pair production samples. The generator used in the simulation, the PDF set, the showering model and the set of tuned parameters are also provided.

Process	Generator	PDF set	Showering	Tune
$X \to SH$	Pythia 8.2 [30]	NNPDF2.3LO [31]	Pythia 8.2 [30]	A14 [32]
$\gamma\gamma$+jets	Sherpa 2.2.4 [33]	NNPDF3.0NNLO [34]	–	–
$t\bar{t}\gamma\gamma$	MadGraph5_aMC@NLO [35]	NNPDF2.3LO	Pythia 8.2	A14
$Z(\to q\bar{q})\gamma\gamma$	Sherpa 2.2.11 [33]	NNPDF3.0NNLO	–	–
ggF H	Nnlops [36–38] [39, 40]	PDF4LHC15 [41]	Pythia 8.2	AZNLO [42]
VBF H	Powheg Box v2 [43–46]	PDF4LHC15	Pythia 8.2	AZNLO
WH	Powheg Box v2 [47, 48]	PDF4LHC15	Pythia 8.2	AZNLO
$qq \to ZH$	Powheg Box v2 [47, 48]	PDF4LHC15	Pythia 8.2	AZNLO
$gg \to ZH$	Powheg Box v2 [47, 48]	PDF4LHC15	Pythia 8.2	AZNLO
$t\bar{t}H$	Powheg Box v2 [49]	NNPDF3.0NLO	Pythia 8.2	A14
$b\bar{b}H$	Powheg Box v2 [37]	NNPDF3.0NLO	Pythia 8.2	A14
tHq	MadGraph5_aMC@NLO	NNPDF3.0NLO	Pythia 8.2	A14
tHW	MadGraph5_aMC@NLO	NNPDF3.0NLO	Pythia 8.2	A14
ggF HH	Powheg Box v2 +FT [46, 50, 51]	PDFLHC	Pythia 8.2	A14
VBF HH	MadGraph5_aMC@NLO	NNPDF3.0NLO	Pythia 8.2	A14

The second largest background category consists of processes with photons from a single Higgs boson decay, this includes processes where the Higgs boson may be produced in association with other particles. This includes single Higgs boson production via gluon–gluon fusion (ggF), vector-boson fusion (VBF), WH, ZH ($qq \to ZH$ and $gg \to ZH$), $t\bar{t}H$, $b\bar{b}H$, tHq and tHW. The cross sections of the single Higgs boson processes are set to the most precise available theoretical values [56].

The last background category consists of Standard Model Higgs boson pair production (HH) processes via ggF and VBF. The ggF Higgs boson pair production cross section is calculated at next-to-next-to-leading-order (NNLO) accuracy including finite top-quark mass effects [57–60]. The cross section for Higgs boson pair production via VBF is calculated at next-to-next-to-next-to-leading-order (N^3LO) [57]. The analysis assumes a branching ratio of 0.227% for the Higgs boson decay into two photons and a branching ratio of 58.2% for the Higgs boson decay into two b-quarks [56, 61].

The samples use EvtGen [62] for the modelling of b- and c-hadron decays. A full simulation of the ATLAS detector [63] based on Geant4 [64] is used to reproduce the detector response for single Higgs boson processes. The samples for signal, non-resonant photon production and Standard Model Higgs boson pair production are processed with the fast simulation AtlFastII [65] which employs Geant4 except for a parameterisation of the calorimeter response.

Varying numbers of minimum-bias interactions produced with Pythia 8.186 [66] using the NNPDF2.3LO PDF set with the A3 tune [67] are overlaid on the hard-scattering event of all samples to simulate the effect of multiple pp interactions (pile-up) in the same or nearby bunch crossings. The events are reweighted as a function of the number of interactions per bunch crossing to match the distribution in data.

4 Object definitions

Events are required to have at least one reconstructed collision vertex, defined as a vertex associated with at least two tracks with transverse momentum (p_T) larger than 0.5 GeV. The primary vertex is selected from the reconstructed collision vertices using a neural network algorithm [68] based on extrapolated photon trajectories and the tracks associated with each candidate vertex.

Photons are reconstructed from topologically connected clusters [29] of energy deposits in the electromagnetic calorimeter in the region $|\eta| < 2.37$, excluding the transition region between the barrel and endcap calorimeters $1.37 < |\eta| < 1.52$. Photon candidates are classified as converted or unconverted based on whether or not they can be associated to conversion vertices or tracks consistent with photon conversions.

The calibration of the photon energy is based on a multivariate regression algorithm trained with MC samples, where the simulated distributions of the input variables are corrected with data-driven techniques. The calibrated energy is brought to the absolute scale by applying scale factors derived from $Z \rightarrow e^+e^-$ events [29]. The photon direction is reconstructed using the longitudinal development of the shower in the calorimeters constrained to the luminous region of the proton-beam collisions. In the case of converted photons the information about the position of the conversion vertex and the tracks associated with conversion is also used.

Photon identification is based on the lateral shower profile of the energy deposits in the first and second electromagnetic calorimeter layers and on the energy leakage fraction into the hadronic calorimeter [29]. It reduces the misidentification of hadronic jets containing large neutral components, primarily neutral pions, which decay into a pair of highly collimated photons. Identification criteria are tuned for converted and unconverted photons separately, and the *Tight* criteria defined in Ref. [29] are applied.

To improve rejection of misidentified photons, two isolation variables are defined to quantify the amount of activity around a photon. Calorimeter-based isolation E_T^{iso} is defined as the sum of the transverse energy of topological clusters within a cone of size $\Delta R = \sqrt{\Delta\eta^2 + \Delta\phi^2} = 0.2$ around the photon, after first correcting for the energy of the photon candidate itself and for an average expected pile-up contribution. Track-based isolation p_T^{iso} is defined as the scalar sum of the transverse momenta of all tracks with $p_T > 1$ GeV originating from the primary vertex and within a cone of size $\Delta R = 0.2$ around the photon. To be considered isolated a photon must have $E_T^{iso}/E_T < 0.065$ and $p_T^{iso}/E_T < 0.05$. For isolated photons with transverse energies between 30 GeV and 250 GeV, the identification efficiency ranges from 84% to 98% [29].

Electrons are reconstructed from energy deposits measured in the electromagnetic calorimeter that are matched to ID tracks [29]. They are required to be in the region $|\eta| < 2.37$, excluding the transition region between the barrel and endcap calorimeters $1.37 < |\eta| < 1.52$, and to have $p_T > 10$ GeV. Electrons are required to satisfy a *Medium* identification criterion based on the shower shape, track-cluster matching and TRT information in a likelihood-based algorithm [29]. Muons are reconstructed from high-quality tracks found in the MS [69]. A matching of the MS tracks to ID tracks is required in the region $|\eta| < 2.5$. Muons are required to have $|\eta| < 2.7$ and $p_T > 10$ GeV and to satisfy a *Medium* identification criterion [70]. Electrons and muons are both matched to the primary vertex via requirements on the longitudinal and transverse impact parameters on the tracks, $|z_0|$ and $|d_0|$, respectively. These requirements are $|z_0| \sin\theta < 0.5$ mm, and $|d_0|/\sigma_{d_0} < 5$ (3) for electrons (muons).

Reconstructed jets are based on particle-flow objects built from noise-suppressed positive-energy topological clusters in the calorimeter and reconstructed tracks [71]. The anti-k_t algorithm [72, 73] with radius

parameter $R = 0.4$ is used. The jet energy is calibrated by applying several simulation-based corrections and techniques correcting for differences between simulation and data [74]. Jets are required to have rapidity $|y| < 4.4$ and $p_T > 25$ GeV. To suppress jets produced in pile-up interactions, each jet within the tracking acceptance of $|\eta| < 2.4$ and with $p_T < 60$ GeV is required to satisfy the *Tight* jet-vertex tagger [75] criteria used to identify jets from the selected primary vertex.

The flavour of jets is determined using a deep-learning neural network, DL1r [76]. The DL1r b-tagging is based on distinctive features of b-hadron decays in terms of the impact parameters of the tracks and the displaced vertices reconstructed in the ID. The inputs of the DL1r network also include discriminating variables constructed by a recurrent neural network (RNNIP) [77], which exploits the spatial and kinematic correlations between tracks originating from the same b-hadron. For each jet, DL1r gives three different probabilities p_b-, p_c- and p_{light} for the jet to originate from a b, c or light quark respectively. The three probabilities are combined to define the final discriminant. The DL1r algorithm is optimised to maximise performance on particle-flow jets and extends the algorithm performance to very high jet p_T. Only central jets with $|\eta| < 2.5$ are considered for flavour tagging. Working points are defined by single requirement values on the DL1r discriminant output distribution, and can be chosen to provide a specific b-jet efficiency for an inclusive $t\bar{t}$ MC sample. The analysis makes use of the DL1r working point with a 77% efficiency to select jets containing b-hadrons in simulated $t\bar{t}$ events. For this working point the misidentification rate is 1/130 for light-flavour jets and 1/4.9 for charm jets. Scale factors are applied to correct for differences in b-tagging efficiency between data and simulation. The scale factors are measured as a function of the jet p_T using a likelihood-based method in a sample enriched in $t\bar{t}$ events [78].

Scale factors are applied to correct for differences in b-tagging efficiency between data and simulation. The scale factors for jets originating from a b quark are measured as a function of the jet p_T using a likelihood-based method in a sample enriched in $t\bar{t}$ events [78]. The scale factors for jets originating from a c quark are measured in $t\bar{t}$ events containing a $W \rightarrow cs$ decay [79]. For light flavour jets, the scale factors are derived using Z+jets events [80].

The energy of b-tagged jets is corrected for the possible contribution of muons from semileptonic b-hadron decays. Additionally, the undetected energy of neutrinos and out-of-cone effects are corrected for with scale factors derived as a function of the b-jet p_T from a $t\bar{t}$ MC sample. The two corrections together improve the resolution of the invariant mass of the two jets with the highest b-tagging discriminant by about 20%. This procedure closely follows that in Ref. [81].

Overlap removal procedures are applied to avoid using the same detector signals to reconstruct multiple objects. In this analysis priority is given to photons, by removing jets, electrons and muons within $\Delta R < 0.4$ of a selected photon. Next, jets within $\Delta R < 0.2$ of electrons are removed. Finally, electrons and muons within $\Delta R < 0.4$ of any remaining jet are removed.

5 Analysis strategy

A wide range of masses is considered for the scalars X and S, leading to significantly varying event kinematics at different hypothetical values of m_X and m_S. When $m_X \gg m_S + m_H$, the scalar S can become so boosted that its decay products, two b-quarks, become very collimated and are reconstructed within the same $R = 0.4$ jet. For smaller values of $m_X - (m_S + m_H)$, two separate b-tagged jets are reconstructed. Therefore two mutually exclusive regions are defined with either one or two b-tagged jets, referred to as the 1 b-tagged and 2 b-tagged regions, and respectively dedicated to the boosted and non-boosted scenarios. A

preselection, common to both regions, is introduced below. A final discriminating variable is then defined for each signal hypothesis using parameterised neural networks. The final experimental constraint on the signal is obtained from a signal-plus-background fit to the distribution of the discriminating variable in data. In the special case where m_S =125 GeV, this analysis strategy can be compared with an alternative strategy similar to that applied in the ATLAS search for $HH \to b\bar{b}\gamma\gamma$ [82], and it was found that for any given signal point the difference between estimated upper limits on $\sigma(X \to SH \to b\bar{b}\gamma\gamma)$ is small.

5.1 Event preselection

Events are selected using diphoton triggers described in Section 3. Beyond the trigger requirements, events are selected if:

- At least two photons satisfy the requirements in Section 4.

- The invariant mass of the two leading photons satisfies $105 < m_{\gamma\gamma} < 160$ GeV.

- The leading photon has $p_T > 0.35 m_{\gamma\gamma}$ and the subleading photon has $p_T > 0.25 m_{\gamma\gamma}$.

- No electrons or muons, as defined in Section 4, are present.

- The number of central ($|\eta| < 2.5$) jets is at least two and no more than five. This reduces the $t\bar{t}H$ background where top quarks decay hadronically.

- There is exactly one or two b-tagged jet at the 77% working point. Events with more than two b-tagged jets are removed to ensure orthogonality with the $b\bar{b}b\bar{b}$ final state from the same signal.

5.2 Signal region definitions

The number of b-tagged jets is used to categorise events in two regions, requiring 1 or 2 b-tagged jets. The signal events contain the characteristic $H \to \gamma\gamma$ decay with the $m_{\gamma\gamma}$ distribution peaking around the Higgs boson mass at ~125 GeV. Therefore, two mutually exclusive signal regions (SR) dedicated respectively to the boosted and non-boosted scenarios are defined requiring $120 < m_{\gamma\gamma} < 130$ GeV. The shape of the final signal-to-background discriminant, defined in Section 5.3 for each signal hypothesis, and obtained in the signal region, is used for the final statistical test of the signal-plus-background and background only hypothesis.

Events with $m_{\gamma\gamma}$ outside the [120, 130] GeV interval are instead used to construct the sideband control regions for background estimation as described in Section 6. The 2 b-tagged and 1 b-tagged sideband regions (SB) are found to contain about 85% of $\gamma\gamma$+jets with two real photons and are expected to contain less than 0.1% of Higgs boson processes.

The fraction of signal events with two resolved b-tagged jets is below 50% if $m_S/m_X < 0.09$, as derived from simulations. The 1 b-tagged signal region is thus used to analyse signal points for which $m_S/m_X \lesssim 0.09$ and, conversely, the 2 b-tagged selection is used to analyse signal points for which $m_S/m_X \gtrsim 0.09$.

5.3 Final signal-to-background discriminant

Multivariate discriminants are used to separate signal from background events in the signal regions. Two distinct parameterised neural networks (PNNs) [83] are trained with events in the 2 b-tagged and the 1 b-tagged signal and sideband regions. PNNs take as input a vector of event characteristics $\bar{x}$ and a vector of phase space parameters $\bar{\theta}$ and yield a response function that is parameterised in $\bar{\theta}$. The parameterisation provides a unique discriminant for each signal hypothesis, separating the targeted signal events from background events. Therefore, for each value of $\bar{\theta} = (m_S, m_X)$, the PNN($\bar{\theta}$) is effectively a different observable. The PNNs provide sensitivity over the considered mass range and allow interpolation to values of $\bar{\theta}$ not explicitly included in the training. In the 2 b-tagged signal region the PNN is parameterised in the plane of the two particle masses $\bar{\theta} = (m_S, m_X)$, and as a function of $\bar{\theta} = (m_X)$ in the 1 b-tagged region.

The decay chain $X \rightarrow S(\rightarrow b\bar{b})H(\rightarrow \gamma\gamma)$ and the masses m_S and m_X are encoded in the invariant mass of the final state particles, thus the most effective features to train the PNNs are the invariant masses of the final state photons and b-tagged jets.

For the 2 b-tagged signal region the input features are $\bar{x} = (m_{bb}, m^*_{bb\gamma\gamma})$ where $m^*_{bb\gamma\gamma} = m_{bb\gamma\gamma} - (m_{\gamma\gamma} - 125\,\text{GeV})$. The replacement of $m_{\gamma\gamma}$ by the Higgs boson mass of 125 GeV allows to remove correlations between the PNN score and $m_{\gamma\gamma}$, allowing to create sideband regions for background normalisation as described in Section 6.1. For the 1 b-tagged signal region the input variables are $\bar{x} = (p^b_{\mathrm{T}}, m^*_{b\gamma\gamma})$ where p^b_{T} is the p_{T} of the b-tagged jet, and $m^*_{b\gamma\gamma}$ is derived from the invariant mass $m_{b\gamma\gamma}$ of the only available b-tagged jet and the two photons as $m^*_{b\gamma\gamma} = m_{b\gamma\gamma} - (m_{\gamma\gamma} - 125\,\text{GeV})$. Additional variables were considered in the training but did not bring significant improvements and were therefore disregarded. The usage of the variables m_{bb} and $m^*_{bb\gamma\gamma}$ alone allows for the signal interpolation applied in the 2 b-tagged signal region and described in Section 5.4.

The PNNs are trained using Keras [84] with the Tensorflow [85] backend. The training is performed using 69 simulated signal samples chosen from the entire investigated mass grid, as well as the largest background processes: non-resonant diphoton+jets, $t\bar{t}H$, ZH and ggF H. In the 1 b-tagged signal region the VBF H, and Higgs boson pair production processes are also considered for training. As the vector of parameters $\bar{\theta}$ is not meaningful for the background samples, each background event has $\bar{\theta}$ values assigned at random from the distribution of values in the signal samples during training.

After the signal region selections, most events arise from the $\gamma\gamma$ + jets background category, leading to very unbalanced training classes, which makes it difficult for the PNNs to differentiate between signal and background. The imbalance is reduced by giving a unit weight to all MC events used in the training. The effect of using a unit event weight on the shape of the input features $\bar{x}$ is found to be negligible.

The PNN internal architectures are optimised using KerasTuner [84], which chooses the hyper-parameters maximizing the Area-Under-Curve calculated on an evaluation set and using Bayesian Optimisation [86]. The class weight defined as $w_c = 0.5 n_{\mathrm{tot}}/n_c$ is used, where c is either signal or background, n_c is the number of events in the given class and n_{tot} is the total number of events. Furthermore, given the number n_s (n_b) of signal (background) events, an initial bias of $\log(n_s/n_b)$ is applied to the last layer of the PNN.

The PNNs use binary cross entropy as the loss function and stochastic gradient-based optimisation using the Adam algorithm [87]. All hidden layers have a standard dense training layer using a rectified linear unit activation function and each has a dropout layer with a dropout rate between 2% and 20%. The output layers have a single node and use a sigmoid activation function. The PNN used in the 2 b-tagged signal region is trained with signal samples with $m_X \geq 170$ GeV and $m_S \geq 30$ GeV. For the 1 b-tagged signal

region, only signal points where S has enough boost are used, this includes eleven points with $15 \leq m_S \leq 70$ GeV. The PNN of the 2 b-tagged signal region has four hidden layers with 85, 49, 45 and 81 nodes. The PNN of the 1 b-tagged signal region has three hidden layers with 101, 29 and 101 nodes. After training, the PNN output shape is compared between data and MC in dedicated sideband regions to validate the modelling of the PNN distribution. The results of these comparisons are covered in Section 8.2.

5.4 Signal interpolation

To set continuous limits in the (m_X, m_S) plane, it is desirable to set limits on intermediate signal models where no sample is simulated. In order to constrain an intermediate signal point defined by $(m_X^{\text{int}}, m_S^{\text{int}})$, the shape of the PNN output is interpolated from a nearby reference signal sample simulated with low statistical uncertainty and referred to as $(m_X^{\text{ref}}, m_S^{\text{ref}})$. The distributions of the input features for $(m_X^{\text{int}}, m_S^{\text{int}})$ are derived from the reference sample in two steps: first a rescaling step that takes into account the different masses at the reference and intermediate points, and second a reweighting step that takes different mass resolutions at different mass points into account. The interpolated input features are then used as input to the PNN to obtain the PNN(θ) distribution for the interpolated signal.

For each selected event in the reference sample, the four-vectors of H, S and X are measured using the selected b-jets and photons. The four-vectors of H and S are recomputed in the rest frame of X using a Lorentz transformation defined by the four-vector of X. In absence of any experimental effects, the four-vectors of H and S in the X rest frame would be set to ideal values defined by the kinematics of the $X \rightarrow SH$ two-body decay and the specific values of m_X and m_S. In practice, the rest frame quantities are distributions around their ideal values, while the shape of the distributions are determined by experimental effects. The kinematics at the intermediate point $(m_X^{\text{int}}, m_S^{\text{int}})$ are emulated from $(m_X^{\text{ref}}, m_S^{\text{ref}})$ by rescaling the rest frame four-vectors of H and S so that they are distributed around their new ideal theoretical values at $(m_X^{\text{int}}, m_S^{\text{int}})$, and events of the reference sample are weighted to reproduce the expected experimental resolution at the intermediate mass.

The resolution effects are much larger for jets than for photons; therefore, the resolution weighting only considers the m_{bb} resolution. The m_{bb} resolution is measured for the simulated points and modelled with a Bukin probability [88]. Each parameter of the Bukin probability becomes a 2D map in the (m_X, m_S) plane. The values of the Bukin parameters can then be interpolated to any mass point $(m_X^{\text{int}}, m_S^{\text{int}})$ using Delaunay triangulation [89]. The final distribution of PNN($m_X^{\text{int}}, m_S^{\text{int}}$) is obtained by feeding the values of m_{bb} and $m_{bb\gamma\gamma}^*$ to the PNN, after four-vector rescaling and resolution weighting. This technique works well at high momenta where the change in resolution effects between nearby simulated points is small. For this reason the interpolation is only applied in parts of the 2 b-tagged signal region, defined by $m_X > 300$ GeV and $m_S > 70$ GeV.

The quality of the PNN shape interpolation is evaluated by studying its impact on the expected upper limits on $\sigma(X \rightarrow SH \rightarrow b\bar{b}\gamma\gamma)$. The upper limits obtained with the PNN output shape from simulated signal events are compared with those obtained with the interpolated PNN output shape. In the domain where the interpolation is applied the expected limits on $\sigma(X \rightarrow SH \rightarrow b\bar{b}\gamma\gamma)$ change by less than 5% for $m_S \geq 100$ GeV when replacing the actual PNN output shape with the interpolated one.

For lower masses (below $m_S = 70$ GeV) fast changes in resolution mean that the limits obtained from interpolated PNN shapes can differ by more than 10% from those obtained with the actual PNN shape. For this reason the interpolation procedure is not applied at low masses or in the 1 b-tagged region. Instead a much finer grid of simulated signal samples in the (m_X, m_S) plane is used. The required granularity is

studied by performing injection tests and checking the sensitivity of one PNN at a given $\bar{\theta}$ to neighbouring signal samples generated at a different (m_X, m_S) point. The grid spacing is chosen small enough so that a signal excess at one simulated grid point would also appear in the PNN output of at least one nearby simulated signal sample.

6 Background estimation

The final interpretation in terms of a search for a possible $X \rightarrow S(\rightarrow b\bar{b})H(\rightarrow\gamma\gamma)$ signal requires the ability to predict for each background process the number of events in the signal region, and the shape of the PNN output. In the following sections several methods are employed: a data-driven technique to study the composition of the non-resonant diphoton background category in terms of events with zero, one or two misidentified photons, a data-driven method to normalise the non-resonant diphoton background category, and finally simulations to evaluate contributions from irreducible backgrounds.

6.1 Non-resonant diphoton background

The largest background category is the non-resonant $\gamma\gamma$+jets background, which includes instrumental components such as γ+jets and dijets where jets are misidentified as photons. Other contributions to this category are the $t\bar{t}\gamma\gamma$ process which represents less than 2% (0.5%) of the background in the 2 b-tagged (1 b-tagged) signal region, and the $Z(\rightarrow q\bar{q})\gamma\gamma$ process, which represents less than 1% (0.3%) in the 2 b-tagged (1 b-tagged) region. These last two processes are estimated directly from simulation.

The fractions of $\gamma\gamma$+jets events with zero, one or two misidentified photons and their associated systematic uncertainties are determined by the double two-dimensional sideband method, a data-driven technique which relies on several photon identification criteria, already employed in the search for Higgs boson pair production in the $b\bar{b}\gamma\gamma$ final state [19], the method is described in Ref. [90] and references therein. The fractions of misidentified photon backgrounds are derived individually in the 1 and 2 b-tagged regions. The fraction of events with two real photons is found to be 87% in the 1 b-tagged region and 84% in the 2 b-tagged region. The data-driven method is also used later to derive the $m_{bb\gamma\gamma}$, $m_{\gamma\gamma}$, m_{bb} and PNN distributions for the different components with true or misidentified photons. These distributions are compared in the sideband regions with the data and the SHERPA $\gamma\gamma$+jets MC sample. No large difference is found between the shapes of the components, indicating that it is possible to directly build high-statistics templates from SHERPA samples without adding contributions from misidentified photons.

Based on these studies, the zero, one or two misidentified photon components of the $\gamma\gamma$+jets background category are modelled directly with the SHERPA $\gamma\gamma$+jets MC sample, with appropriate systematic uncertainties described in Section 7. The normalisation of the SHERPA $\gamma\gamma$+jets MC sample is fitted to the data in the sideband and signal regions according to the statistical model described in Section 8.1, the fit effectively rescales the SHERPA $\gamma\gamma$+jets MC sample to the sum of the zero, one and two misidentified photon components of the non-resonant diphoton background in data. The rescaling of the SHERPA $\gamma\gamma$+jets MC sample therefore reflects both misidentified photon contributions and higher order processes present in data but not in the simulation. Several systematic uncertainties can affect the ratio of the $\gamma\gamma$+jets background in the signal region over the corresponding sideband as detailed in Section 7. In a background-only fit where only the data in the sidebands are considered, this procedure scales the SHERPA $\gamma\gamma$+jets MC sample by a factor 1.03 ± 0.01 in the 1 b-tagged region and a factor 1.26 ± 0.03 in the 2 b-tagged region.

The shape of the PNN output for the non-resonant diphoton category is studied in the sideband regions in both data and simulation, and in the signal regions with simulation. It is observed that the shapes of the PNN output for the zero, one or two misidentified photon components are well reproduced by the SHERPA $\gamma\gamma$+jets MC sample. In the SHERPA $\gamma\gamma$+jets simulation the input variables to the PNN are observed to be consistent within statistical uncertainties between the signal regions and two narrow sidebands defined by $m_{\gamma\gamma} \in [115,120] \cup [130,135]$ GeV. Finally the modelling of the PNN output by simulation is validated in the full sideband control regions, by comparing the predicted PNN distributions from SHERPA $\gamma\gamma$+jets simulations, with the observed PNN distributions in data. Theoretical and experimental systematic uncertainties in the PNN output shapes for the $\gamma\gamma$+jets background category are considered in Section 7.

6.2 Higgs boson processes

This category of background consists of all processes that contain single Higgs boson production via ggF or VBF, WH, ZH ($qq \rightarrow ZH$ and $gg \rightarrow ZH$), $t\bar{t}H$, $b\bar{b}H$, tHq and tHW. Higgs boson pair production via ggF and VBF is also included in this category. Following the strategy in Ref. [19], the normalisation and shape of these processes are obtained from simulated MC samples generated at NLO, and normalised using state-of-the-art theoretical cross sections [56]. Several systematic uncertainties are assigned to these processes as discussed in Section 7.

7 Systematic uncertainties

Three categories of systematic uncertainties are considered. Experimental systematic uncertainties account for possible differences between the performance of the detector in simulation and in data, they are applied to all quantities derived from simulation and are described in Section 7.1. Theoretical systematic uncertainties arise where theoretical inputs are used, such as cross sections, or where effects on shapes from higher-order corrections should be considered, this is described in Section 7.2. The $\gamma\gamma$+jets background is derived from a combination of MC simulation and a data-driven technique, and the related sytematic uncertainties are detailed in Section 7.3.

7.1 Experimental systematic uncertainties

Experimental systematic uncertainties affect selection efficiencies and PNN shapes for all Higgs boson processes and the $X \rightarrow S(\rightarrow b\bar{b})H(\rightarrow \gamma\gamma)$ signal. The effect of experimental systematic uncertainties is also propagated to the PNN shape of the $\gamma\gamma$+jets background. The experimental systematic uncertainties are categorised into four groups, in order of decreasing impact on the expected upper limits on $\sigma(X \rightarrow SH \rightarrow b\bar{b}\gamma\gamma)$: flavour tagging, photons, jets and pile-up. The limits on $\sigma(X \rightarrow SH \rightarrow b\bar{b}\gamma\gamma)$ are compared with and without experimental systematic uncertainties. For m_X above ~400 GeV the effect of experimental systematic uncertainties on the limits is less than 1% but grows to 2%–20% at lower m_X values.

Flavour tagging uncertainties [78–80] are the leading source of experimental uncertainties in this search. They include the uncertainties in the efficiency to b-tag a jet containing a b-hadron, and the probability to b-tag a jet containing a c-hadron or a light-flavour jet by mistake. The combined effect of all flavour tagging uncertainties is the largest in the 2 b-tagged signal region with a 5% uncertainty in the signal

efficiency for models with low m_S and decreasing to 2% at high m_S. In the 1 b-tagged signal region that uncertainty remains in the range 0.5%–1.5%. The corresponding uncertainty in the predicted number of single and double Higgs boson processes is about 3%. Once incorporated into the fit and taking into account the effect on both the yields and the PNN shapes of signal and backgrounds, flavour tagging uncertainties impact the upper limits by about 6%.

The category of photon-related uncertainties includes uncertainties from efficiencies of the photon triggers, photon identification and isolation, and uncertainties in the photon energy resolution and scale. These are computed in data using data-driven techniques [28, 29] and are propagated to the simulation-based estimates of background yields and signal efficiencies. The combined effect of all photon uncertainties on the predicted signal efficiency and predicted number of events from single and double Higgs boson processes is about 2.5% in both the signal regions. Once incorporated into the fit and taking into account the effect on both the yields and the PNN shapes on signal and backgrounds, these translate into an uncertainty of 2%–4.5% in the signal sensitivity.

The category of jet-related uncertainties include uncertainties in the jet energy scale and jet energy resolution. These are derived using data-driven techniques [74] and compared with their counterpart in simulation. These uncertainties are propagated to the signal efficiency and background estimates. The combined effect of all jet-related uncertainties is largest in the 2 b-tagged signal region with up to 14% uncertainty in the signal efficiency for models with low m_S and decreasing to about 2% at high m_S. In the 1 b-tagged signal region that uncertainty remains smaller than 3%. The corresponding uncertainty in the predicted number of single and double Higgs boson processes is 5% (7%) in the 1 b-tagged (2 b-tagged) signal region. However the effect of these systematic uncertainties on the PNN shape remains small, of the order of 1% in the most signal-like PNN bin. Once incorporated into the fit and taking into account the effect on both the yields and the PNN shapes of signal and backgrounds, these translate into an uncertainty of about 1.5% in the signal sensitivity for $m_S > 110$ GeV. The impact grows at lower masses where it can reach up to 15%.

The category of pile-up related uncertainties comes from the reweighting of the MC simulation to the pile-up profile in data. This results in an uncertainty of at most 1% in the predicted number of events from Higgs boson processes. The effect on the signal efficiency is smaller than 1% in both the signal regions and for most of the parameter space, except in the 2 b-tagged signal region for low m_X where it can reach 1.8%. Finally the 0.83% uncertainty in the measured ATLAS Run 2 integrated luminosity is propagated to all processes normalised with their theoretical cross sections.

7.2 Theoretical systematic uncertainties

Theoretical systematic uncertainties affect the backgrounds normalised by their theoretical cross sections, but also the signal efficiency, and the non-resonant diphoton background. The latter is discussed in Section 7.3.

For processes with significant contributions to the 1 b-tagged and 2 b-tagged signal regions and where the dominant heavy-flavour production is already taken into account at LO (ttH and ZH), several theoretical systematic uncertainties are considered. Scale uncertainties due to missing higher-order corrections in the production rates are estimated by varying the factorisation and renormalisation scales up and down from their nominal values by a factor two, taking the envelope of these variations. Parton shower uncertainties are evaluated by comparing against alternative samples where the parton shower is performed with HERWIG 7.1.5 [91, 92]. The resulting bin-to-bin variations of the PNN output range from a few percent up

to 10% in some bins, while the resulting impact on the exclusion limits is below 1%. Effects of the choice of PDF and α_S are estimated by varying them following the prescription in Ref. [41]. These systematic uncertainties can lead to up to 5% bin-to-bin variations in the shape of the PNN discriminant output, but have a small impact on the limits.

For smaller Higgs boson backgrounds where the dominant heavy flavour production occurs at LO, the inclusive cross section uncertainties from Ref. [56] are used along with scale, parton shower, PDF and α_S uncertainties derived as described above. The same procedure is followed for the $Z(\rightarrow q\bar{q})\gamma\gamma$ process. The final impact of these uncertainties on the results is small.

In single Higgs boson processes where b-quarks are not produced at LO (VBF H, WH, ggF H), a single 100% normalisation uncertainty is used. This is motivated by studies of heavy-flavour production in association with top-quark pairs [93, 94] and of W-boson production in association with b-jets [95]. These have a very small impact on the final sensitivity, except when searching for models with low m_S, where the 100% uncertainty in ggF H can lead to a 10% decrease in sensitivity to the signal.

The uncertainties in the Higgs boson decay branching ratios $BR(H \rightarrow \gamma\gamma)$ and $BR(H \rightarrow b\bar{b})$ propagate to the background yields, impacting the $\sigma(X \rightarrow SH \rightarrow b\bar{b}\gamma\gamma)$ limits by ~3% and ~1.5% respectively.

To better understand the overall impact of theoretical background systematic uncertainties, the limits on $\sigma(X \rightarrow SH \rightarrow b\bar{b}\gamma\gamma)$ are computed with and without the theoretical background systematic uncertainties described above. It is observed that the limits worsen by about 4% when including theoretical background systematic uncertainties. It can be noted that this is smaller than the effect of systematic uncertainties in the non-resonant diphoton background described in the next section and smaller than the effect of theoretical signal systematic uncertainties.

Theoretical systematic uncertainties are also considered for the $X \rightarrow S(\rightarrow b\bar{b})H(\rightarrow \gamma\gamma)$ signal, both in terms of the shape of the PNN output and the predicted event yields. They include scale, parton shower, PDF and α_S uncertainties calculated as described earlier. The impact of these systematic uncertainties on the signal efficiency and the shape of the PNN output are taken into account. These uncertainties lead to 2%–10% bin-to-bin variations of the PNN output shape, it is most pronounced for the parton shower uncertainty. The systematic uncertainties obtained by changing to an alternative PDF and α_S lead to up to 11% change in the predicted signal yield, particularly at high m_X ~1000 GeV. The impact of theoretical signal uncertainties on the sensitivity to $\sigma(X \rightarrow SH \rightarrow b\bar{b}\gamma\gamma)$ can reach 10%. A systematic uncertainty associated with the interpolation of the PNN score in the region m_X >300 GeV and m_S >70 GeV is estimated by considering a shape systematic uncertainty in the PNN score, derived by varying the parameters of the Bukin probabilities within their errors. The impact on the exclusion limits at interpolated (m_X, m_S) points is at most 10%.

7.3 Systematic uncertainties in the non-resonant diphoton background

The normalisation of the non-resonant diphoton background is derived in a fit which includes the sideband control regions. The following theoretical uncertainties, introduced earlier, affect the PNN output shape and the overall estimated number of events in the signal and sideband regions: scale uncertainties, choice of PDF, α_s and parton shower. The uncertainties associated with the scales, PDFs and α_s are calculated using the same methods as described in Section 7.2. The parton shower uncertainties are evaluated by using alternative samples generated with MADGRAPH [35] for the parton shower. An additional MC modelling uncertainty is considered by using an alternative $\gamma\gamma$+jets sample generated with MADGRAPH5_AMC@NLO.

This sample models diphoton production with up to two jets at NLO. The corresponding uncertainty is found to be the most significant in the analysis; its impact in the 2 b-tagged signal region degrades the expected upper limits on the signal by up to 20%. This impact is larger for low values of m_X, while for m_X above 600 GeV the impact is always below 5%. For the 1 b-tagged signal region the modelling uncertainty has an impact of a few percent on the upper limits, except for two signal points at (500, 30) GeV and (230, 15) GeV where the effect is around 40% due to statistical fluctuations in the alternative MADGRAPH samples.

8 Results

8.1 Statistical model

The results of the analysis are obtained from a maximum-likelihood fit of the binned PNN output distribution, performed simultaneously over a signal region and its corresponding sideband region. The PNN binning is constructed starting from the rightmost signal-like bin. The size of this bin is chosen to maximise the signal-to-background ratio and widened until there is at least one background event. The same procedure is repeated with the next bin, and requiring that the number of background events is above a certain threshold, in order to avoid bins with large statistical errors. When the signal-to-background ratio in the bin drops below that of the full un-binned distribution, the iterative process is stopped and a single background-like bin is constructed for the remaining distribution at PNN outputs close to zero. The binning is optimised independently for each signal hypothesis. For the 1 b-jet selection a similar method is used.

The likelihood function is defined as:

$$
\mathcal{L} = \mathrm{Pois}\left(n_{\mathrm{SB}} \,\middle|\, \mu_{\gamma\gamma} N_{\mathrm{SB}}^{\gamma\gamma}(\boldsymbol{\theta}) + \sum_p N_{\mathrm{SB}}^p(\boldsymbol{\theta})\right) \cdot \prod_i \mathrm{Pois}\left(n_{\mathrm{SR},i} \,\middle|\, \mu_{\gamma\gamma} N_{\mathrm{SR}}^{\gamma\gamma}(\boldsymbol{\theta}) f_i^{\gamma\gamma}(\boldsymbol{\theta}) + \sum_p N_{\mathrm{SR}}^p(\boldsymbol{\theta}) f_i^p(\boldsymbol{\theta})\right) \cdot G(\boldsymbol{\theta})
$$

(1)

where the index p runs over physics processes other than $\gamma\gamma$+jets, the index i runs over the bins of the PNN output, $n_{\mathrm{SR},i}$ and n_{SB} are the observed number of events in the signal region PNN bin i and in the corresponding sideband region, $N_{\mathrm{SR}}^p(\boldsymbol{\theta})$ is the expected number of events from process p in the signal region, and $N_{\mathrm{SB}}(\boldsymbol{\theta})$ is the total expected number of events in the corresponding sideband region. The superscript $\gamma\gamma$ is used for parameters that specifically apply to the $\gamma\gamma$+jets background. The factor $\mu_{\gamma\gamma}$ is the free parameter that fits the $\gamma\gamma$+jets normalisation to the data. The function f_i^p gives the shape or probability density function (pdf) of the PNN output discriminant for each background or signal process; therefore $N_{\mathrm{SR}}^p f_i^p$ is the expected number of events of process p in the PNN bin i. Finally $\boldsymbol{\theta}$ is a vector of nuisance parameters, and $G(\boldsymbol{\theta})$ are constrained pdfs for the nuisance parameters. Correlation of the nuisance parameters across different signal and background components, as well as categories, is taken into account.

The nominal yields of the single and double Higgs boson background processes are initially set to values from simulation. The likelihood function includes all the nuisance parameters that describe the systematic uncertainties. The signal cross section is a free parameter in the fit. The measurement of the parameter of interest is carried out using a statistical test based on the profile likelihood ratio [96]. In the absence of signal, upper limits on $\sigma(X \to SH \to b\bar{b}\gamma\gamma)$ at the 95% CL are set. The limits are calculated using
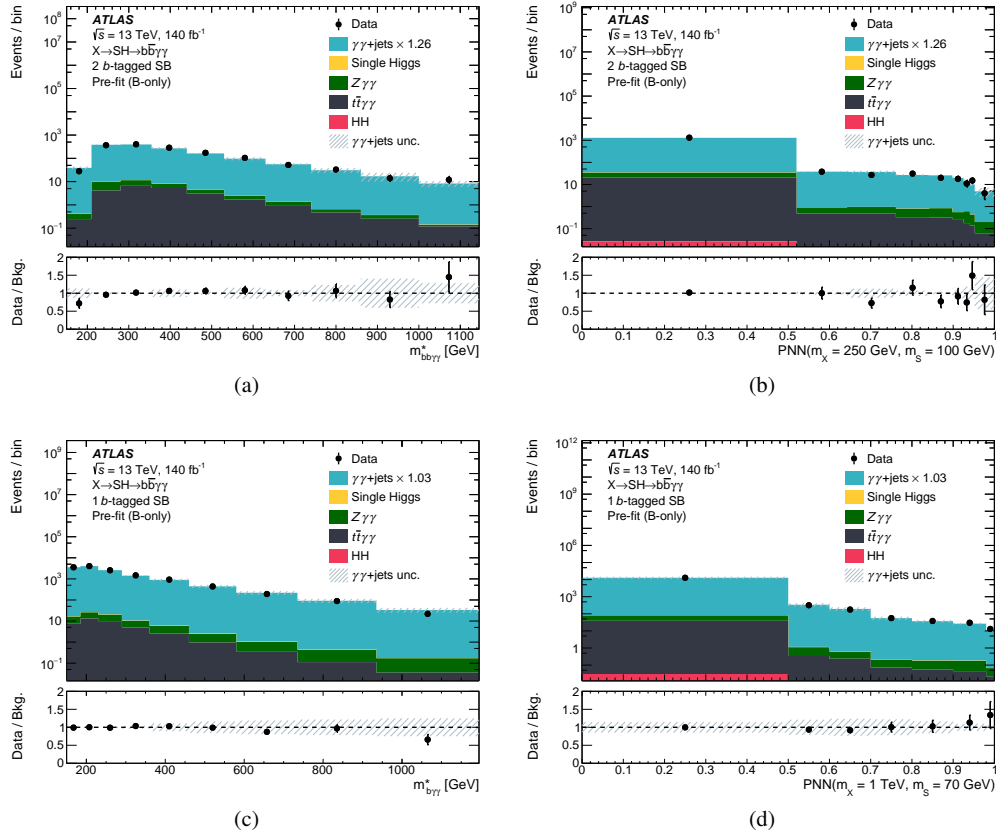
Figure 2: Distributions of (a) $m^*_{bb\gamma\gamma}$, (c) $m^*_{b\gamma\gamma}$ and (b,d) PNN for two choices of $\bar{\theta} = (m_S, m_X)$ in data and in the predicted model, in the sidebands of the 2 b-tagged region (top) and 1 b-tagged region (bottom). The $\gamma\gamma$ + jets background is rescaled to its post-fit normalisation in a background-only fit. The variables $m^*_{bb\gamma\gamma}$ and $m^*_{b\gamma\gamma}$ are defined as $m^*_{bb\gamma\gamma} = m_{bb\gamma\gamma} - (m_{\gamma\gamma} - 125 \text{ GeV})$ and $m^*_{b\gamma\gamma} = m_{b\gamma\gamma} - (m_{\gamma\gamma} - 125 \text{ GeV})$. The $\gamma\gamma$ + jets category represents the sum of $\gamma\gamma$ + jets, γ + jets and dijet backgrounds. The error band corresponds to the dominant uncertainty, which arises from the non-resonant $\gamma\gamma$ + jets background.

the asymptotic formula with a profile-likelihood-ratio-based test statistic [96], and are based on the CL_S method [97]. The binning in PNN score was chosen to ensure that the asymptotic approximation would be valid.

8.2 Control region validation

The ability of the background model to reproduce the data is studied in the sideband regions where a background-only fit is performed to the data. Distributions are then compared between the post-fit model and the data as shown in Figure 2. A good agreement between the data and the model shows the ability of the model to reproduce the PNN discriminant output in both the 2 b-tagged and 1 b-tagged regions. For each value of $\bar{\theta} = (m_S, m_X)$ the PNN($\bar{\theta}$) is effectively a different observable, for this reason the post-fit data-to-prediction comparison in the sideband is performed for all analysed signal mass points, and good agreement is observed.

8.3 Result and interpretation

The results of the background-only fit in the signal regions and sidebands to the data is shown in Table 2. The signal region and sideband yields are independent of the parameterised neural network, while the column "Signal-like bin" illustrates the signal and background yields in the most signal-like bin of the PNN for two choices of $\bar{\theta}$, namely (250, 100) GeV and (1000, 70) GeV. Figure 3 illustrates the post-fit distribution of the PNN in the 2 b-tagged and 1 b-tagged regions at two different $\bar{\theta}$. PNN($\bar{\theta}$) is sensitive not only to a signal at the same masses defined by $\bar{\theta}$, but also to signals with nearby masses $\bar{\theta}'$. To check for discovery of a wide range of signal masses, the background-only hypothesis is tested against the data for a highly granular grid of PNN parameters $\bar{\theta}$. The step size between two consecutive parameters $\bar{\theta}$ is selected by studying the sensitivity of PNN($\bar{\theta}$) to a signal with different masses $\bar{\theta}'$. If there was an excess in data due to a signal with masses $\bar{\theta}'$ observed with the discriminant PNN($\bar{\theta}$), the significance of this excess would degrade with increasing distance between $\bar{\theta}'$ and $\bar{\theta}$. A step size in the $\bar{\theta}$ grid is chosen such that the degradation of the significance does not exceed 10% between two consecutive grid points. In practice the step size goes from 5 GeV in the densest regions to 25 GeV for $m_X \geq 250$ GeV, and to 50 GeV for $m_X \geq 600$ GeV and $m_S \geq 200$ GeV.

For most mass points good agreement is observed between data and the SM background-only expectation; however some deviation is observed for a few points. The largest excess of the observation over the SM background-only hypothesis occurs for $(m_X, m_S) = (575, 200)$ GeV with a local significance of 3.5σ. The 'look-elsewhere effect' is taken into account using the asymptotic method described in Ref. [98]. An asymptotic formula for the Euler characteristic as a function of the maximum of the test statistic across each signal point is derived using toy MC experiments. The resulting global significance is calculated to be 2.0σ. At this mass point the signal PNN output shape was initially derived from interpolation. The analysis was repeated using a simulated sample; the observed significance remained however unchanged, confirming the validity of the interpolation method.

A parameter point of particular interest is $(m_X, m_S) = (650, 90)$ GeV where the CMS Collaboration reports a deviation between observation and background-only expectation, corresponding to a local (global) significance of 3.8 (2.8) standard deviations [17]. Injecting a MC signal with a production cross section of 0.35 fb (the best fit reported by the CMS experiment) in the analysis performed in this paper yields a local excess in observation to SM expectation of 2.7 standard deviations, demonstrating the sensitivity of this analysis to a signal consistent with the excess observed by CMS. The results of the analysis of ATLAS data for this specific parameter point instead shows good agreement between observation and SM background expectation (the p-value of the background-only hypothesis is larger than 0.5). The 95% CL upper limit on $\sigma(X \to SH \to b\bar{b}\gamma\gamma)$ for this specific mass point is 0.2 fb.

The statistical analysis sets 95% CL upper limits on $\sigma(X \to SH \to b\bar{b}\gamma\gamma)$ for all values of $\bar{\theta} = (m_X, m_S)$ by performing a signal-plus-background fit to the PNN output distribution in data. For each mass point the signal region which gives the best expected upper limit is selected. The resulting expected and observed upper limits are presented in Figure 4, and range from observed (expected) limits of 39 (25) fb at $m_X = 170$ GeV and $m_S = 30$ GeV, to 0.09 (0.14) fb at $m_X = 1000$ GeV and m_S between 250 and 300 GeV. The upper limits improve at higher masses, consistent with the fact that signals with higher m_X become easier to differentiate from SM processes. In contrast, they worsen in the boosted signal regime at lower m_S, where the 1 b-tagged region is employed, and consistent with the lower signal-to-background ratio shown in Table 2 for the 1 b-tagged region. At low m_X the sensitivity suffers from an increasing fraction of b-jets falling below the jet p_T reconstruction threshold.
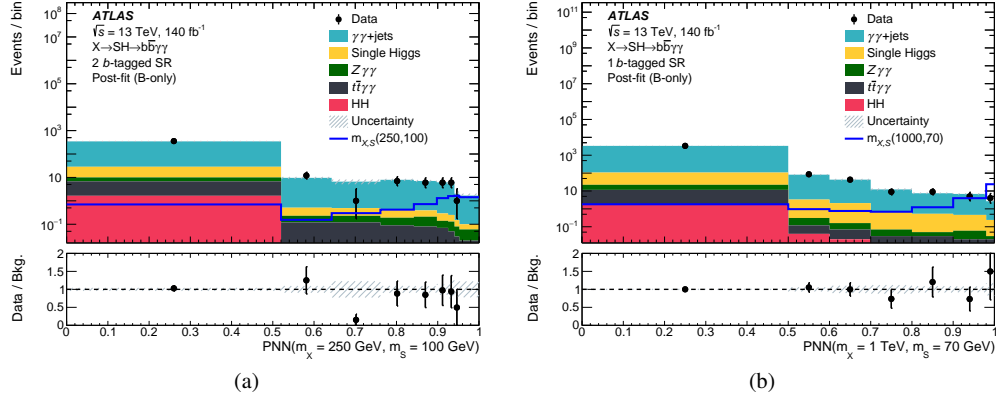
Figure 3: Post-fit distributions of the PNN discriminant output in the (a) 2 *b*-tagged signal region for m_X = 250 GeV and m_S = 100 GeV and (b) 1 *b*-tagged signal region for m_X = 1000 GeV and m_S = 70 GeV, after a background-only fit to data. The signals corresponding to the two PNN parameterisations, normalised to a 1 fb cross section, are illustrated for comparison. The $\gamma\gamma$+ jets category represents the sum of $\gamma\gamma$+ jets, γ + jets and dijet backgrounds. The error band corresponds to the total systematic uncertainty after fit.
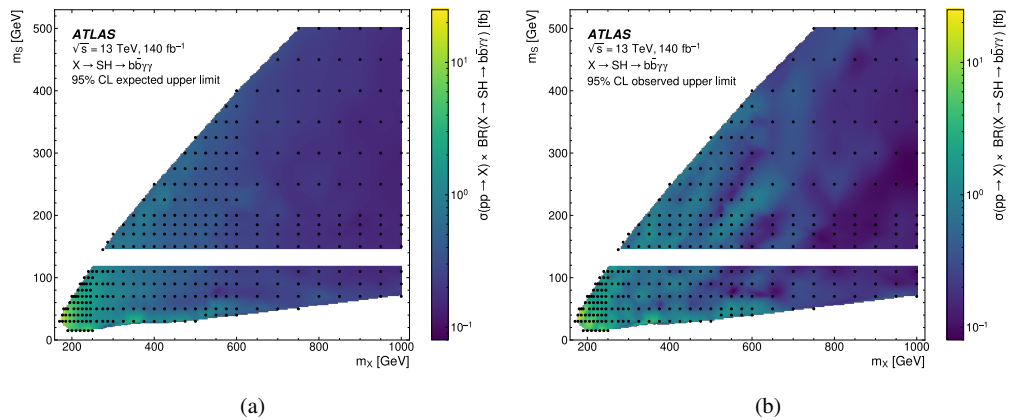
Figure 4: (a) Expected and (b) observed 95% CL upper limits on the signal cross section times branching fraction for the $X \rightarrow SH$ signal, in the (m_X, m_S) plane. The points show where the limits were evaluated. The band at m_S = 125 GeV is not shown as those points are equivalent to those already probed in Ref. [19].

18

Table 2: Number of events for the different process categories obtained from a background-only fit to data in the signal regions and sidebands. Observed and fitted event yields in the two signal regions and sidebands, independent of phase space parameters $\bar{\theta}$, are given in the columns "Signal region" and "Sideband". The yields in the most signal-like bin of the PNN distribution depend on the selected phase space parameters $\bar{\theta}$, here shown under the column "Signal-like bin" for $\bar{\theta} = (m_X, m_S) = (250, 100)$ GeV and $(1000, 70)$ GeV. The expected number of events from the two corresponding benchmark signals with a 1 fb cross section is also given. The uncertainties are symmetrised around the central value. The uncertainty in the total background is calculated taking correlations between the individual contributions into account. For the single Higgs boson processes, "Other" includes the following production modes: VBF, WH, tHq, and tHW.

Background	2 b-tagged region			1 b-tagged region		
	Sideband	Signal region	Signal-like bin	Sideband	Signal region	Signal-like bin
Non-res. $\gamma\gamma$	1480 ± 37	372 ± 16	1.64 ± 0.37	13450 ± 110	3392 ± 53	2.45 ± 0.43
Single Higgs	0.46 ± 0.11	19.9 ± 5.3	0.04 ± 0.01	2.3 ± 1.1	92 ± 44	0.21 ± 0.10
ggF+$b\bar{b}H$	0.14 ± 0.11	6.5 ± 5.2	0.01 ± 0.01	1.5 ± 1.1	56 ± 43	0.11 ± 0.09
$t\bar{t}H$	0.21 ± 0.01	7.91 ± 0.77	0.01 ± 0.01	0.31 ± 0.01	11.4 ± 1.1	0.03 ± 0.01
ZH	0.08 ± 0.01	3.56 ± 0.30	0.02 ± 0.01	0.17 ± 0.01	7.35 ± 0.60	0.02 ± 0.01
Other	0.03 ± 0.01	1.94 ± 0.70	< 0.005	0.40 ± 0.23	17 ± 10	0.05 ± 0.03
Double Higgs	0.03 ± 0.01	1.65 ± 0.25	< 0.005	0.03 ± 0.01	1.79 ± 0.27	0.01 ± 0.01
Total	1480 ± 37	394 ± 16	1.67 ± 0.37	13450 ± 110	3486 ± 48	2.67 ± 0.45
Signal (m_X, m_S)						
(250, 100) GeV	0.38 ± 0.04	8.3 ± 1.2	1.43 ± 0.21			
(1000, 70) GeV				0.97 ± 0.10	33.3 ± 5.8	23.9 ± 4.2
Data	1479	395	0	13450	3491	4

9 Conclusion

A search for a signal from a hypothetical scalar X is performed, considering the case where it decays into another hypothetical scalar S and a Higgs boson, which subsequently decay into pairs of b-quarks and photons, respectively. Two signal regions targeting resolved or boosted $S \to b\bar{b}$ decays are analysed using parameterised neural networks, which provide continuous sensitivity in the probed (m_X, m_S) plane. In the region $m_X > 300$ GeV and $m_S > 70$ GeV the validity of the limits for intermediate mass points is ensured by interpolating the signal shapes to a much finer signal grid, and the finer grid spacing is guided by the sensitivity range of the PNN to values of (m_X, m_S) where it was not trained. At lower masses the validity of the limits for intermediate mass points is ensured by using a very fine grid of simulated signal samples.

No significant excess with respect to the Standard Model background is found. Therefore, 95% CL upper limits are set on $\sigma(X \to SH \to b\bar{b}\gamma\gamma)$ in the ranges $170 \leq m_X \leq 1000$ GeV and $15 \leq m_S \leq 500$ GeV, expanding earlier LHC results to lower masses and providing higher sensitivity. The largest deviation from the background-only expectation occurs for $(m_X, m_S) = (575, 200)$ GeV with a local (global) significance of 3.5 (2.0) standard deviations. For the mass point $(m_X, m_S) = (650, 90)$ GeV, where CMS reported an excess with a local (global) significance of 3.8 (2.8) standard deviations, this analysis shows good

agreement with the background-only hypothesis and sets a 95% CL upper limit on the signal cross section of 0.2 fb.

Acknowledgements

References

[1] ATLAS Collaboration, *Observation of a new particle in the search for the Standard Model Higgs boson with the ATLAS detector at the LHC*, Phys. Lett. B **716** (2012) 1, arXiv: `1207.7214 [hep-ex]`.

[2] CMS Collaboration, *Observation of a new boson at a mass of 125 GeV with the CMS experiment at the LHC*, Phys. Lett. B **716** (2012) 30, arXiv: `1207.7235 [hep-ex]`.

[3] CMS Collaboration, *A portrait of the Higgs boson by the CMS experiment ten years after the discovery*, Nature **607** (2022) 60, arXiv: `2207.00043 [hep-ex]`, Erratum: Nature **623** (2023) E4.

[4] ATLAS Collaboration, *A detailed map of Higgs boson interactions by the ATLAS experiment ten years after the discovery*, Nature **607** (2022) 52, arXiv: `2207.00092 [hep-ex]`, Erratum: Nature **612** (2022) E24.

[5] A. Ferrari and N. Rompotis, *Exploration of Extended Higgs Sectors with Run-2 Proton–Proton Collision Data at the LHC*, Symmetry **13** (2021) 2144, Erratum: Symmetry **14** (2022) 1546.

[6] V. Barger, P. Langacker, M. McCaskey, M. Ramsey-Musolf and G. Shaughnessy, *Complex singlet extension of the standard model*, Phys. Rev. D **79** (2009) 015018, arXiv: `0811.0393 [hep-ph]`.

[7] T. Robens, T. Stefaniak and J. Wittbrodt, *Two-real-scalar-singlet extension of the SM: LHC phenomenology and benchmark scenarios*, Eur. Phys. J. C **80** (2020) 151, arXiv: `1908.08554 [hep-ph]`.

[8] I. F. Ginzburg, M. Krawczyk and P. Osland, *Two-Higgs-Doublet Models with CP violation*, 2002, arXiv: `hep-ph/0211371 [hep-ph]`.

[9] X.-G. He, T. Li, X.-Q. Li, J. Tandean and H.-C. Tsai, *Constraints on scalar dark matter from direct experimental searches*, Phys. Rev. D **79** (2009) 023521, arXiv: `0811.0658 [hep-ph]`.

[10] M. Mühlleitner, M. O. P. Sampaio, R. Santos and J. Wittbrodt, *The N2HDM under theoretical and experimental scrutiny*, JHEP **03** (2017) 94, arXiv: `1612.01309 [hep-ph]`.

[11] U. Ellwanger, C. Hugonie and A. M. Teixeira, *The Next-to-Minimal Supersymmetric Standard Model*, Phys. Rept. **496** (2010) 1, arXiv: `0910.1785 [hep-ph]`.

[12] M. Maniatis, *The next-to-minimal supersymmetric extension of the standard model reviewed*, Int. J. Mod. Phys. A **25** (2010), arXiv: `0906.0777 [hep-ph]`.

[13] P. Basler, S. Dawson, C. Englert and M. Mühlleitner, *Showcasing HH production: Benchmarks for the LHC and HL-LHC*, Phys. Rev. D **99** (2019) 055048, arXiv: `1812.03542 [hep-ph]`.

[14] S. Baum and N. R. Shah, *Benchmark Suggestions for Resonant Double Higgs Production at the LHC for Extended Higgs Sectors*, (2019), arXiv: `1904.10810 [hep-ph]`.

[15] CMS Collaboration, *Search for a massive scalar resonance decaying to a light scalar and a Higgs boson in the four b quarks final state with boosted topology*, Phys. Lett. B **842** (2023) 137392, arXiv: `2204.12413 [hep-ex]`.

[16] CMS Collaboration, *Search for a heavy Higgs boson decaying into two lighter Higgs bosons in the $\tau\tau bb$ final state at 13 TeV*, JHEP **11** (2021) 57, arXiv: `2106.10361 [hep-ex]`.

[17] CMS Collaboration, *Search for a new resonance decaying into two spin-0 bosons in a final state with two photons and two bottom quarks in proton-proton collisions at $\sqrt{s} = 13$ TeV*, JHEP **05** (2024) 316, arXiv: `2310.01643 [hep-ex]`.

[18] ATLAS Collaboration, *Search for a new heavy scalar particle decaying into a Higgs boson and a new scalar singlet in final states with one or two light leptons and a pair of τ-leptons with the ATLAS detector*, JHEP **10** (2023) 009, arXiv: `2307.11120 [hep-ex]`.

[19] ATLAS Collaboration, *Search for Higgs boson pair production in the two bottom quarks plus two photons final state in pp collisions at $\sqrt{s} = 13$ TeV with the ATLAS detector*, Phys. Rev. D **106** (2022) 052001, arXiv: `2112.11876 [hep-ex]`.

[20] ATLAS Collaboration, *The ATLAS Experiment at the CERN Large Hadron Collider*, JINST **3** (2008) S08003.

[21] ATLAS Collaboration, *ATLAS Insertable B-Layer: Technical Design Report*, ATLAS-TDR-19; CERN-LHCC-2010-013, 2010, URL: `https://cds.cern.ch/record/1291633`, Addendum: ATLAS-TDR-19-ADD-1; CERN-LHCC-2012-009, 2012, URL: `https://cds.cern.ch/record/1451888`.

[22] B. Abbott et al., *Production and integration of the ATLAS Insertable B-Layer*, JINST **13** (2018) T05008, arXiv: `1803.00844 [physics.ins-det]`.

[23] G. Avoni et al., *The new LUCID-2 detector for luminosity measurement and monitoring in ATLAS*, JINST **13** (2018) P07017.

[24] ATLAS Collaboration, *Performance of the ATLAS trigger system in 2015*, Eur. Phys. J. C **77** (2017) 317, arXiv: 1611.09661 [hep-ex].

[25] ATLAS Collaboration, *The ATLAS Collaboration Software and Firmware*, ATL-SOFT-PUB-2021-001, 2021, URL: https://cds.cern.ch/record/2767187.

[26] ATLAS Collaboration, *ATLAS data quality operations and performance for 2015–2018 data-taking*, JINST **15** (2020) P04003, arXiv: 1911.04632 [physics.ins-det].

[27] *Luminosity determination in pp collisions at $\sqrt{s}$=13 TeV using the ATLAS detector at the LHC*, Eur. Phys. J. C **83** (2023), arXiv: 2212.09379 [hep-ex].

[28] ATLAS Collaboration, *Performance of electron and photon triggers in ATLAS during LHC Run 2*, Eur. Phys. J. C **80** (2020) 47, arXiv: 1909.00761 [hep-ex].

[29] ATLAS Collaboration, *Electron and photon performance measurements with the ATLAS detector using the 2015–2017 LHC proton–proton collision data*, JINST **14** (2019) P12006, arXiv: 1908.00005 [hep-ex].

[30] T. Sjöstrand et al., *An introduction to PYTHIA 8.2*, Comput. Phys. Commun. **191** (2015) 159, arXiv: 1410.3012 [hep-ph].

[31] NNPDF Collaboration, R. D. Ball et al., *Parton distributions with LHC data*, Nucl. Phys. B **867** (2013) 244, arXiv: 1207.1303 [hep-ph].

[32] ATLAS Collaboration, *ATLAS Pythia 8 tunes to 7 TeV data*, ATL-PHYS-PUB-2014-021, 2014, URL: https://cds.cern.ch/record/1966419.

[33] E. Bothmann et al., *Event generation with Sherpa 2.2*, SciPost Phys. **7** (2019) 034, arXiv: 1905.09127 [hep-ph].

[34] NNPDF Collaboration, R. D. Ball et al., *Parton distributions for the LHC run II*, JHEP **04** (2015) 040, arXiv: 1410.8849 [hep-ph].

[35] J. Alwall et al., *The automated computation of tree-level and next-to-leading order differential cross sections, and their matching to parton shower simulations*, JHEP **07** (2014) 079, arXiv: 1405.0301 [hep-ph].

[36] K. Hamilton, P. Nason and G. Zanderighi, *MINLO: multi-scale improved NLO*, JHEP **10** (2012) 155, arXiv: 1206.3572 [hep-ph].

[37] J. M. Campbell et al., *NLO Higgs boson production plus one and two jets using the POWHEG BOX, MadGraph4 and MCFM*, JHEP **07** (2012) 092, arXiv: 1202.5475 [hep-ph].

[38] K. Hamilton, P. Nason, C. Oleari and G. Zanderighi, *Merging H/W/Z + 0 and 1 jet at NLO with no merging scale: a path to parton shower + NNLO matching*, JHEP **05** (2013) 082, arXiv: 1212.4504 [hep-ph].

[39] G. Bozzi, S. Catani, D. de Florian and M. Grazzini, *Transverse-momentum resummation and the spectrum of the Higgs boson at the LHC*, Nucl. Phys. B **737** (2006) 73, arXiv: hep-ph/0508068 [hep-ph].

[40] D. de Florian, G. Ferrera, M. Grazzini and D. Tommasini, *Transverse-momentum resummation: Higgs boson production at the Tevatron and the LHC*, JHEP **11** (2011) 064, arXiv: 1109.2109 [hep-ph].

[41] J. Butterworth et al., *PDF4LHC recommendations for LHC Run II*, J. Phys. G **43** (2016) 023001, arXiv: 1510.03865 [hep-ph].

[42] ATLAS Collaboration, *Measurement of the Z/γ^* boson transverse momentum distribution in pp collisions at $\sqrt{s} = 7$ TeV with the ATLAS detector*, JHEP **09** (2014) 145, arXiv: 1406.3660 [hep-ex].

[43] P. Nason, *A new method for combining NLO QCD with shower Monte Carlo algorithms*, JHEP **11** (2004) 040, arXiv: hep-ph/0409146.

[44] S. Frixione, P. Nason and C. Oleari, *Matching NLO QCD computations with parton shower simulations: the POWHEG method*, JHEP **11** (2007) 070, arXiv: 0709.2092 [hep-ph].

[45] S. Alioli, P. Nason, C. Oleari and E. Re, *A general framework for implementing NLO calculations in shower Monte Carlo programs: the POWHEG BOX*, JHEP **06** (2010) 043, arXiv: 1002.2581 [hep-ph].

[46] P. Nason and C. Oleari, *NLO Higgs boson production via vector-boson fusion matched with shower in POWHEG*, JHEP **02** (2010) 037, arXiv: 0911.5299 [hep-ph].

[47] K. Mimasu, V. Sanz and C. Williams, *Higher order QCD predictions for associated Higgs production with anomalous couplings to gauge bosons*, JHEP **08** (2016) 039, arXiv: 1512.02572 [hep-ph].

[48] G. Luisoni, P. Nason, C. Oleari and F. Tramontano, *$HW^\pm/HZ + 0$ and 1 jet at NLO with the POWHEG BOX interfaced to GoSam and their merging within MiNLO*, JHEP **10** (2013) 083, arXiv: 1306.2542 [hep-ph].

[49] H. B. Hartanto, B. Jäger, L. Reina and D. Wackeroth, *Higgs boson production in association with top quarks in the POWHEG BOX*, Phys. Rev. D **91** (2015) 094003, arXiv: 1501.04498 [hep-ph].

[50] G. Heinrich, S. P. Jones, M. Kerner, G. Luisoni and E. Vryonidou, *NLO predictions for Higgs boson pair production with full top quark mass dependence matched to parton showers*, JHEP **08** (2017) 088, arXiv: 1703.09252 [hep-ph].

[51] G. Heinrich, S. Jones, M. Kerner, G. Luisoni and L. Scyboz, *Probing the trilinear Higgs boson coupling in di-Higgs production at NLO QCD including parton shower effects*, JHEP **06** (2019) 066, arXiv: 1903.08137 [hep-ph].

[52] T. Gleisberg and S. Höche, *Comix, a new matrix element generator*, JHEP **12** (2008) 039, arXiv: 0808.3674 [hep-ph].

[53] F. Buccioni et al., *OpenLoops 2*, Eur. Phys. J. C **79** (2019) 866, arXiv: 1907.13071 [hep-ph].

[54] F. Cascioli, P. Maierhöfer and S. Pozzorini, *Scattering Amplitudes with Open Loops*, Phys. Rev. Lett. **108** (2012) 111601, arXiv: 1111.5206 [hep-ph].

[55] A. Denner, S. Dittmaier and L. Hofer, *Collier: A fortran-based complex one-loop library in extended regularizations*, Comput. Phys. Commun. **212** (2017) 220, arXiv: 1604.06792 [hep-ph].

[56] D. de Florian et al., *Handbook of LHC Higgs Cross Sections: 4. Deciphering the Nature of the Higgs Sector*, (2017), arXiv: 1610.07922 [hep-ph].

[57] B. D. Micco, M. Gouzevitch, J. Mazzitelli and C. Vernieri,
Higgs boson potential at colliders: Status and perspectives, Rev. Phys. **5** (2020) 100045,
arXiv: 1910.00012 [hep-ph].

[58] D. Y. Shao, C. S. Li, H. T. Li and J. Wang,
Threshold resummation effects in Higgs boson pair production at the LHC, JHEP **07** (2013) 169,
arXiv: 1301.1245 [hep-ph].

[59] D. de Florian and J. Mazzitelli,
Higgs pair production at next-to-next-to-leading logarithmic accuracy at the LHC,
JHEP **09** (2015) 053, arXiv: 1505.07122 [hep-ph].

[60] J. Baglio et al., $gg \rightarrow HH$: *Combined uncertainties*, Phys. Rev. D **103** (2021) 056002,
arXiv: 2008.11626 [hep-ph].

[61] A. Djouadi, J. Kalinowski and M. Spira, *HDECAY: a program for Higgs boson decays in the
Standard Model and its supersymmetric extension*, Comput. Phys. Commun. **108** (1998) 56,
arXiv: hep-ph/9704448.

[62] D. J. Lange, *The EvtGen particle decay simulation package*,
Nucl. Instrum. Meth. A **462** (2001) 152.

[63] ATLAS Collaboration, *The ATLAS Simulation Infrastructure*, Eur. Phys. J. C **70** (2010) 823,
arXiv: 1005.4568 [physics.ins-det].

[64] S. Agostinelli et al., GEANT4 – *a simulation toolkit*, Nucl. Instrum. Meth. A **506** (2003) 250.

[65] ATLAS Collaboration,
The simulation principle and performance of the ATLAS fast calorimeter simulation FastCaloSim,
(2010), ATL-PHYS-PUB-2010-013, URL: http://cdsweb.cern.ch/record/1300517.

[66] T. Sjöstrand, S. Mrenna and P. Skands, *A brief introduction to PYTHIA 8.1*,
Comput. Phys. Commun. **178** (2008) 852, arXiv: 0710.3820 [hep-ph].

[67] ATLAS Collaboration, *The Pythia 8 A3 tune description of ATLAS minimum bias and inelastic
measurements incorporating the Donnachie–Landshoff diffractive model*,
ATL-PHYS-PUB-2016-017, 2016, URL: https://cds.cern.ch/record/2206965.

[68] ATLAS Collaboration, *Measurement of Higgs boson production in the diphoton decay channel in
pp collisions at center-of-mass energies of* 7 *and* 8 *TeV with the ATLAS detector*,
Phys. Rev. D **90** (2014) 112015, arXiv: 1408.7084 [hep-ex].

[69] ATLAS Collaboration, *Muon reconstruction performance of the ATLAS detector in proton–proton
collision data at* $\sqrt{s}$ = 13 *TeV*, Eur. Phys. J. C **76** (2016) 292, arXiv: 1603.05598 [hep-ex].

[70] ATLAS Collaboration, *Muon reconstruction and identification efficiency in ATLAS using the full
Run 2 pp collision data set at* $\sqrt{s}$ = 13 *TeV*, Eur. Phys. J. C **81** (2021) 578,
arXiv: 2012.00578 [hep-ex].

[71] ATLAS Collaboration,
Jet reconstruction and performance using particle flow with the ATLAS Detector,
Eur. Phys. J. C **77** (2017) 466, arXiv: 1703.10485 [hep-ex].

[72] M. Cacciari, G. P. Salam and G. Soyez, *The anti-k_t jet clustering algorithm*, JHEP **04** (2008) 063,
arXiv: 0802.1189 [hep-ph].

[73] M. Cacciari, G. P. Salam and G. Soyez, *FastJet user manual*, Eur. Phys. J. C **72** (2012) 1896,
arXiv: 1111.6097 [hep-ph].

[74] ATLAS Collaboration, *Jet energy scale and resolution measured in proton–proton collisions at $\sqrt{s}$ = 13 TeV with the ATLAS detector*, Eur. Phys. J. C **81** (2021) 689, arXiv: 2007.02645 [hep-ex].

[75] ATLAS Collaboration, *Performance of pile-up mitigation techniques for jets in pp collisions at $\sqrt{s}$ = 8 TeV using the ATLAS detector*, Eur. Phys. J. C **76** (2016) 581, arXiv: 1510.03823 [hep-ex].

[76] ATLAS Collaboration, *ATLAS flavour-tagging algorithms for the LHC Run 2 pp collision dataset*, Eur. Phys. J. C **83** (2023) 681, arXiv: 2211.16345 [physics.data-an].

[77] ATLAS Collaboration, *Identification of Jets Containing b-Hadrons with Recurrent Neural Networks at the ATLAS Experiment*, ATL-PHYS-PUB-2017-003, 2017, URL: https://cds.cern.ch/record/2255226.

[78] ATLAS Collaboration, *ATLAS b-jet identification performance and efficiency measurement with $t\bar{t}$ events in pp collisions at $\sqrt{s}$ = 13 TeV*, Eur. Phys. J. C **79** (2019) 970, arXiv: 1907.05120 [hep-ex].

[79] ATLAS Collaboration, *Measurement of the c-jet mistagging efficiency in $t\bar{t}$ events using pp collision data at $\sqrt{s}$ = 13 TeV collected with the ATLAS detector*, Eur. Phys. J. C **82** (2022) 95, arXiv: 2109.10627 [hep-ex].

[80] ATLAS Collaboration, *Calibration of the light-flavour jet mistagging efficiency of the b-tagging algorithms with Z+jets events using 139 fb^{-1} of ATLAS proton–proton collision data at $\sqrt{s}$ = 13 TeV*, Eur. Phys. J. C **83** (2023) 728, arXiv: 2301.06319 [hep-ex].

[81] ATLAS Collaboration, *Evidence for the $H \rightarrow b\bar{b}$ decay with the ATLAS detector*, JHEP **12** (2017) 024, arXiv: 1708.03299 [hep-ex].

[82] ATLAS Collaboration, *Search for Higgs boson pair production in the two bottom quarks plus two photons final state in pp collisions at $\sqrt{s}$ = 13 TeV with the ATLAS detector*, Phys. Rev. D **106** (5 2022) 052001.

[83] P. Baldi, K. Cranmer, T. Faucett, P. Sadowski and D. Whiteson, *Parameterized neural networks for high-energy physics*, Eur. Phys. J. C **76** (2016) 235, arXiv: 1601.07913 [hep-ex].

[84] F. Chollet et al., *Keras*, 2015, URL: https://keras.io.

[85] M. Abadi et al., *TensorFlow: Large-Scale Machine Learning on Heterogeneous Systems*, 2015, URL: https://www.tensorflow.org/.

[86] R. Garnett, *Bayesian Optimization*, Cambridge University Press, 2023, ISBN: 978-1-108-42578-0.

[87] D. P. Kingma and J. Ba, *Adam: A Method for Stochastic Optimization*, 2014, arXiv: 1412.6980 [cs.LG].

[88] A. D. Bukin, *Fitting function for asymmetric peaks*, (2007), arXiv: 0711.4449 [physics.data-an].

[89] B. N. Delaunay, *Sur la sphère vide*, French, Bull. Acad. Sci. URSS **1934** (1934) 793.

[90] ATLAS Collaboration, *Measurement of the production cross section of pairs of isolated photons in pp collisions at 13 TeV with the ATLAS detector*, JHEP **11** (2021) 169, arXiv: 2107.09330 [hep-ex].

[91] M. Bähr et al., *Herwig++ physics and manual*, Eur. Phys. J. C **58** (2008) 639,
      arXiv: 0803.0883 [hep-ph].

[92] J. Bellm et al., *Herwig 7.0/Herwig++ 3.0 release note*, Eur. Phys. J. C **76** (2016) 196,
      arXiv: 1512.01178 [hep-ph].

[93] ATLAS Collaboration,
      *Measurements of inclusive and differential fiducial cross-sections of $t\bar{t}$ production with additional
      heavy-flavour jets in proton–proton collisions at $\sqrt{s} = 13\,TeV$ with the ATLAS detector*,
      JHEP **04** (2019) 046, arXiv: 1811.12113 [hep-ex].

[94] ATLAS Collaboration, *Study of heavy-flavor quarks produced in association with top-quark pairs at
      $\sqrt{s} = 7\,TeV$ using the ATLAS detector*, Phys. Rev. D **89** (2014) 072012,
      arXiv: 1304.6386 [hep-ex].

[95] ATLAS Collaboration, *Measurement of the cross-section for W boson production in association
      with b-jets in pp collisions at $\sqrt{s} = 7\,TeV$ with the ATLAS detector*, JHEP **06** (2013) 084,
      arXiv: 1302.2929 [hep-ex].

[96] G. Cowan, K. Cranmer, E. Gross and O. Vitells,
      Asymptotic formulae for likelihood-based tests of new physics, Eur. Phys. J. C **71** (2011) 1554,
      arXiv: 1007.1727 [physics.data-an], Erratum: Eur. Phys. J. C **73** (2013) 2501.

[97] A. L. Read, *Presentation of search results: the CL_S technique*, J. Phys. G **28** (2002) 2693.

[98] E. Gross and O. Vitells, *Trial factors for the look elsewhere effect in high energy physics*,
      Eur. Phys. J. C **70** (2010) 525, arXiv: 1005.1891 [physics.data-an].

[99] ATLAS Collaboration, *ATLAS Computing Acknowledgements*, ATL-SOFT-PUB-2023-001, 2023,
      URL: https://cds.cern.ch/record/2869272.

The ATLAS Collaboration

G. Aad [103], E. Aakvaag [16], B. Abbott [121], K. Abeling [55], N.J. Abicht [49], S.H. Abidi [29],
M. Aboelela [44], A. Aboulhorma [35e], H. Abramowicz [152], H. Abreu [151], Y. Abulaiti [118],
B.S. Acharya [69a,69b,l], A. Ackermann [63a], C. Adam Bourdarios [4], L. Adamczyk [86a],
S.V. Addepalli [26], M.J. Addison [102], J. Adelman [116], A. Adiguzel [21c], T. Adye [135],
A.A. Affolder [137], Y. Afik [39], M.N. Agaras [13], J. Agarwala [73a,73b], A. Aggarwal [101],
C. Agheorghiesei [27c], A. Ahmad [36], F. Ahmadov [38,z], W.S. Ahmed [105], S. Ahuja [96], X. Ai [62e],
G. Aielli [76a,76b], A. Aikot [164], M. Ait Tamlihat [35e], B. Aitbenchikh [35a], I. Aizenberg [170],
M. Akbiyik [101], T.P.A. Åkesson [99], A.V. Akimov [37], D. Akiyama [169], N.N. Akolkar [24],
S. Aktas [21a], K. Al Khoury [41], G.L. Alberghi [23b], J. Albert [166], P. Albicocco [53], G.L. Albouy [60],
S. Alderweireldt [52], Z.L. Alegria [122], M. Aleksa [36], I.N. Aleksandrov [38], C. Alexa [27b],
T. Alexopoulos [10], F. Alfonsi [23b], M. Algren [56], M. Alhroob [142], B. Ali [133], H.M.J. Ali [92],
S. Ali [149], S.W. Alibocus [93], M. Aliev [33c], G. Alimonti [71a], W. Alkakhi [55], C. Allaire [66],
B.M.M. Allbrooke [147], J.F. Allen [52], C.A. Allendes Flores [138f], P.P. Allport [20], A. Aloisio [72a,72b],
F. Alonso [91], C. Alpigiani [139], M. Alvarez Estevez [100], A. Alvarez Fernandez [101],
M. Alves Cardoso [56], M.G. Alviggi [72a,72b], M. Aly [102], Y. Amaral Coutinho [83b], A. Ambler [105],
C. Amelung [36], M. Amerl [102], C.G. Ames [110], D. Amidei [107], K.J. Amirie [156],
S.P. Amor Dos Santos [131a], K.R. Amos [164], V. Ananiev [126], C. Anastopoulos [140], T. Andeen [11],
J.K. Anders [36], S.Y. Andrean [47a,47b], A. Andreazza [71a,71b], S. Angelidakis [9], A. Angerami [41,ab],
A.V. Anisenkov [37], A. Annovi [74a], C. Antel [56], M.T. Anthony [140], E. Antipov [146],
M. Antonelli [53], F. Anulli [75a], M. Aoki [84], T. Aoki [154], J.A. Aparisi Pozo [164], M.A. Aparo [147],
L. Aperio Bella [48], C. Appelt [18], A. Apyan [26], S.J. Arbiol Val [87], C. Arcangeletti [53],
A.T.H. Arce [51], E. Arena [93], J-F. Arguin [109], S. Argyropoulos [54], J.-H. Arling [48], O. Arnaez [4],
H. Arnold [115], G. Artoni [75a,75b], H. Asada [112], K. Asai [119], S. Asai [154], N.A. Asbah [36],
K. Assamagan [29], R. Astalos [28a], S. Atashi [160], R.J. Atkin [33a], M. Atkinson[163], H. Atmani[35f],
P.A. Atmasiddha [129], K. Augsten [133], S. Auricchio [72a,72b], A.D. Auriol [20], V.A. Austrup [102],
G. Avolio [36], K. Axiotis [56], G. Azuelos [109,af], D. Babal [28b], H. Bachacou [136], K. Bachas [153,p],
A. Bachiu [34], F. Backman [47a,47b], A. Badea [39], T.M. Baer [107], P. Bagnaia [75a,75b],
M. Bahmani [18], D. Bahner [54], K. Bai [124], A.J. Bailey [164], J.T. Baines [135], L. Baines [95],
O.K. Baker [173], E. Bakos [15], D. Bakshi Gupta [8], V. Balakrishnan [121], R. Balasubramanian [115],
E.M. Baldin [37], P. Balek [86a], E. Ballabene [23b,23a], F. Balli [136], L.M. Baltes [63a], W.K. Balunas [32],
J. Balz [101], E. Banas [87], M. Bandieramonte [130], A. Bandyopadhyay [24], S. Bansal [24],
L. Barak [152], M. Barakat [48], E.L. Barberio [106], D. Barberis [57b,57a], M. Barbero [103],
M.Z. Barel [115], K.N. Barends [33a], T. Barillari [111], M-S. Barisits [36], T. Barklow [144], P. Baron [123],
D.A. Baron Moreno [102], A. Baroncelli [62a], G. Barone [29], A.J. Barr [127], J.D. Barr [97],
F. Barreiro [100], J. Barreiro Guimarães da Costa [14a], U. Barron [152], M.G. Barros Teixeira [131a],
S. Barsov [37], F. Bartels [63a], R. Bartoldus [144], A.E. Barton [92], P. Bartos [28a], A. Basan [101],
M. Baselga [49], A. Bassalat [66,b], M.J. Basso [157a], R.L. Bates [59], S. Batlamous[35e], B. Batool [142],
M. Battaglia [137], D. Battulga [18], M. Bauce [75a,75b], M. Bauer [36], P. Bauer [24],
L.T. Bazzano Hurrell [30], J.B. Beacham [51], T. Beau [128], J.Y. Beaucamp [91], P.H. Beauchemin [159],
P. Bechtle [24], H.P. Beck [19,o], K. Becker [168], A.J. Beddall [82], V.A. Bednyakov [38], C.P. Bee [146],
L.J. Beemster [15], T.A. Beermann [36], M. Begalli [83d], M. Begel [29], A. Behera [146], J.K. Behr [48],
J.F. Beirer [36], F. Beisiegel [24], M. Belfkir [117b], G. Bella [152], L. Bellagamba [23b], A. Bellerive [34],
P. Bellos [20], K. Beloborodov [37], D. Benchekroun [35a], F. Bendebba [35a], Y. Benhammou [152],
K.C. Benkendorfer [61], L. Beresford [48], M. Beretta [53], E. Bergeaas Kuutmann [162], N. Berger [4],

B. Bergmann [133], J. Beringer [17a], G. Bernardi [5], C. Bernius [144], F.U. Bernlochner [24],
F. Bernon [36,103], A. Berrocal Guardia [13], T. Berry [96], P. Berta [134], A. Berthold [50], S. Bethke [111],
A. Betti [75a,75b], A.J. Bevan [95], N.K. Bhalla [54], M. Bhamjee [33c], S. Bhatta [146],
D.S. Bhattacharya [167], P. Bhattarai [144], K.D. Bhide [54], V.S. Bhopatkar [122], R.M. Bianchi [130],
G. Bianco [23b,23a], O. Biebel [110], R. Bielski [124], M. Biglietti [77a], C.S. Billingsley [44], M. Bindi [55],
A. Bingul [21b], C. Bini [75a,75b], A. Biondini [93], C.J. Birch-sykes [102], G.A. Bird [32], M. Birman [170],
M. Biros [134], S. Biryukov [147], T. Bisanz [49], E. Bisceglie [43b,43a], J.P. Biswal [135], D. Biswas [142],
K. Bjørke [126], I. Bloch [48], A. Blue [59], U. Blumenschein [95], J. Blumenthal [101],
V.S. Bobrovnikov [37], M. Boehler [54], B. Boehm [167], D. Bogavac [36], A.G. Bogdanchikov [37],
C. Bohm [47a], V. Boisvert [96], P. Bokan [36], T. Bold [86a], M. Bomben [5], M. Bona [95],
M. Boonekamp [136], C.D. Booth [96], A.G. Borbély [59], I.S. Bordulev [37], H.M. Borecka-Bielska [109],
G. Borissov [92], D. Bortoletto [127], D. Boscherini [23b], M. Bosman [13], J.D. Bossio Sola [36],
K. Bouaouda [35a], N. Bouchhar [164], J. Boudreau [130], E.V. Bouhova-Thacker [92], D. Boumediene [40],
R. Bouquet [57b,57a], A. Boveia [120], J. Boyd [36], D. Boye [29], I.R. Boyko [38], J. Bracinik [20],
N. Brahimi [4], G. Brandt [172], O. Brandt [32], F. Braren [48], B. Brau [104], J.E. Brau [124],
R. Brener [170], L. Brenner [115], R. Brenner [162], S. Bressler [170], D. Britton [59], D. Britzger [111],
I. Brock [24], R. Brock [108], G. Brooijmans [41], E. Brost [29], L.M. Brown [166], L.E. Bruce [61],
T.L. Bruckler [127], P.A. Bruckman de Renstrom [87], B. Brüers [48], A. Bruni [23b], G. Bruni [23b],
D. Brunner [47b], M. Bruschi [23b], N. Bruscino [75a,75b], T. Buanes [16], Q. Buat [139], D. Buchin [111],
A.G. Buckley [59], O. Bulekov [37], B.A. Bullard [144], S. Burdin [93], C.D. Burgard [49],
A.M. Burger [36], B. Burghgrave [8], O. Burlayenko [54], J.T.P. Burr [32], C.D. Burton [11],
J.C. Burzynski [143], E.L. Busch [41], V. Büscher [101], P.J. Bussey [59], J.M. Butler [25], C.M. Buttar [59],
J.M. Butterworth [97], W. Buttinger [135], C.J. Buxo Vazquez [108], A.R. Buzykaev [37],
S. Cabrera Urbán [164], L. Cadamuro [66], D. Caforio [58], H. Cai [130], Y. Cai [14a,14e], Y. Cai [14c],
V.M.M. Cairo [36], O. Cakir [3a], N. Calace [36], P. Calafiura [17a], G. Calderini [128], P. Calfayan [68],
G. Callea [59], L.P. Caloba [83b], D. Calvet [40], S. Calvet [40], M. Calvetti [74a,74b], R. Camacho Toro [128],
S. Camarda [36], D. Camarero Munoz [26], P. Camarri [76a,76b], M.T. Camerlingo [72a,72b],
D. Cameron [36], C. Camincher [166], M. Campanelli [97], A. Camplani [42], V. Canale [72a,72b],
A.C. Canbay [3a], J. Cantero [164], Y. Cao [163], F. Capocasa [26], M. Capua [43b,43a], A. Carbone [71a,71b],
R. Cardarelli [76a], J.C.J. Cardenas [8], F. Cardillo [164], G. Carducci [43b,43a], T. Carli [36],
G. Carlino [72a], J.I. Carlotto [13], B.T. Carlson [130,q], E.M. Carlson [166,157a], L. Carminati [71a,71b],
A. Carnelli [136], M. Carnesale [75a,75b], S. Caron [114], E. Carquin [138f], S. Carrá [71a],
G. Carratta [23b,23a], A.M. Carroll [124], T.M. Carter [52], M.P. Casado [13,i], M. Caspar [48],
F.L. Castillo [4], L. Castillo Garcia [13], V. Castillo Gimenez [164], N.F. Castro [131a,131e],
A. Catinaccio [36], J.R. Catmore [126], T. Cavaliere [4], V. Cavaliere [29], N. Cavalli [23b,23a],
Y.C. Cekmecelioglu [48], E. Celebi [21a], S. Cella [36], F. Celli [127], M.S. Centonze [70a,70b],
V. Cepaitis [56], K. Cerny [123], A.S. Cerqueira [83a], A. Cerri [147], L. Cerrito [76a,76b], F. Cerutti [17a],
B. Cervato [142], A. Cervelli [23b], G. Cesarini [53], S.A. Cetin [82], D. Chakraborty [116], J. Chan [17a],
W.Y. Chan [154], J.D. Chapman [32], E. Chapon [136], B. Chargeishvili [150b], D.G. Charlton [20],
M. Chatterjee [19], C. Chauhan [134], Y. Che [14c], S. Chekanov [6], S.V. Chekulaev [157a],
G.A. Chelkov [38,a], A. Chen [107], B. Chen [152], B. Chen [166], H. Chen [14c], H. Chen [29],
J. Chen [62c], J. Chen [143], M. Chen [127], S. Chen [154], S.J. Chen [14c], X. Chen [62c,136],
X. Chen [14b,ae], Y. Chen [62a], C.L. Cheng [171], H.C. Cheng [64a], S. Cheong [144], A. Cheplakov [38],
E. Cheremushkina [48], E. Cherepanova [115], R. Cherkaoui El Moursli [35e], E. Cheu [7], K. Cheung [65],
L. Chevalier [136], V. Chiarella [53], G. Chiarelli [74a], N. Chiedde [103], G. Chiodini [70a],
A.S. Chisholm [20], A. Chitan [27b], M. Chitishvili [164], M.V. Chizhov [38,r], K. Choi [11], Y. Chou [139],
E.Y.S. Chow [114], K.L. Chu [170], M.C. Chu [64a], X. Chu [14a,14e], J. Chudoba [132],

J.J. Chwastowski [87], D. Cieri [111], K.M. Ciesla [86a], V. Cindro [94], A. Ciocio [17a], F. Cirotto [72a,72b], Z.H. Citron [170], M. Citterio [71a], D.A. Ciubotaru[27b], A. Clark [56], P.J. Clark [52], C. Clarry [156], J.M. Clavijo Columbie [48], S.E. Clawson [48], C. Clement [47a,47b], J. Clercx [48], Y. Coadou [103], M. Cobal [69a,69c], A. Coccaro [57b], R.F. Coelho Barrue [131a], R. Coelho Lopes De Sa [104], S. Coelli [71a], B. Cole [41], J. Collot [60], P. Conde Muiño [131a,131g], M.P. Connell [33c], S.H. Connell [33c], E.I. Conroy [127], F. Conventi [72a,ag], H.G. Cooke [20], A.M. Cooper-Sarkar [127], A. Cordeiro Oudot Choi [128], L.D. Corpe [40], M. Corradi [75a,75b], F. Corriveau [105,x], A. Cortes-Gonzalez [18], M.J. Costa [164], F. Costanza [4], D. Costanzo [140], B.M. Cote [120], G. Cowan [96], K. Cranmer [171], D. Cremonini [23b,23a], S. Crépé-Renaudin [60], F. Crescioli [128], M. Cristinziani [142], M. Cristoforetti [78a,78b], V. Croft [115], J.E. Crosby [122], G. Crosetti [43b,43a], A. Cueto [100], T. Cuhadar Donszelmann [160], H. Cui [14a,14e], Z. Cui [7], W.R. Cunningham [59], F. Curcio [164], J.R. Curran [52], P. Czodrowski [36], M.M. Czurylo [36], M.J. Da Cunha Sargedas De Sousa [57b,57a], J.V. Da Fonseca Pinto [83b], C. Da Via [102], W. Dabrowski [86a], T. Dado [49], S. Dahbi [149], T. Dai [107], D. Dal Santo [19], C. Dallapiccola [104], M. Dam [42], G. D'amen [29], V. D'Amico [110], J. Damp [101], J.R. Dandoy [34], M. Danninger [143], V. Dao [36], G. Darbo [57b], S. Darmora [6], S.J. Das [29,ah], S. D'Auria [71a,71b], A. D'Avanzo [131a], C. David [33a], T. Davidek [134], B. Davis-Purcell [34], I. Dawson [95], H.A. Day-hall [133], K. De [8], R. De Asmundis [72a], N. De Biase [48], S. De Castro [23b,23a], N. De Groot [114], P. de Jong [115], H. De la Torre [116], A. De Maria [14c], A. De Salvo [75a], U. De Sanctis [76a,76b], F. De Santis [70a,70b], A. De Santo [147], J.B. De Vivie De Regie [60], D.V. Dedovich[38], J. Degens [115], A.M. Deiana [44], F. Del Corso [23b,23a], J. Del Peso [100], F. Del Rio [63a], L. Delagrange [128], F. Deliot [136], C.M. Delitzsch [49], M. Della Pietra [72a,72b], D. Della Volpe [56], A. Dell'Acqua [36], L. Dell'Asta [71a,71b], M. Delmastro [4], P.A. Delsart [60], S. Demers [173], M. Demichev[38], S.P. Denisov [37], L. D'Eramo [40], D. Derendarz [87], F. Derue [128], P. Dervan [93], K. Desch [24], C. Deutsch [24], F.A. Di Bello [57b,57a], A. Di Ciaccio [76a,76b], L. Di Ciaccio [4], A. Di Domenico [75a,75b], C. Di Donato [72a,72b], A. Di Girolamo [36], G. Di Gregorio [36], A. Di Luca [78a,78b], B. Di Micco [77a,77b], R. Di Nardo [77a,77b], M. Diamantopoulou [34], F.A. Dias [115], T. Dias Do Vale [143], M.A. Diaz [138a,138b], F.G. Diaz Capriles [24], M. Didenko [164], E.B. Diehl [107], S. Díez Cornell [48], C. Diez Pardos [142], C. Dimitriadi [162,24], A. Dimitrievska [17a], J. Dingfelder [24], I-M. Dinu [27b], S.J. Dittmeier [63b], F. Dittus [36], M. Divisek [134], F. Djama [103], T. Djobava [150b], C. Doglioni [102,99], A. Dohnalova [28a], J. Dolejsi [134], Z. Dolezal [134], K.M. Dona [39], M. Donadelli [83c], B. Dong [108], J. Donini [40], A. D'Onofrio [72a,72b], M. D'Onofrio [93], J. Dopke [135], A. Doria [72a], N. Dos Santos Fernandes [131a], P. Dougan [102], M.T. Dova [91], A.T. Doyle [59], M.A. Draguet [127], E. Dreyer [170], I. Drivas-koulouris [10], M. Drnevich [118], M. Drozdova [56], D. Du [62a], T.A. du Pree [115], F. Dubinin [37], M. Dubovsky [28a], E. Duchovni [170], G. Duckeck [110], O.A. Ducu [27b], D. Duda [52], A. Dudarev [36], E.R. Duden [26], M. D'uffizi [102], L. Duflot [66], M. Dührssen [36], A.E. Dumitriu [27b], M. Dunford [63a], S. Dungs [49], K. Dunne [47a,47b], A. Duperrin [103], H. Duran Yildiz [3a], M. Düren [58], A. Durglishvili [150b], B.L. Dwyer [116], G.I. Dyckes [17a], M. Dyndal [86a], B.S. Dziedzic [87], Z.O. Earnshaw [147], G.H. Eberwein [127], B. Eckerova [28a], S. Eggebrecht [55], E. Egidio Purcino De Souza [128], L.F. Ehrke [56], G. Eigen [16], K. Einsweiler [17a], T. Ekelof [162], P.A. Ekman [99], S. El Farkh [35b], Y. El Ghazali [35b], H. El Jarrari [36], A. El Moussaouy [109], V. Ellajosyula [162], M. Ellert [162], F. Ellinghaus [172], N. Ellis [36], J. Elmsheuser [29], M. Elsing [36], D. Emeliyanov [135], Y. Enari [154], I. Ene [17a], S. Epari [13], P.A. Erland [87], M. Errenst [172], M. Escalier [66], C. Escobar [164], E. Etzion [152], G. Evans [131a], H. Evans [68], L.S. Evans [96], A. Ezhilov [37], S. Ezzarqtouni [35a], F. Fabbri [23b,23a], L. Fabbri [23b,23a], G. Facini [97], V. Fadeyev [137], R.M. Fakhrutdinov [37], D. Fakoudis [101], S. Falciano [75a], L.F. Falda Ulhoa Coelho [36], P.J. Falke [24], J. Faltova [134], C. Fan [163], Y. Fan [14a],

30

Y. Fang[14a,14e], M. Fanti[71a,71b], M. Faraj[69a,69b], Z. Farazpay[98], A. Farbin[8], A. Farilla[77a],
T. Farooque[108], S.M. Farrington[52], F. Fassi[35e], D. Fassouliotis[9], M. Faucci Giannelli[76a,76b],
W.J. Fawcett[32], L. Fayard[66], P. Federic[134], P. Federicova[132], O.L. Fedin[37,a], M. Feickert[171],
L. Feligioni[103], D.E. Fellers[124], C. Feng[62b], M. Feng[14b], Z. Feng[115], M.J. Fenton[160],
L. Ferencz[48], R.A.M. Ferguson[92], S.I. Fernandez Luengo[138f], P. Fernandez Martinez[13],
M.J.V. Fernoux[103], J. Ferrando[92], A. Ferrari[162], P. Ferrari[115,114], R. Ferrari[73a], D. Ferrere[56],
C. Ferretti[107], F. Fiedler[101], P. Fiedler[133], A. Filipčič[94], E.K. Filmer[1], F. Filthaut[114],
M.C.N. Fiolhais[131a,131c,c], L. Fiorini[164], W.C. Fisher[108], T. Fitschen[102], P.M. Fitzhugh[136],
I. Fleck[142], P. Fleischmann[107], T. Flick[172], M. Flores[33d,ac], L.R. Flores Castillo[64a],
L. Flores Sanz De Acedo[36], F.M. Follega[78a,78b], N. Fomin[16], J.H. Foo[156], A. Formica[136],
A.C. Forti[102], E. Fortin[36], A.W. Fortman[17a], M.G. Foti[17a], L. Fountas[9,j], D. Fournier[66],
H. Fox[92], P. Francavilla[74a,74b], S. Francescato[61], S. Franchellucci[56], M. Franchini[23b,23a],
S. Franchino[63a], D. Francis[36], L. Franco[114], V. Franco Lima[36], L. Franconi[48], M. Franklin[61],
G. Frattari[26], W.S. Freund[83b], Y.Y. Frid[152], J. Friend[59], N. Fritzsche[50], A. Froch[54],
D. Froidevaux[36], J.A. Frost[127], Y. Fu[62a], S. Fuenzalida Garrido[138f], M. Fujimoto[103],
K.Y. Fung[64a], E. Furtado De Simas Filho[83e], M. Furukawa[154], J. Fuster[164], A. Gabrielli[23b,23a],
A. Gabrielli[156], P. Gadow[36], G. Gagliardi[57b,57a], L.G. Gagnon[17a], S. Galantzan[152],
E.J. Gallas[127], B.J. Gallop[135], K.K. Gan[120], S. Ganguly[154], Y. Gao[52],
F.M. Garay Walls[138a,138b], B. Garcia[29], C. García[164], A. Garcia Alonso[115],
A.G. Garcia Caffaro[173], J.E. García Navarro[164], M. Garcia-Sciveres[17a], G.L. Gardner[129],
R.W. Gardner[39], N. Garelli[159], D. Garg[80], R.B. Garg[144,m], J.M. Gargan[52], C.A. Garner[156],
C.M. Garvey[33a], P. Gaspar[83b], V.K. Gassmann[159], G. Gaudio[73a], V. Gautam[13], P. Gauzzi[75a,75b],
I.L. Gavrilenko[37], A. Gavrilyuk[37], C. Gay[165], G. Gaycken[48], E.N. Gazis[10], A.A. Geanta[27b],
C.M. Gee[137], A. Gekow[120], C. Gemme[57b], M.H. Genest[60], A.D. Gentry[113], S. George[96],
W.F. George[20], T. Geralis[46], P. Gessinger-Befurt[36], M.E. Geyik[172], M. Ghani[168],
M. Ghneimat[142], K. Ghorbanian[95], A. Ghosal[142], A. Ghosh[160], A. Ghosh[7], B. Giacobbe[23b],
S. Giagu[75a,75b], T. Giani[115], P. Giannetti[74a], A. Giannini[62a], S.M. Gibson[96], M. Gignac[137],
D.T. Gil[86b], A.K. Gilbert[86a], B.J. Gilbert[41], D. Gillberg[34], G. Gilles[115], L. Ginabat[128],
D.M. Gingrich[2,af], M.P. Giordani[69a,69c], P.F. Giraud[136], G. Giugliarelli[69a,69c], D. Giugni[71a],
F. Giuli[36], I. Gkialas[9,j], L.K. Gladilin[37], C. Glasman[100], G.R. Gledhill[124], G. Glemža[48],
M. Glisic[124], I. Gnesi[43b,f], Y. Go[29], M. Goblirsch-Kolb[36], B. Gocke[49], D. Godin[109],
B. Gokturk[21a], S. Goldfarb[106], T. Golling[56], M.G.D. Gololo[33g], D. Golubkov[37],
J.P. Gombas[108], A. Gomes[131a,131b], G. Gomes Da Silva[142], A.J. Gomez Delegido[164],
R. Gonçalo[131a,131c], L. Gonella[20], A. Gongadze[150c], F. Gonnella[20], J.L. Gonski[144],
R.Y. González Andana[52], S. González de la Hoz[164], R. Gonzalez Lopez[93],
C. Gonzalez Renteria[17a], M.V. Gonzalez Rodrigues[48], R. Gonzalez Suarez[162],
S. Gonzalez-Sevilla[56], L. Goossens[36], B. Gorini[36], E. Gorini[70a,70b], A. Gorišek[94],
T.C. Gosart[129], A.T. Goshaw[51], M.I. Gostkin[38], S. Goswami[122], C.A. Gottardo[36],
S.A. Gotz[110], M. Gouighri[35b], V. Goumarre[48], A.G. Goussiou[139], N. Govender[33c],
I. Grabowska-Bold[86a], K. Graham[34], E. Gramstad[126], S. Grancagnolo[70a,70b], C.M. Grant[1,136],
P.M. Gravila[27f], F.G. Gravili[70a,70b], H.M. Gray[17a], M. Greco[70a,70b], C. Grefe[24],
I.M. Gregor[48], P. Grenier[144], S.G. Grewe[111], A.A. Grillo[137], K. Grimm[31], S. Grinstein[13,t],
J.-F. Grivaz[66], E. Gross[170], J. Grosse-Knetter[55], J.C. Grundy[127], L. Guan[107], C. Gubbels[165],
J.G.R. Guerrero Rojas[164], G. Guerrieri[69a,69c], F. Guescini[111], R. Gugel[101], J.A.M. Guhit[107],
A. Guida[18], E. Guilloton[168], S. Guindon[36], F. Guo[14a,14e], J. Guo[62c], L. Guo[48], Y. Guo[107],
R. Gupta[48], R. Gupta[130], S. Gurbuz[24], S.S. Gurdasani[54], G. Gustavino[36], M. Guth[56],
P. Gutierrez[121], L.F. Gutierrez Zagazeta[129], M. Gutsche[50], C. Gutschow[97], C. Gwenlan[127],

C.B. Gwilliam [93], E.S. Haaland [126], A. Haas [118], M. Habedank [48], C. Haber [17a],
H.K. Hadavand [8], A. Hadef [50], S. Hadzic [111], A.I. Hagan [92], J.J. Hahn [142], E.H. Haines [97],
M. Haleem [167], J. Haley [122], J.J. Hall [140], G.D. Hallewell [103], L. Halser [19], K. Hamano [166],
M. Hamer [24], G.N. Hamity [52], E.J. Hampshire [96], J. Han [62b], K. Han [62a], L. Han [14c],
L. Han [62a], S. Han [17a], Y.F. Han [156], K. Hanagaki [84], M. Hance [137], D.A. Hangal [41],
H. Hanif [143], M.D. Hank [129], J.B. Hansen [42], P.H. Hansen [42], K. Hara [158], D. Harada [56],
T. Harenberg [172], S. Harkusha [37], M.L. Harris [104], Y.T. Harris [127], J. Harrison [13],
N.M. Harrison [120], P.F. Harrison[168], N.M. Hartman [111], N.M. Hartmann [110], Y. Hasegawa [141],
R. Hauser [108], C.M. Hawkes [20], R.J. Hawkings [36], Y. Hayashi [154], S. Hayashida [112],
D. Hayden [108], C. Hayes [107], R.L. Hayes [115], C.P. Hays [127], J.M. Hays [95], H.S. Hayward [93],
F. He [62a], M. He [14a,14e], Y. He [155], Y. He [48], Y. He [97], N.B. Heatley [95], V. Hedberg [99],
A.L. Heggelund [126], N.D. Hehir [95,*], C. Heidegger [54], K.K. Heidegger [54], W.D. Heidorn [81],
J. Heilman [34], S. Heim [48], T. Heim [17a], J.G. Heinlein [129], J.J. Heinrich [124], L. Heinrich [111,ad],
J. Hejbal [132], A. Held [171], S. Hellesund [16], C.M. Helling [165], S. Hellman [47a,47b],
R.C.W. Henderson[92], L. Henkelmann [32], A.M. Henriques Correia[36], H. Herde [99],
Y. Hernández Jiménez [146], L.M. Herrmann [24], T. Herrmann [50], G. Herten [54], R. Hertenberger [110],
L. Hervas [36], M.E. Hesping [101], N.P. Hessey [157a], E. Hill [156], S.J. Hillier [20], J.R. Hinds [108],
F. Hinterkeuser [24], M. Hirose [125], S. Hirose [158], D. Hirschbuehl [172], T.G. Hitchings [102],
B. Hiti [94], J. Hobbs [146], R. Hobincu [27e], N. Hod [170], M.C. Hodgkinson [140],
B.H. Hodkinson [127], A. Hoecker [36], D.D. Hofer [107], J. Hofer [48], T. Holm [24], M. Holzbock [111],
L.B.A.H. Hommels [32], B.P. Honan [102], J. Hong [62c], T.M. Hong [130], B.H. Hooberman [163],
W.H. Hopkins [6], Y. Horii [112], S. Hou [149], A.S. Howard [94], J. Howarth [59], J. Hoya [6],
M. Hrabovsky [123], A. Hrynevich [48], T. Hryn'ova [4], P.J. Hsu [65], S.-C. Hsu [139], Q. Hu [62a],
S. Huang [64b], X. Huang [14a,14e], Y. Huang [140], Y. Huang [14a], Z. Huang [102], Z. Hubacek [133],
M. Huebner [24], F. Huegging [24], T.B. Huffman [127], C.A. Hugli [48], M. Huhtinen [36],
S.K. Huiberts [16], R. Hulsken [105], N. Huseynov [12], J. Huston [108], J. Huth [61], R. Hyneman [144],
G. Iacobucci [56], G. Iakovidis [29], I. Ibragimov [142], L. Iconomidou-Fayard [66], J.P. Iddon [36],
P. Iengo [72a,72b], R. Iguchi [154], T. Iizawa [127], Y. Ikegami [84], N. Ilic [156], H. Imam [35a],
M. Ince Lezki [56], T. Ingebretsen Carlson [47a,47b], G. Introzzi [73a,73b], M. Iodice [77a],
V. Ippolito [75a,75b], R.K. Irwin [93], M. Ishino [154], W. Islam [171], C. Issever [18,48], S. Istin [21a,aj],
H. Ito [169], R. Iuppa [78a,78b], A. Ivina [170], J.M. Izen [45], V. Izzo [72a], P. Jacka [132,133], P. Jackson [1],
B.P. Jaeger [143], C.S. Jagfeld [110], G. Jain [157a], P. Jain [54], K. Jakobs [54], T. Jakoubek [170],
J. Jamieson [59], K.W. Janas [86a], M. Javurkova [104], L. Jeanty [124], J. Jejelava [150a,aa], P. Jenni [54,g],
C.E. Jessiman [34], C. Jia [62b], J. Jia [146], X. Jia [61], X. Jia [14a,14e], Z. Jia [14c], S. Jiggins [48],
J. Jimenez Pena [13], S. Jin [14c], A. Jinaru [27b], O. Jinnouchi [155], P. Johansson [140], K.A. Johns [7],
J.W. Johnson [137], D.M. Jones [32], E. Jones [48], P. Jones [32], R.W.L. Jones [92], T.J. Jones [93],
H.L. Joos [55,36], R. Joshi [120], J. Jovicevic [15], X. Ju [17a], J.J. Junggeburth [104], T. Junkermann [63a],
A. Juste Rozas [13,t], M.K. Juzek [87], S. Kabana [138e], A. Kaczmarska [87], M. Kado [111],
H. Kagan [120], M. Kagan [144], A. Kahn[41], A. Kahn [129], C. Kahra [101], T. Kaji [154],
E. Kajomovitz [151], N. Kakati [170], I. Kalaitzidou [54], C.W. Kalderon [29], N.J. Kang [137],
D. Kar [33g], K. Karava [127], M.J. Kareem [157b], E. Karentzos [54], I. Karkanias [153], O. Karkout [115],
S.N. Karpov [38], Z.M. Karpova [38], V. Kartvelishvili [92], A.N. Karyukhin [37], E. Kasimi [153],
J. Katzy [48], S. Kaur [34], K. Kawade [141], M.P. Kawale [121], C. Kawamoto [88], T. Kawamoto [62a],
E.F. Kay [36], F.I. Kaya [159], S. Kazakos [108], V.F. Kazanin [37], Y. Ke [146], J.M. Keaveney [33a],
R. Keeler [166], G.V. Kehris [61], J.S. Keller [34], A.S. Kelly[97], J.J. Kempster [147], P.D. Kennedy [101],
O. Kepka [132], B.P. Kerridge [135], S. Kersten [172], B.P. Kerševan [94], L. Keszeghova [28a],
S. Ketabchi Haghighat [156], R.A. Khan [130], A. Khanov [122], A.G. Kharlamov [37], T. Kharlamova [37],

E.E. Khoda [139], M. Kholodenko [37], T.J. Khoo [18], G. Khoriauli [167], J. Khubua [150b,*],
Y.A.R. Khwaira [66], B. Kibirige [33g], A. Kilgallon [124], D.W. Kim [47a,47b], Y.K. Kim [39],
N. Kimura [97], M.K. Kingston [55], A. Kirchhoff [55], C. Kirfel [24], F. Kirfel [24], J. Kirk [135],
A.E. Kiryunin [111], C. Kitsaki [10], O. Kivernyk [24], M. Klassen [63a], C. Klein [34], L. Klein [167],
M.H. Klein [44], S.B. Klein [56], U. Klein [93], P. Klimek [36], A. Klimentov [29], T. Klioutchnikova [36],
P. Kluit [115], S. Kluth [111], E. Kneringer [79], T.M. Knight [156], A. Knue [49], R. Kobayashi [88],
D. Kobylianskii [170], S.F. Koch [127], M. Kocian [144], P. Kodyš [134], D.M. Koeck [124],
P.T. Koenig [24], T. Koffas [34], O. Kolay [50], I. Koletsou [4], T. Komarek [123], K. Köneke [54],
A.X.Y. Kong [1], T. Kono [119], N. Konstantinidis [97], P. Kontaxakis [56], B. Konya [99],
R. Kopeliansky [41], S. Koperny [86a], K. Korcyl [87], K. Kordas [153,e], A. Korn [97], S. Korn [55],
I. Korolkov [13], N. Korotkova [37], B. Kortman [115], O. Kortner [111], S. Kortner [111],
W.H. Kostecka [116], V.V. Kostyukhin [142], A. Kotsokechagia [136], A. Kotwal [51], A. Koulouris [36],
A. Kourkoumeli-Charalampidi [73a,73b], C. Kourkoumelis [9], E. Kourlitis [111,ad], O. Kovanda [124],
R. Kowalewski [166], W. Kozanecki [136], A.S. Kozhin [37], V.A. Kramarenko [37], G. Kramberger [94],
P. Kramer [101], M.W. Krasny [128], A. Krasznahorkay [36], J.W. Kraus [172], J.A. Kremer [48],
T. Kresse [50], J. Kretzschmar [93], K. Kreul [18], P. Krieger [156], S. Krishnamurthy [104],
M. Krivos [134], K. Krizka [20], K. Kroeninger [49], H. Kroha [111], J. Kroll [132], J. Kroll [129],
K.S. Krowpman [108], U. Kruchonak [38], H. Krüger [24], N. Krumnack [81], M.C. Kruse [51],
O. Kuchinskaia [37], S. Kuday [3a], S. Kuehn [36], R. Kuesters [54], T. Kuhl [48], V. Kukhtin [38],
Y. Kulchitsky [37,a], S. Kuleshov [138d,138b], M. Kumar [33g], N. Kumari [48], P. Kumari [157b],
A. Kupco [132], T. Kupfer [49], A. Kupich [37], O. Kuprash [54], H. Kurashige [85], L.L. Kurchaninov [157a],
O. Kurdysh [66], Y.A. Kurochkin [37], A. Kurova [37], M. Kuze [155], A.K. Kvam [104], J. Kvita [123],
T. Kwan [105], N.G. Kyriacou [107], L.A.O. Laatu [103], C. Lacasta [164], F. Lacava [75a,75b],
H. Lacker [18], D. Lacour [128], N.N. Lad [97], E. Ladygin [38], A. Lafarge [40], B. Laforge [128],
T. Lagouri [173], F.Z. Lahbabi [35a], S. Lai [55], I.K. Lakomiec [86a], N. Lalloue [60], J.E. Lambert [166],
S. Lammers [68], W. Lampl [7], C. Lampoudis [153,e], G. Lamprinoudis [101], A.N. Lancaster [116],
E. Lançon [29], U. Landgraf [54], M.P.J. Landon [95], V.S. Lang [54], O.K.B. Langrekken [126],
A.J. Lankford [160], F. Lanni [36], K. Lantzsch [24], A. Lanza [73a], A. Lapertosa [57b,57a],
J.F. Laporte [136], T. Lari [71a], F. Lasagni Manghi [23b], M. Lassnig [36], V. Latonova [132],
A. Laudrain [101], A. Laurier [151], S.D. Lawlor [140], Z. Lawrence [102], R. Lazaridou [168],
M. Lazzaroni [71a,71b], B. Le [102], E.M. Le Boulicaut [51], B. Leban [23b,23a], A. Lebedev [81],
M. LeBlanc [102], F. Ledroit-Guillon [60], A.C.A. Lee [97], S.C. Lee [149], S. Lee [47a,47b], T.F. Lee [93],
L.L. Leeuw [33c], H.P. Lefebvre [96], M. Lefebvre [166], C. Leggett [17a], G. Lehmann Miotto [36],
M. Leigh [56], W.A. Leight [104], W. Leinonen [114], A. Leisos [153,s], M.A.L. Leite [83c],
C.E. Leitgeb [18], R. Leitner [134], K.J.C. Leney [44], T. Lenz [24], S. Leone [74a], C. Leonidopoulos [52],
A. Leopold [145], C. Leroy [109], R. Les [108], C.G. Lester [32], M. Levchenko [37], J. Levêque [4],
L.J. Levinson [170], G. Levrini [23b,23a], M.P. Lewicki [87], D.J. Lewis [4], A. Li [5], B. Li [62b], C. Li [62a],
C-Q. Li [111], H. Li [62a], H. Li [62b], H. Li [14c], H. Li [14b], H. Li [62b], J. Li [62c], K. Li [139],
L. Li [62c], M. Li [14a,14e], Q.Y. Li [62a], S. Li [14a,14e], S. Li [62d,62c,d], T. Li [5], X. Li [105], Z. Li [127],
Z. Li [154], Z. Li [14a,14e], S. Liang [14a,14e], Z. Liang [14a], M. Liberatore [136], B. Liberti [76a],
K. Lie [64c], J. Lieber Marin [83b], H. Lien [68], K. Lin [108], R.E. Lindley [7], J.H. Lindon [2],
E. Lipeles [129], A. Lipniacka [16], A. Lister [165], J.D. Little [4], B. Liu [14a], B.X. Liu [143],
D. Liu [62d,62c], E.H.L. Liu [20], J.B. Liu [62a], J.K.K. Liu [32], K. Liu [62d], K. Liu [62d,62c], M. Liu [62a],
M.Y. Liu [62a], P. Liu [14a], Q. Liu [62d,139,62c], X. Liu [62a], X. Liu [62b], Y. Liu [14d,14e], Y.L. Liu [62b],
Y.W. Liu [62a], J. Llorente Merino [143], S.L. Lloyd [95], E.M. Lobodzinska [48], P. Loch [7],
T. Lohse [18], K. Lohwasser [140], E. Loiacono [48], M. Lokajicek [132,*], J.D. Lomas [20],
J.D. Long [163], I. Longarini [160], L. Longo [70a,70b], R. Longo [163], I. Lopez Paz [67],

A. Lopez Solis [48], N. Lorenzo Martinez [4], A.M. Lory [110], G. Löschcke Centeno [147],
O. Loseva [37], X. Lou [47a,47b], X. Lou [14a,14e], A. Lounis [66], P.A. Love [92], G. Lu [14a,14e],
M. Lu [80], S. Lu [129], Y.J. Lu [65], H.J. Lubatti [139], C. Luci [75a,75b], F.L. Lucio Alves [14c],
F. Luehring [68], I. Luise [146], O. Lukianchuk [66], O. Lundberg [145], B. Lund-Jensen [145,*],
N.A. Luongo [6], M.S. Lutz [36], A.B. Lux [25], D. Lynn [29], R. Lysak [132], E. Lytken [99],
V. Lyubushkin [38], T. Lyubushkina [38], M.M. Lyukova [146], H. Ma [29], K. Ma [62a], L.L. Ma [62b],
W. Ma [62a], Y. Ma [122], D.M. Mac Donell [166], G. Maccarrone [53], J.C. MacDonald [101],
P.C. Machado De Abreu Farias [83b], R. Madar [40], T. Madula [97], J. Maeda [85], T. Maeno [29],
H. Maguire [140], V. Maiboroda [136], A. Maio [131a,131b,131d], K. Maj [86a], O. Majersky [48],
S. Majewski [124], N. Makovec [66], V. Maksimovic [15], B. Malaescu [128], Pa. Malecki [87],
V.P. Maleev [37], F. Malek [60,n], M. Mali [94], D. Malito [96], U. Mallik [80,*], S. Maltezos [10],
S. Malyukov [38], J. Mamuzic [13], G. Mancini [53], M.N. Mancini [26], G. Manco [73a,73b],
J.P. Mandalia [95], I. Mandić [94], L. Manhaes de Andrade Filho [83a], I.M. Maniatis [170],
J. Manjarres Ramos [90], D.C. Mankad [170], A. Mann [110], S. Manzoni [36], L. Mao [62c],
X. Mapekula [33c], A. Marantis [153,s], G. Marchiori [5], M. Marcisovsky [132], C. Marcon [71a],
M. Marinescu [20], S. Marium [48], M. Marjanovic [121], M. Markovitch [66], E.J. Marshall [92],
Z. Marshall [17a], S. Marti-Garcia [164], T.A. Martin [168], V.J. Martin [52], B. Martin dit Latour [16],
L. Martinelli [75a,75b], M. Martinez [13,t], P. Martinez Agullo [164], V.I. Martinez Outschoorn [104],
P. Martinez Suarez [13], S. Martin-Haugh [135], G. Martinovicova [134], V.S. Martoiu [27b],
A.C. Martyniuk [97], A. Marzin [36], D. Mascione [78a,78b], L. Masetti [101], T. Mashimo [154],
J. Masik [102], A.L. Maslennikov [37], P. Massarotti [72a,72b], P. Mastrandrea [74a,74b],
A. Mastroberardino [43b,43a], T. Masubuchi [154], T. Mathisen [162], J. Matousek [134], N. Matsuzawa[154],
J. Maurer [27b], A.J. Maury [66], B. Maček [94], D.A. Maximov [37], R. Mazini [149], I. Maznas [116],
M. Mazza [108], S.M. Mazza [137], E. Mazzeo [71a,71b], C. Mc Ginn [29], J.P. Mc Gowan [166],
S.P. Mc Kee [107], C.C. McCracken [165], E.F. McDonald [106], A.E. McDougall [115],
J.A. Mcfayden [147], R.P. McGovern [129], G. Mchedlidze [150b], R.P. Mckenzie [33g],
T.C. Mclachlan [48], D.J. Mclaughlin [97], S.J. McMahon [135], C.M. Mcpartland [93],
R.A. McPherson [166,x], S. Mehlhase [110], A. Mehta [93], D. Melini [164], B.R. Mellado Garcia [33g],
A.H. Melo [55], F. Meloni [48], A.M. Mendes Jacques Da Costa [102], H.Y. Meng [156], L. Meng [92],
S. Menke [111], M. Mentink [36], E. Meoni [43b,43a], G. Mercado [116], C. Merlassino [69a,69c],
L. Merola [72a,72b], C. Meroni [71a,71b], J. Metcalfe [6], A.S. Mete [6], C. Meyer [68], J-P. Meyer [136],
R.P. Middleton [135], L. Mijović [52], G. Mikenberg [170], M. Mikestikova [132], M. Mikuž [94],
H. Mildner [101], A. Milic [36], D.W. Miller [39], E.H. Miller [144], L.S. Miller [34], A. Milov [170],
D.A. Milstead [47a,47b], T. Min [14c], A.A. Minaenko [37], I.A. Minashvili [150b], L. Mince [59],
A.I. Mincer [118], B. Mindur [86a], M. Mineev [38], Y. Mino [88], L.M. Mir [13], M. Miralles Lopez [59],
M. Mironova [17a], A. Mishima [154], M.C. Missio [114], A. Mitra [168], V.A. Mitsou [164],
Y. Mitsumori [112], O. Miu [156], P.S. Miyagawa [95], T. Mkrtchyan [63a], M. Mlinarevic [97],
T. Mlinarevic [97], M. Mlynarikova [36], S. Mobius [19], P. Mogg [110], M.H. Mohamed Farook [113],
A.F. Mohammed [14a,14e], S. Mohapatra [41], G. Mokgatitswane [33g], L. Moleri [170], B. Mondal [142],
S. Mondal [133], K. Mönig [48], E. Monnier [103], L. Monsonis Romero[164], J. Montejo Berlingen [13],
M. Montella [120], F. Montereali [77a,77b], F. Monticelli [91], S. Monzani [69a,69c], N. Morange [66],
A.L. Moreira De Carvalho [131a], M. Moreno Llácer [164], C. Moreno Martinez [56], P. Morettini [57b],
S. Morgenstern [36], M. Morii [61], M. Morinaga [154], F. Morodei [75a,75b], L. Morvaj [36],
P. Moschovakos [36], B. Moser [36], M. Mosidze [150b], T. Moskalets [54], P. Moskvitina [114],
J. Moss [31,k], A. Moussa [35d], E.J.W. Moyse [104], O. Mtintsilana [33g], S. Muanza [103],
J. Mueller [130], D. Muenstermann [92], R. Müller [19], G.A. Mullier [162], A.J. Mullin[32], J.J. Mullin[129],
D.P. Mungo [156], D. Munoz Perez [164], F.J. Munoz Sanchez [102], M. Murin [102], W.J. Murray [168,135],

M. Muškinja [94], C. Mwewa [29], A.G. Myagkov [37,a], A.J. Myers [8], G. Myers [107], M. Myska [133],
B.P. Nachman [17a], O. Nackenhorst [49], K. Nagai [127], K. Nagano [84], J.L. Nagle [29,ah], E. Nagy [103],
A.M. Nairz [36], Y. Nakahama [84], K. Nakamura [84], K. Nakkalil [5], H. Nanjo [125], R. Narayan [44],
E.A. Narayanan [113], I. Naryshkin [37], M. Naseri [34], S. Nasri [117b], C. Nass [24], G. Navarro [22a],
J. Navarro-Gonzalez [164], R. Nayak [152], A. Nayaz [18], P.Y. Nechaeva [37], F. Nechansky [48],
L. Nedic [127], T.J. Neep [20], A. Negri [73a,73b], M. Negrini [23b], C. Nellist [115], C. Nelson [105],
K. Nelson [107], S. Nemecek [132], M. Nessi [36,h], M.S. Neubauer [163], F. Neuhaus [101],
J. Neundorf [48], R. Newhouse [165], P.R. Newman [20], C.W. Ng [130], Y.W.Y. Ng [48], B. Ngair [117a],
H.D.N. Nguyen [109], R.B. Nickerson [127], R. Nicolaidou [136], J. Nielsen [137], M. Niemeyer [55],
J. Niermann [55], N. Nikiforou [36], V. Nikolaenko [37,a], I. Nikolic-Audit [128], K. Nikolopoulos [20],
P. Nilsson [29], I. Ninca [48], H.R. Nindhito [56], G. Ninio [152], A. Nisati [75a], N. Nishu [2],
R. Nisius [111], J-E. Nitschke [50], E.K. Nkadimeng [33g], T. Nobe [154], D.L. Noel [32],
T. Nommensen [148], M.B. Norfolk [140], R.R.B. Norisam [97], B.J. Norman [34], M. Noury [35a],
J. Novak [94], T. Novak [48], L. Novotny [133], R. Novotny [113], L. Nozka [123], K. Ntekas [160],
N.M.J. Nunes De Moura Junior [83b], J. Ocariz [128], A. Ochi [85], I. Ochoa [131a], S. Oerdek [48,u],
J.T. Offermann [39], A. Ogrodnik [134], A. Oh [102], C.C. Ohm [145], H. Oide [84], R. Oishi [154],
M.L. Ojeda [48], Y. Okumura [154], L.F. Oleiro Seabra [131a], S.A. Olivares Pino [138d],
D. Oliveira Damazio [29], D. Oliveira Goncalves [83a], J.L. Oliver [160], Ö.O. Öncel [54],
A.P. O'Neill [19], A. Onofre [131a,131e], P.U.E. Onyisi [11], M.J. Oreglia [39], G.E. Orellana [91],
D. Orestano [77a,77b], N. Orlando [13], R.S. Orr [156], V. O'Shea [59], L.M. Osojnak [129],
R. Ospanov [62a], G. Otero y Garzon [30], H. Otono [89], P.S. Ott [63a], G.J. Ottino [17a], M. Ouchrif [35d],
F. Ould-Saada [126], T. Ovsiannikova [139], M. Owen [59], R.E. Owen [135], K.Y. Oyulmaz [21a],
V.E. Ozcan [21a], F. Ozturk [87], N. Ozturk [8], S. Ozturk [82], H.A. Pacey [127], A. Pacheco Pages [13],
C. Padilla Aranda [13], G. Padovano [75a,75b], S. Pagan Griso [17a], G. Palacino [68], A. Palazzo [70a,70b],
J. Pampel [24], J. Pan [173], T. Pan [64a], D.K. Panchal [11], C.E. Pandini [115], J.G. Panduro Vazquez [96],
H.D. Pandya [1], H. Pang [14b], P. Pani [48], G. Panizzo [69a,69c], L. Panwar [128], L. Paolozzi [56],
S. Parajuli [163], A. Paramonov [6], C. Paraskevopoulos [53], D. Paredes Hernandez [64b],
A. Pareti [73a,73b], K.R. Park [41], T.H. Park [156], M.A. Parker [32], F. Parodi [57b,57a], E.W. Parrish [116],
V.A. Parrish [52], J.A. Parsons [41], U. Parzefall [54], B. Pascual Dias [109], L. Pascual Dominguez [152],
E. Pasqualucci [75a], S. Passaggio [57b], F. Pastore [96], P. Patel [87], U.M. Patel [51], J.R. Pater [102],
T. Pauly [36], C.I. Pazos [159], J. Pearkes [144], M. Pedersen [126], R. Pedro [131a], S.V. Peleganchuk [37],
O. Penc [36], E.A. Pender [52], G.D. Penn [173], K.E. Penski [110], M. Penzin [37], B.S. Peralva [83d],
A.P. Pereira Peixoto [139], L. Pereira Sanchez [144], D.V. Perepelitsa [29,ah], E. Perez Codina [157a],
M. Perganti [10], H. Pernegger [36], O. Perrin [40], K. Peters [48], R.F.Y. Peters [102], B.A. Petersen [36],
T.C. Petersen [42], E. Petit [103], V. Petousis [133], C. Petridou [153,e], T. Petru [134], A. Petrukhin [142],
M. Pettee [17a], N.E. Pettersson [36], A. Petukhov [37], K. Petukhova [134], R. Pezoa [138f],
L. Pezzotti [36], G. Pezzullo [173], T.M. Pham [171], T. Pham [106], P.W. Phillips [135], G. Piacquadio [146],
E. Pianori [17a], F. Piazza [124], R. Piegaia [30], D. Pietreanu [27b], A.D. Pilkington [102],
M. Pinamonti [69a,69c], J.L. Pinfold [2], B.C. Pinheiro Pereira [131a], A.E. Pinto Pinoargote [101,136],
L. Pintucci [69a,69c], K.M. Piper [147], A. Pirttikoski [56], D.A. Pizzi [34], L. Pizzimento [64b],
A. Pizzini [115], M.-A. Pleier [29], V. Plesanovs [54], V. Pleskot [134], E. Plotnikova [38], G. Poddar [95],
R. Poettgen [99], L. Poggioli [128], I. Pokharel [55], S. Polacek [134], G. Polesello [73a], A. Poley [143,157a],
A. Polini [23b], C.S. Pollard [168], Z.B. Pollock [120], E. Pompa Pacchi [75a,75b], D. Ponomarenko [114],
L. Pontecorvo [36], S. Popa [27a], G.A. Popeneciu [27d], A. Poreba [36], D.M. Portillo Quintero [157a],
S. Pospisil [133], M.A. Postill [140], P. Postolache [27c], K. Potamianos [168], P.A. Potepa [86a],
I.N. Potrap [38], C.J. Potter [32], H. Potti [1], J. Poveda [164], M.E. Pozo Astigarraga [36],
A. Prades Ibanez [164], J. Pretel [54], D. Price [102], M. Primavera [70a], M.A. Principe Martin [100],

R. Privara [123], T. Procter [59], M.L. Proffitt [139], N. Proklova [129], K. Prokofiev [64c], G. Proto [111], J. Proudfoot [6], M. Przybycien [86a], W.W. Przygoda [86b], A. Psallidas [46], J.E. Puddefoot [140], D. Pudzha [37], D. Pyatiizbyantseva [37], J. Qian [107], D. Qichen [102], Y. Qin [13], T. Qiu [52], A. Quadt [55], M. Queitsch-Maitland [102], G. Quetant [56], R.P. Quinn [165], G. Rabanal Bolanos [61], D. Rafanoharana [54], F. Ragusa [71a,71b], J.L. Rainbolt [39], J.A. Raine [56], S. Rajagopalan [29], E. Ramakoti [37], I.A. Ramirez-Berend [34], K. Ran [48,14e], N.P. Rapheeha [33g], H. Rasheed [27b], V. Raskina [128], D.F. Rassloff [63a], A. Rastogi [17a], S. Rave [101], B. Ravina [55], I. Ravinovich [170], M. Raymond [36], A.L. Read [126], N.P. Readioff [140], D.M. Rebuzzi [73a,73b], G. Redlinger [29], A.S. Reed [111], K. Reeves [26], J.A. Reidelsturz [172], D. Reikher [152], A. Rej [49], C. Rembser [36], M. Renda [27b], M.B. Rendel [111], F. Renner [48], A.G. Rennie [160], A.L. Rescia [48], S. Resconi [71a], M. Ressegotti [57b,57a], S. Rettie [36], J.G. Reyes Rivera [108], E. Reynolds [17a], O.L. Rezanova [37], P. Reznicek [134], H. Riani [35d], N. Ribaric [92], E. Ricci [78a,78b], R. Richter [111], S. Richter [47a,47b], E. Richter-Was [86b], M. Ridel [128], S. Ridouani [35d], P. Rieck [118], P. Riedler [36], E.M. Riefel [47a,47b], J.O. Rieger [115], M. Rijssenbeek [146], M. Rimoldi [36], L. Rinaldi [23b,23a], T.T. Rinn [29], M.P. Rinnagel [110], G. Ripellino [162], I. Riu [13], J.C. Rivera Vergara [166], F. Rizatdinova [122], E. Rizvi [95], B.R. Roberts [17a], S.H. Robertson [105,x], D. Robinson [32], C.M. Robles Gajardo [138f], M. Robles Manzano [101], A. Robson [59], A. Rocchi [76a,76b], C. Roda [74a,74b], S. Rodriguez Bosca [36], Y. Rodriguez Garcia [22a], A. Rodriguez Rodriguez [54], A.M. Rodríguez Vera [116], S. Roe[36], J.T. Roemer [160], A.R. Roepe-Gier [137], J. Roggel [172], O. Røhne [126], R.A. Rojas [104], C.P.A. Roland [128], J. Roloff [29], A. Romaniouk [37], E. Romano [73a,73b], M. Romano [23b], A.C. Romero Hernandez [163], N. Rompotis [93], L. Roos [128], S. Rosati [75a], B.J. Rosser [39], E. Rossi [127], E. Rossi [72a,72b], L.P. Rossi [61], L. Rossini [54], R. Rosten [120], M. Rotaru [27b], B. Rottler [54], C. Rougier [90], D. Rousseau [66], D. Rousso [32], A. Roy [163], S. Roy-Garand [156], A. Rozanov [103], Z.M.A. Rozario [59], Y. Rozen [151], A. Rubio Jimenez [164], A.J. Ruby [93], V.H. Ruelas Rivera [18], T.A. Ruggeri [1], A. Ruggiero [127], A. Ruiz-Martinez [164], A. Rummler [36], Z. Rurikova [54], N.A. Rusakovich [38], H.L. Russell [166], G. Russo [75a,75b], J.P. Rutherfoord [7], S. Rutherford Colmenares [32], K. Rybacki[92], M. Rybar [134], E.B. Rye [126], A. Ryzhov [44], J.A. Sabater Iglesias [56], P. Sabatini [164], H.F-W. Sadrozinski [137], F. Safai Tehrani [75a], B. Safarzadeh Samani [135], M. Safdari [144], S. Saha [1], M. Sahinsoy [111], A. Saibel [164], M. Saimpert [136], M. Saito [154], T. Saito [154], D. Salamani [36], A. Salnikov [144], J. Salt [164], A. Salvador Salas [152], D. Salvatore [43b,43a], F. Salvatore [147], A. Salzburger [36], D. Sammel [54], E. Sampson [92], D. Sampsonidis [153,e], D. Sampsonidou [124], J. Sánchez [164], V. Sanchez Sebastian [164], H. Sandaker [126], C.O. Sander [48], J.A. Sandesara [104], M. Sandhoff [172], C. Sandoval [22b], D.P.C. Sankey [135], T. Sano [88], A. Sansoni [53], L. Santi [75a,75b], C. Santoni [40], H. Santos [131a,131b], A. Santra [170], K.A. Saoucha [161], J.G. Saraiva [131a,131d], J. Sardain [7], O. Sasaki [84], K. Sato [158], C. Sauer[63b], F. Sauerburger [54], E. Sauvan [4], P. Savard [156,af], R. Sawada [154], C. Sawyer [135], L. Sawyer [98], I. Sayago Galvan[164], C. Sbarra [23b], A. Sbrizzi [23b,23a], T. Scanlon [97], J. Schaarschmidt [139], U. Schäfer [101], A.C. Schaffer [66,44], D. Schaile [110], R.D. Schamberger [146], C. Scharf [18], M.M. Schefer [19], V.A. Schegelsky [37], D. Scheirich [134], F. Schenck [18], M. Schernau [160], C. Scheulen [55], C. Schiavi [57b,57a], M. Schioppa [43b,43a], B. Schlag [144,m], K.E. Schleicher [54], S. Schlenker [36], J. Schmeing [172], M.A. Schmidt [172], K. Schmieden [101], C. Schmitt [101], N. Schmitt [101], S. Schmitt [48], L. Schoeffel [136], A. Schoening [63b], P.G. Scholer [34], E. Schopf [127], M. Schott [101], J. Schovancova [36], S. Schramm [56], T. Schroer [56], H-C. Schultz-Coulon [63a], M. Schumacher [54], B.A. Schumm [137], Ph. Schune [136], A.J. Schuy [139], H.R. Schwartz [137], A. Schwartzman [144], T.A. Schwarz [107], Ph. Schwemling [136], R. Schwienhorst [108], A. Sciandra [137], G. Sciolla [26], F. Scuri [74a], C.D. Sebastiani [93], K. Sedlaczek [116], P. Seema [18], S.C. Seidel [113], A. Seiden [137],

B.D. Seidlitz [41], C. Seitz [48], J.M. Seixas [83b], G. Sekhniaidze [72a], L. Selem [60],
N. Semprini-Cesari [23b,23a], D. Sengupta [56], V. Senthilkumar [164], L. Serin [66], L. Serkin [69a,69b],
M. Sessa [76a,76b], H. Severini [121], F. Sforza [57b,57a], A. Sfyrla [56], Q. Sha [14a], E. Shabalina [55],
R. Shaheen [145], J.D. Shahinian [129], D. Shaked Renous [170], L.Y. Shan [14a], M. Shapiro [17a],
A. Sharma [36], A.S. Sharma [165], P. Sharma [80], P.B. Shatalov [37], K. Shaw [147], S.M. Shaw [102],
A. Shcherbakova [37], Q. Shen [62c,5], D.J. Sheppard [143], P. Sherwood [97], L. Shi [97], X. Shi [14a],
C.O. Shimmin [173], J.D. Shinner [96], I.P.J. Shipsey [127], S. Shirabe [89], M. Shiyakova [38,v],
J. Shlomi [170], M.J. Shochet [39], J. Shojaii [106], D.R. Shope [126], B. Shrestha [121], S. Shrestha [120,ai],
E.M. Shrif [33g], M.J. Shroff [166], P. Sicho [132], A.M. Sickles [163], E. Sideras Haddad [33g],
A. Sidoti [23b], F. Siegert [50], Dj. Sijacki [15], F. Sili [91], J.M. Silva [52], M.V. Silva Oliveira [29],
S.B. Silverstein [47a], S. Simion [66], R. Simoniello [36], E.L. Simpson [59], H. Simpson [147],
L.R. Simpson [107], N.D. Simpson [99], S. Simsek [82], S. Sindhu [55], P. Sinervo [156], S. Singh [156],
S. Sinha [48], S. Sinha [102], M. Sioli [23b,23a], I. Siral [36], E. Sitnikova [48], J. Sjölin [47a,47b],
A. Skaf [55], E. Skorda [20], P. Skubic [121], M. Slawinska [87], V. Smakhtin [170], B.H. Smart [135],
S.Yu. Smirnov [37], Y. Smirnov [37], L.N. Smirnova [37,a], O. Smirnova [99], A.C. Smith [41],
E.A. Smith [39], H.A. Smith [127], J.L. Smith [102], R. Smith [144], M. Smizanska [92], K. Smolek [133],
A.A. Snesarev [37], S.R. Snider [156], H.L. Snoek [115], S. Snyder [29], R. Sobie [166,x], A. Soffer [152],
C.A. Solans Sanchez [36], E.Yu. Soldatov [37], U. Soldevila [164], A.A. Solodkov [37], S. Solomon [26],
A. Soloshenko [38], K. Solovieva [54], O.V. Solovyanov [40], V. Solovyev [37], P. Sommer [36],
A. Sonay [13], W.Y. Song [157b], A. Sopczak [133], A.L. Sopio [97], F. Sopkova [28b], J.D. Sorenson [113],
I.R. Sotarriva Alvarez [155], V. Sothilingam [63a], O.J. Soto Sandoval [138c,138b], S. Sottocornola [68],
R. Soualah [161], Z. Soumaimi [35e], D. South [48], N. Soybelman [170], S. Spagnolo [70a,70b],
M. Spalla [111], D. Sperlich [54], G. Spigo [36], S. Spinali [92], D.P. Spiteri [59], M. Spousta [134],
E.J. Staats [34], R. Stamen [63a], A. Stampekis [20], M. Standke [24], E. Stanecka [87], M.V. Stange [50],
B. Stanislaus [17a], M.M. Stanitzki [48], B. Stapf [48], E.A. Starchenko [37], G.H. Stark [137], J. Stark [90],
P. Staroba [132], P. Starovoitov [63a], S. Stärz [105], R. Staszewski [87], G. Stavropoulos [46],
J. Steentoft [162], P. Steinberg [29], B. Stelzer [143,157a], H.J. Stelzer [130], O. Stelzer-Chilton [157a],
H. Stenzel [58], T.J. Stevenson [147], G.A. Stewart [36], J.R. Stewart [122], M.C. Stockton [36],
G. Stoicea [27b], M. Stolarski [131a], S. Stonjek [111], A. Straessner [50], J. Strandberg [145],
S. Strandberg [47a,47b], M. Stratmann [172], M. Strauss [121], T. Strebler [103], P. Strizenec [28b],
R. Ströhmer [167], D.M. Strom [124], R. Stroynowski [44], A. Strubig [47a,47b], S.A. Stucci [29],
B. Stugu [16], J. Stupak [121], N.A. Styles [48], D. Su [144], S. Su [62a], W. Su [62d], X. Su [62a],
D. Suchy [28a], K. Sugizaki [154], V.V. Sulin [37], M.J. Sullivan [93], D.M.S. Sultan [127],
L. Sultanaliyeva [37], S. Sultansoy [3b], T. Sumida [88], S. Sun [107], S. Sun [171],
O. Sunneborn Gudnadottir [162], N. Sur [103], M.R. Sutton [147], H. Suzuki [158], M. Svatos [132],
M. Swiatlowski [157a], T. Swirski [167], I. Sykora [28a], M. Sykora [134], T. Sykora [134], D. Ta [101],
K. Tackmann [48,u], A. Taffard [160], R. Tafirout [157a], J.S. Tafoya Vargas [66], Y. Takubo [84],
M. Talby [103], A.A. Talyshev [37], K.C. Tam [64b], N.M. Tamir [152], A. Tanaka [154], J. Tanaka [154],
R. Tanaka [66], M. Tanasini [57b,57a], Z. Tao [165], S. Tapia Araya [138f], S. Tapprogge [101],
A. Tarek Abouelfadl Mohamed [108], S. Tarem [151], K. Tariq [14a], G. Tarna [103,27b], G.F. Tartarelli [71a],
P. Tas [134], M. Tasevsky [132], E. Tassi [43b,43a], A.C. Tate [163], G. Tateno [154], Y. Tayalati [35e,w],
G.N. Taylor [106], W. Taylor [157b], A.S. Tee [171], R. Teixeira De Lima [144], P. Teixeira-Dias [96],
J.J. Teoh [156], K. Terashi [154], J. Terron [100], S. Terzo [13], M. Testa [53], R.J. Teuscher [156,x],
A. Thaler [79], O. Theiner [56], N. Themistokleous [52], T. Theveneaux-Pelzer [103], O. Thielmann [172],
D.W. Thomas [96], J.P. Thomas [20], E.A. Thompson [17a], P.D. Thompson [20], E. Thomson [129],
R.E. Thornberry [44], Y. Tian [55], V. Tikhomirov [37,a], Yu.A. Tikhonov [37], S. Timoshenko [37],
D. Timoshyn [134], E.X.L. Ting [1], P. Tipton [173], S.H. Tlou [33g], K. Todome [155],

S. Todorova-Nova [134], S. Todt[50], M. Togawa [84], J. Tojo [89], S. Tokár [28a], K. Tokushuku [84],
O. Toldaiev [68], R. Tombs [32], M. Tomoto [84,112], L. Tompkins [144,m], K.W. Topolnicki [86b],
E. Torrence [124], H. Torres [90], E. Torró Pastor [164], M. Toscani [30], C. Tosciri [39], M. Tost [11],
D.R. Tovey [140], A. Traeet[16], I.S. Trandafir [27b], T. Trefzger [167], A. Tricoli [29], I.M. Trigger [157a],
S. Trincaz-Duvoid [128], D.A. Trischuk [26], B. Trocmé [60], L. Truong [33c], M. Trzebinski [87],
A. Trzupek [87], F. Tsai [146], M. Tsai [107], A. Tsiamis [153,e], P.V. Tsiareshka[37], S. Tsigaridas [157a],
A. Tsirigotis [153,s], V. Tsiskaridze [156], E.G. Tskhadadze [150a], M. Tsopoulou [153], Y. Tsujikawa [88],
I.I. Tsukerman [37], V. Tsulaia [17a], S. Tsuno [84], K. Tsuri [119], D. Tsybychev [146], Y. Tu [64b],
A. Tudorache [27b], V. Tudorache [27b], A.N. Tuna [61], S. Turchikhin [57b,57a], I. Turk Cakir [3a],
R. Turra [71a], T. Turtuvshin [38,y], P.M. Tuts [41], S. Tzamarias [153,e], E. Tzovara [101], F. Ukegawa [158],
P.A. Ulloa Poblete [138c,138b], E.N. Umaka [29], G. Unal [36], A. Undrus [29], G. Unel [160], J. Urban [28b],
P. Urquijo [106], P. Urrejola [138a], G. Usai [8], R. Ushioda [155], M. Usman [109], Z. Uysal [82],
V. Vacek [133], B. Vachon [105], K.O.H. Vadla [126], T. Vafeiadis [36], A. Vaitkus [97], C. Valderanis [110],
E. Valdes Santurio [47a,47b], M. Valente [157a], S. Valentinetti [23b,23a], A. Valero [164],
E. Valiente Moreno [164], A. Vallier [90], J.A. Valls Ferrer [164], D.R. Van Arneman [115],
T.R. Van Daalen [139], A. Van Der Graaf [49], P. Van Gemmeren [6], M. Van Rijnbach [126],
S. Van Stroud [97], I. Van Vulpen [115], P. Vana [134], M. Vanadia [76a,76b], W. Vandelli [36],
E.R. Vandewall [122], D. Vannicola [152], L. Vannoli [53], R. Vari [75a], E.W. Varnes [7], C. Varni [17b],
T. Varol [149], D. Varouchas [66], L. Varriale [164], K.E. Varvell [148], M.E. Vasile [27b], L. Vaslin[84],
G.A. Vasquez [166], A. Vasyukov [38], R. Vavricka[101], F. Vazeille [40], T. Vazquez Schroeder [36],
J. Veatch [31], V. Vecchio [102], M.J. Veen [104], I. Veliscek [29], L.M. Veloce [156], F. Veloso [131a,131c],
S. Veneziano [75a], A. Ventura [70a,70b], S. Ventura Gonzalez [136], A. Verbytskyi [111],
M. Verducci [74a,74b], C. Vergis [24], M. Verissimo De Araujo [83b], W. Verkerke [115],
J.C. Vermeulen [115], C. Vernieri [144], M. Vessella [104], M.C. Vetterli [143,af], A. Vgenopoulos [153,e],
N. Viaux Maira [138f], T. Vickey [140], O.E. Vickey Boeriu [140], G.H.A. Viehhauser [127], L. Vigani [63b],
M. Villa [23b,23a], M. Villaplana Perez [164], E.M. Villhauer[52], E. Vilucchi [53], M.G. Vincter [34],
G.S. Virdee [20], A. Vishwakarma [52], A. Visibile[115], C. Vittori [36], I. Vivarelli [23b,23a],
E. Voevodina [111], F. Vogel [110], J.C. Voigt [50], P. Vokac [133], Yu. Volkotrub [86b], J. Von Ahnen [48],
E. Von Toerne [24], B. Vormwald [36], V. Vorobel [134], K. Vorobev [37], M. Vos [164], K. Voss [142],
M. Vozak [115], L. Vozdecky [121], N. Vranjes [15], M. Vranjes Milosavljevic [15], M. Vreeswijk [115],
N.K. Vu [62d,62c], R. Vuillermet [36], O. Vujinovic [101], I. Vukotic [39], S. Wada [158], C. Wagner[104],
J.M. Wagner [17a], W. Wagner [172], S. Wahdan [172], H. Wahlberg [91], M. Wakida [112], J. Walder [135],
R. Walker [110], W. Walkowiak [142], A. Wall [129], E.J. Wallin [99], T. Wamorkar [6], A.Z. Wang [137],
C. Wang [101], C. Wang [11], H. Wang [17a], J. Wang [64c], R.-J. Wang [101], R. Wang [61], R. Wang [6],
S.M. Wang [149], S. Wang [62b], T. Wang [62a], W.T. Wang [80], W. Wang [14a], X. Wang [14c],
X. Wang [163], X. Wang [62c], Y. Wang [62d], Y. Wang [14c], Z. Wang [107], Z. Wang [62d,51,62c],
Z. Wang [107], A. Warburton [105], R.J. Ward [20], N. Warrack [59], S. Waterhouse [96], A.T. Watson [20],
H. Watson [59], M.F. Watson [20], E. Watton [59,135], G. Watts [139], B.M. Waugh [97], C. Weber [29],
H.A. Weber [18], M.S. Weber [19], S.M. Weber [63a], C. Wei [62a], Y. Wei [127], A.R. Weidberg [127],
E.J. Weik [118], J. Weingarten [49], M. Weirich [101], C. Weiser [54], C.J. Wells [48], T. Wenaus [29],
B. Wendland [49], T. Wengler [36], N.S. Wenke[111], N. Wermes [24], M. Wessels [63a], A.M. Wharton [92],
A.S. White [61], A. White [8], M.J. White [1], D. Whiteson [160], L. Wickremasinghe [125],
W. Wiedenmann [171], M. Wielers [135], C. Wiglesworth [42], D.J. Wilbern[121], H.G. Wilkens [36],
D.M. Williams [41], H.H. Williams[129], S. Williams [32], S. Willocq [104], B.J. Wilson [102],
P.J. Windischhofer [39], F.I. Winkel [30], F. Winklmeier [124], B.T. Winter [54], J.K. Winter [102],
M. Wittgen[144], M. Wobisch [98], Z. Wolffs [115], J. Wollrath[160], M.W. Wolter [87], H. Wolters [131a,131c],
M.C. Wong [137], E.L. Woodward [41], S.D. Worm [48], B.K. Wosiek [87], K.W. Woźniak [87],

38

S. Wozniewski [55], K. Wraight [59], C. Wu [20], M. Wu [14d], M. Wu [114], S.L. Wu [171], X. Wu [56],
Y. Wu [62a], Z. Wu [4], J. Wuerzinger [111,ad], T.R. Wyatt [102], B.M. Wynne [52], S. Xella [42],
L. Xia [14c], M. Xia [14b], J. Xiang [64c], M. Xie [62a], X. Xie [62a], S. Xin [14a,14e], A. Xiong [124],
J. Xiong [17a], D. Xu [14a], H. Xu [62a], L. Xu [62a], R. Xu [129], T. Xu [107], Y. Xu [14b], Z. Xu [52],
Z. Xu [14c], B. Yabsley [148], S. Yacoob [33a], Y. Yamaguchi [155], E. Yamashita [154], H. Yamauchi [158],
T. Yamazaki [17a], Y. Yamazaki [85], J. Yan [62c], S. Yan [59], Z. Yan [104], H.J. Yang [62c,62d],
H.T. Yang [62a], S. Yang [62a], T. Yang [64c], X. Yang [36], X. Yang [14a], Y. Yang [44], Y. Yang [62a],
Z. Yang [62a], W-M. Yao [17a], H. Ye [14c], H. Ye [55], J. Ye [14a], S. Ye [29], X. Ye [62a], Y. Yeh [97],
I. Yeletskikh [38], B. Yeo [17b], M.R. Yexley [97], P. Yin [41], K. Yorita [169], S. Younas [27b],
C.J.S. Young [36], C. Young [144], C. Yu [14a,14e], Y. Yu [62a], M. Yuan [107], R. Yuan [62b], L. Yue [97],
M. Zaazoua [62a], B. Zabinski [87], E. Zaid[52], Z.K. Zak [87], T. Zakareishvili [164], N. Zakharchuk [34],
S. Zambito [56], J.A. Zamora Saa [138d,138b], J. Zang [154], D. Zanzi [54], O. Zaplatilek [133],
C. Zeitnitz [172], H. Zeng [14a], J.C. Zeng [163], D.T. Zenger Jr [26], O. Zenin [37], T. Ženiš [28a],
S. Zenz [95], S. Zerradi [35a], D. Zerwas [66], M. Zhai [14a,14e], D.F. Zhang [140], J. Zhang [62b],
J. Zhang [6], K. Zhang [14a,14e], L. Zhang [14c], P. Zhang [14a,14e], R. Zhang [171], S. Zhang [107],
S. Zhang [44], T. Zhang [154], X. Zhang [62c], X. Zhang [62b], Y. Zhang [62c,5], Y. Zhang [97],
Y. Zhang [14c], Z. Zhang [17a], Z. Zhang [66], H. Zhao [139], T. Zhao [62b], Y. Zhao [137], Z. Zhao [62a],
A. Zhemchugov [38], J. Zheng [14c], K. Zheng [163], X. Zheng [62a], Z. Zheng [144], D. Zhong [163],
B. Zhou [107], H. Zhou [7], N. Zhou [62c], Y. Zhou [14c], Y. Zhou[7], C.G. Zhu [62b], J. Zhu [107],
Y. Zhu [62c], Y. Zhu [62a], X. Zhuang [14a], K. Zhukov [37], N.I. Zimine [38], J. Zinsser [63b],
M. Ziolkowski [142], L. Živković [15], A. Zoccoli [23b,23a], K. Zoch [61], T.G. Zorbas [140],
O. Zormpa [46], W. Zou [41], L. Zwalinski [36].

[1]Department of Physics, University of Adelaide, Adelaide; Australia.

[2]Department of Physics, University of Alberta, Edmonton AB; Canada.

[3][(a)]Department of Physics, Ankara University, Ankara;[(b)]Division of Physics, TOBB University of Economics and Technology, Ankara; Türkiye.

[4]LAPP, Université Savoie Mont Blanc, CNRS/IN2P3, Annecy; France.

[5]APC, Université Paris Cité, CNRS/IN2P3, Paris; France.

[6]High Energy Physics Division, Argonne National Laboratory, Argonne IL; United States of America.

[7]Department of Physics, University of Arizona, Tucson AZ; United States of America.

[8]Department of Physics, University of Texas at Arlington, Arlington TX; United States of America.

[9]Physics Department, National and Kapodistrian University of Athens, Athens; Greece.

[10]Physics Department, National Technical University of Athens, Zografou; Greece.

[11]Department of Physics, University of Texas at Austin, Austin TX; United States of America.

[12]Institute of Physics, Azerbaijan Academy of Sciences, Baku; Azerbaijan.

[13]Institut de Física d'Altes Energies (IFAE), Barcelona Institute of Science and Technology, Barcelona; Spain.

[14][(a)]Institute of High Energy Physics, Chinese Academy of Sciences, Beijing;[(b)]Physics Department, Tsinghua University, Beijing;[(c)]Department of Physics, Nanjing University, Nanjing;[(d)]School of Science, Shenzhen Campus of Sun Yat-sen University;[(e)]University of Chinese Academy of Science (UCAS), Beijing; China.

[15]Institute of Physics, University of Belgrade, Belgrade; Serbia.

[16]Department for Physics and Technology, University of Bergen, Bergen; Norway.

[17][(a)]Physics Division, Lawrence Berkeley National Laboratory, Berkeley CA;[(b)]University of California, Berkeley CA; United States of America.

[18]Institut für Physik, Humboldt Universität zu Berlin, Berlin; Germany.

[19]Albert Einstein Center for Fundamental Physics and Laboratory for High Energy Physics, University of Bern, Bern; Switzerland.

[20]School of Physics and Astronomy, University of Birmingham, Birmingham; United Kingdom.

[21][a]Department of Physics, Bogazici University, Istanbul;[b]Department of Physics Engineering, Gaziantep University, Gaziantep;[c]Department of Physics, Istanbul University, Istanbul; Türkiye.

[22][a]Facultad de Ciencias y Centro de Investigaciónes, Universidad Antonio Nariño, Bogotá;[b]Departamento de Física, Universidad Nacional de Colombia, Bogotá; Colombia.

[23][a]Dipartimento di Fisica e Astronomia A. Righi, Università di Bologna, Bologna;[b]INFN Sezione di Bologna; Italy.

[24]Physikalisches Institut, Universität Bonn, Bonn; Germany.

[25]Department of Physics, Boston University, Boston MA; United States of America.

[26]Department of Physics, Brandeis University, Waltham MA; United States of America.

[27][a]Transilvania University of Brasov, Brasov;[b]Horia Hulubei National Institute of Physics and Nuclear Engineering, Bucharest;[c]Department of Physics, Alexandru Ioan Cuza University of Iasi, Iasi;[d]National Institute for Research and Development of Isotopic and Molecular Technologies, Physics Department, Cluj-Napoca;[e]National University of Science and Technology Politechnica, Bucharest;[f]West University in Timisoara, Timisoara;[g]Faculty of Physics, University of Bucharest, Bucharest; Romania.

[28][a]Faculty of Mathematics, Physics and Informatics, Comenius University, Bratislava;[b]Department of Subnuclear Physics, Institute of Experimental Physics of the Slovak Academy of Sciences, Kosice; Slovak Republic.

[29]Physics Department, Brookhaven National Laboratory, Upton NY; United States of America.

[30]Universidad de Buenos Aires, Facultad de Ciencias Exactas y Naturales, Departamento de Física, y CONICET, Instituto de Física de Buenos Aires (IFIBA), Buenos Aires; Argentina.

[31]California State University, CA; United States of America.

[32]Cavendish Laboratory, University of Cambridge, Cambridge; United Kingdom.

[33][a]Department of Physics, University of Cape Town, Cape Town;[b]iThemba Labs, Western Cape;[c]Department of Mechanical Engineering Science, University of Johannesburg, Johannesburg;[d]National Institute of Physics, University of the Philippines Diliman (Philippines);[e]University of South Africa, Department of Physics, Pretoria;[f]University of Zululand, KwaDlangezwa;[g]School of Physics, University of the Witwatersrand, Johannesburg; South Africa.

[34]Department of Physics, Carleton University, Ottawa ON; Canada.

[35][a]Faculté des Sciences Ain Chock, Université Hassan II de Casablanca;[b]Faculté des Sciences, Université Ibn-Tofail, Kénitra;[c]Faculté des Sciences Semlalia, Université Cadi Ayyad, LPHEA-Marrakech;[d]LPMR, Faculté des Sciences, Université Mohamed Premier, Oujda;[e]Faculté des sciences, Université Mohammed V, Rabat;[f]Institute of Applied Physics, Mohammed VI Polytechnic University, Ben Guerir; Morocco.

[36]CERN, Geneva; Switzerland.

[37]Affiliated with an institute covered by a cooperation agreement with CERN.

[38]Affiliated with an international laboratory covered by a cooperation agreement with CERN.

[39]Enrico Fermi Institute, University of Chicago, Chicago IL; United States of America.

[40]LPC, Université Clermont Auvergne, CNRS/IN2P3, Clermont-Ferrand; France.

[41]Nevis Laboratory, Columbia University, Irvington NY; United States of America.

[42]Niels Bohr Institute, University of Copenhagen, Copenhagen; Denmark.

[43][a]Dipartimento di Fisica, Università della Calabria, Rende;[b]INFN Gruppo Collegato di Cosenza, Laboratori Nazionali di Frascati; Italy.

[44]Physics Department, Southern Methodist University, Dallas TX; United States of America.

[45]Physics Department, University of Texas at Dallas, Richardson TX; United States of America.

[46]National Centre for Scientific Research "Demokritos", Agia Paraskevi; Greece.

[47][(a)]Department of Physics, Stockholm University;[(b)]Oskar Klein Centre, Stockholm; Sweden.

[48]Deutsches Elektronen-Synchrotron DESY, Hamburg and Zeuthen; Germany.

[49]Fakultät Physik , Technische Universität Dortmund, Dortmund; Germany.

[50]Institut für Kern- und Teilchenphysik, Technische Universität Dresden, Dresden; Germany.

[51]Department of Physics, Duke University, Durham NC; United States of America.

[52]SUPA - School of Physics and Astronomy, University of Edinburgh, Edinburgh; United Kingdom.

[53]INFN e Laboratori Nazionali di Frascati, Frascati; Italy.

[54]Physikalisches Institut, Albert-Ludwigs-Universität Freiburg, Freiburg; Germany.

[55]II. Physikalisches Institut, Georg-August-Universität Göttingen, Göttingen; Germany.

[56]Département de Physique Nucléaire et Corpusculaire, Université de Genève, Genève; Switzerland.

[57][(a)]Dipartimento di Fisica, Università di Genova, Genova;[(b)]INFN Sezione di Genova; Italy.

[58]II. Physikalisches Institut, Justus-Liebig-Universität Giessen, Giessen; Germany.

[59]SUPA - School of Physics and Astronomy, University of Glasgow, Glasgow; United Kingdom.

[60]LPSC, Université Grenoble Alpes, CNRS/IN2P3, Grenoble INP, Grenoble; France.

[61]Laboratory for Particle Physics and Cosmology, Harvard University, Cambridge MA; United States of America.

[62][(a)]Department of Modern Physics and State Key Laboratory of Particle Detection and Electronics, University of Science and Technology of China, Hefei;[(b)]Institute of Frontier and Interdisciplinary Science and Key Laboratory of Particle Physics and Particle Irradiation (MOE), Shandong University, Qingdao;[(c)]School of Physics and Astronomy, Shanghai Jiao Tong University, Key Laboratory for Particle Astrophysics and Cosmology (MOE), SKLPPC, Shanghai;[(d)]Tsung-Dao Lee Institute, Shanghai;[(e)]School of Physics and Microelectronics, Zhengzhou University; China.

[63][(a)]Kirchhoff-Institut für Physik, Ruprecht-Karls-Universität Heidelberg, Heidelberg;[(b)]Physikalisches Institut, Ruprecht-Karls-Universität Heidelberg, Heidelberg; Germany.

[64][(a)]Department of Physics, Chinese University of Hong Kong, Shatin, N.T., Hong Kong;[(b)]Department of Physics, University of Hong Kong, Hong Kong;[(c)]Department of Physics and Institute for Advanced Study, Hong Kong University of Science and Technology, Clear Water Bay, Kowloon, Hong Kong; China.

[65]Department of Physics, National Tsing Hua University, Hsinchu; Taiwan.

[66]IJCLab, Université Paris-Saclay, CNRS/IN2P3, 91405, Orsay; France.

[67]Centro Nacional de Microelectrónica (IMB-CNM-CSIC), Barcelona; Spain.

[68]Department of Physics, Indiana University, Bloomington IN; United States of America.

[69][(a)]INFN Gruppo Collegato di Udine, Sezione di Trieste, Udine;[(b)]ICTP, Trieste;[(c)]Dipartimento Politecnico di Ingegneria e Architettura, Università di Udine, Udine; Italy.

[70][(a)]INFN Sezione di Lecce;[(b)]Dipartimento di Matematica e Fisica, Università del Salento, Lecce; Italy.

[71][(a)]INFN Sezione di Milano;[(b)]Dipartimento di Fisica, Università di Milano, Milano; Italy.

[72][(a)]INFN Sezione di Napoli;[(b)]Dipartimento di Fisica, Università di Napoli, Napoli; Italy.

[73][(a)]INFN Sezione di Pavia;[(b)]Dipartimento di Fisica, Università di Pavia, Pavia; Italy.

[74][(a)]INFN Sezione di Pisa;[(b)]Dipartimento di Fisica E. Fermi, Università di Pisa, Pisa; Italy.

[75][(a)]INFN Sezione di Roma;[(b)]Dipartimento di Fisica, Sapienza Università di Roma, Roma; Italy.

[76][(a)]INFN Sezione di Roma Tor Vergata;[(b)]Dipartimento di Fisica, Università di Roma Tor Vergata, Roma; Italy.

[77][(a)]INFN Sezione di Roma Tre;[(b)]Dipartimento di Matematica e Fisica, Università Roma Tre, Roma; Italy.

[78][(a)]INFN-TIFPA;[(b)]Università degli Studi di Trento, Trento; Italy.

[79]Universität Innsbruck, Department of Astro and Particle Physics, Innsbruck; Austria.

[80]University of Iowa, Iowa City IA; United States of America.

[81]Department of Physics and Astronomy, Iowa State University, Ames IA; United States of America.

[82]Istinye University, Sariyer, Istanbul; Türkiye.

[83][(a)]Departamento de Engenharia Elétrica, Universidade Federal de Juiz de Fora (UFJF), Juiz de Fora;[(b)]Universidade Federal do Rio De Janeiro COPPE/EE/IF, Rio de Janeiro;[(c)]Instituto de Física, Universidade de São Paulo, São Paulo;[(d)]Rio de Janeiro State University, Rio de Janeiro;[(e)]Federal University of Bahia, Bahia; Brazil.

[84]KEK, High Energy Accelerator Research Organization, Tsukuba; Japan.

[85]Graduate School of Science, Kobe University, Kobe; Japan.

[86][(a)]AGH University of Krakow, Faculty of Physics and Applied Computer Science, Krakow;[(b)]Marian Smoluchowski Institute of Physics, Jagiellonian University, Krakow; Poland.

[87]Institute of Nuclear Physics Polish Academy of Sciences, Krakow; Poland.

[88]Faculty of Science, Kyoto University, Kyoto; Japan.

[89]Research Center for Advanced Particle Physics and Department of Physics, Kyushu University, Fukuoka ; Japan.

[90]L2IT, Université de Toulouse, CNRS/IN2P3, UPS, Toulouse; France.

[91]Instituto de Física La Plata, Universidad Nacional de La Plata and CONICET, La Plata; Argentina.

[92]Physics Department, Lancaster University, Lancaster; United Kingdom.

[93]Oliver Lodge Laboratory, University of Liverpool, Liverpool; United Kingdom.

[94]Department of Experimental Particle Physics, Jožef Stefan Institute and Department of Physics, University of Ljubljana, Ljubljana; Slovenia.

[95]School of Physics and Astronomy, Queen Mary University of London, London; United Kingdom.

[96]Department of Physics, Royal Holloway University of London, Egham; United Kingdom.

[97]Department of Physics and Astronomy, University College London, London; United Kingdom.

[98]Louisiana Tech University, Ruston LA; United States of America.

[99]Fysiska institutionen, Lunds universitet, Lund; Sweden.

[100]Departamento de Física Teorica C-15 and CIAFF, Universidad Autónoma de Madrid, Madrid; Spain.

[101]Institut für Physik, Universität Mainz, Mainz; Germany.

[102]School of Physics and Astronomy, University of Manchester, Manchester; United Kingdom.

[103]CPPM, Aix-Marseille Université, CNRS/IN2P3, Marseille; France.

[104]Department of Physics, University of Massachusetts, Amherst MA; United States of America.

[105]Department of Physics, McGill University, Montreal QC; Canada.

[106]School of Physics, University of Melbourne, Victoria; Australia.

[107]Department of Physics, University of Michigan, Ann Arbor MI; United States of America.

[108]Department of Physics and Astronomy, Michigan State University, East Lansing MI; United States of America.

[109]Group of Particle Physics, University of Montreal, Montreal QC; Canada.

[110]Fakultät für Physik, Ludwig-Maximilians-Universität München, München; Germany.

[111]Max-Planck-Institut für Physik (Werner-Heisenberg-Institut), München; Germany.

[112]Graduate School of Science and Kobayashi-Maskawa Institute, Nagoya University, Nagoya; Japan.

[113]Department of Physics and Astronomy, University of New Mexico, Albuquerque NM; United States of America.

[114]Institute for Mathematics, Astrophysics and Particle Physics, Radboud University/Nikhef, Nijmegen; Netherlands.

[115]Nikhef National Institute for Subatomic Physics and University of Amsterdam, Amsterdam; Netherlands.

[116]Department of Physics, Northern Illinois University, DeKalb IL; United States of America.

[117][(a)]New York University Abu Dhabi, Abu Dhabi;[(b)]United Arab Emirates University, Al Ain; United

Arab Emirates.

[118]Department of Physics, New York University, New York NY; United States of America.

[119]Ochanomizu University, Otsuka, Bunkyo-ku, Tokyo; Japan.

[120]Ohio State University, Columbus OH; United States of America.

[121]Homer L. Dodge Department of Physics and Astronomy, University of Oklahoma, Norman OK; United States of America.

[122]Department of Physics, Oklahoma State University, Stillwater OK; United States of America.

[123]Palacký University, Joint Laboratory of Optics, Olomouc; Czech Republic.

[124]Institute for Fundamental Science, University of Oregon, Eugene, OR; United States of America.

[125]Graduate School of Science, Osaka University, Osaka; Japan.

[126]Department of Physics, University of Oslo, Oslo; Norway.

[127]Department of Physics, Oxford University, Oxford; United Kingdom.

[128]LPNHE, Sorbonne Université, Université Paris Cité, CNRS/IN2P3, Paris; France.

[129]Department of Physics, University of Pennsylvania, Philadelphia PA; United States of America.

[130]Department of Physics and Astronomy, University of Pittsburgh, Pittsburgh PA; United States of America.

[131][a]Laboratório de Instrumentação e Física Experimental de Partículas - LIP, Lisboa;[b]Departamento de Física, Faculdade de Ciências, Universidade de Lisboa, Lisboa;[c]Departamento de Física, Universidade de Coimbra, Coimbra;[d]Centro de Física Nuclear da Universidade de Lisboa, Lisboa;[e]Departamento de Física, Universidade do Minho, Braga;[f]Departamento de Física Teórica y del Cosmos, Universidad de Granada, Granada (Spain);[g]Departamento de Física, Instituto Superior Técnico, Universidade de Lisboa, Lisboa; Portugal.

[132]Institute of Physics of the Czech Academy of Sciences, Prague; Czech Republic.

[133]Czech Technical University in Prague, Prague; Czech Republic.

[134]Charles University, Faculty of Mathematics and Physics, Prague; Czech Republic.

[135]Particle Physics Department, Rutherford Appleton Laboratory, Didcot; United Kingdom.

[136]IRFU, CEA, Université Paris-Saclay, Gif-sur-Yvette; France.

[137]Santa Cruz Institute for Particle Physics, University of California Santa Cruz, Santa Cruz CA; United States of America.

[138][a]Departamento de Física, Pontificia Universidad Católica de Chile, Santiago;[b]Millennium Institute for Subatomic physics at high energy frontier (SAPHIR), Santiago;[c]Instituto de Investigación Multidisciplinario en Ciencia y Tecnología, y Departamento de Física, Universidad de La Serena;[d]Universidad Andres Bello, Department of Physics, Santiago;[e]Instituto de Alta Investigación, Universidad de Tarapacá, Arica;[f]Departamento de Física, Universidad Técnica Federico Santa María, Valparaíso; Chile.

[139]Department of Physics, University of Washington, Seattle WA; United States of America.

[140]Department of Physics and Astronomy, University of Sheffield, Sheffield; United Kingdom.

[141]Department of Physics, Shinshu University, Nagano; Japan.

[142]Department Physik, Universität Siegen, Siegen; Germany.

[143]Department of Physics, Simon Fraser University, Burnaby BC; Canada.

[144]SLAC National Accelerator Laboratory, Stanford CA; United States of America.

[145]Department of Physics, Royal Institute of Technology, Stockholm; Sweden.

[146]Departments of Physics and Astronomy, Stony Brook University, Stony Brook NY; United States of America.

[147]Department of Physics and Astronomy, University of Sussex, Brighton; United Kingdom.

[148]School of Physics, University of Sydney, Sydney; Australia.

[149]Institute of Physics, Academia Sinica, Taipei; Taiwan.

[150](a)E. Andronikashvili Institute of Physics, Iv. Javakhishvili Tbilisi State University, Tbilisi;(b)High Energy Physics Institute, Tbilisi State University, Tbilisi;(c)University of Georgia, Tbilisi; Georgia.

[151]Department of Physics, Technion, Israel Institute of Technology, Haifa; Israel.

[152]Raymond and Beverly Sackler School of Physics and Astronomy, Tel Aviv University, Tel Aviv; Israel.

[153]Department of Physics, Aristotle University of Thessaloniki, Thessaloniki; Greece.

[154]International Center for Elementary Particle Physics and Department of Physics, University of Tokyo, Tokyo; Japan.

[155]Department of Physics, Tokyo Institute of Technology, Tokyo; Japan.

[156]Department of Physics, University of Toronto, Toronto ON; Canada.

[157](a)TRIUMF, Vancouver BC;(b)Department of Physics and Astronomy, York University, Toronto ON; Canada.

[158]Division of Physics and Tomonaga Center for the History of the Universe, Faculty of Pure and Applied Sciences, University of Tsukuba, Tsukuba; Japan.

[159]Department of Physics and Astronomy, Tufts University, Medford MA; United States of America.

[160]Department of Physics and Astronomy, University of California Irvine, Irvine CA; United States of America.

[161]University of Sharjah, Sharjah; United Arab Emirates.

[162]Department of Physics and Astronomy, University of Uppsala, Uppsala; Sweden.

[163]Department of Physics, University of Illinois, Urbana IL; United States of America.

[164]Instituto de Física Corpuscular (IFIC), Centro Mixto Universidad de Valencia - CSIC, Valencia; Spain.

[165]Department of Physics, University of British Columbia, Vancouver BC; Canada.

[166]Department of Physics and Astronomy, University of Victoria, Victoria BC; Canada.

[167]Fakultät für Physik und Astronomie, Julius-Maximilians-Universität Würzburg, Würzburg; Germany.

[168]Department of Physics, University of Warwick, Coventry; United Kingdom.

[169]Waseda University, Tokyo; Japan.

[170]Department of Particle Physics and Astrophysics, Weizmann Institute of Science, Rehovot; Israel.

[171]Department of Physics, University of Wisconsin, Madison WI; United States of America.

[172]Fakultät für Mathematik und Naturwissenschaften, Fachgruppe Physik, Bergische Universität Wuppertal, Wuppertal; Germany.

[173]Department of Physics, Yale University, New Haven CT; United States of America.

[a] Also Affiliated with an institute covered by a cooperation agreement with CERN.

[b] Also at An-Najah National University, Nablus; Palestine.

[c] Also at Borough of Manhattan Community College, City University of New York, New York NY; United States of America.

[d] Also at Center for High Energy Physics, Peking University; China.

[e] Also at Center for Interdisciplinary Research and Innovation (CIRI-AUTH), Thessaloniki; Greece.

[f] Also at Centro Studi e Ricerche Enrico Fermi; Italy.

[g] Also at CERN, Geneva; Switzerland.

[h] Also at Département de Physique Nucléaire et Corpusculaire, Université de Genève, Genève; Switzerland.

[i] Also at Departament de Fisica de la Universitat Autonoma de Barcelona, Barcelona; Spain.

[j] Also at Department of Financial and Management Engineering, University of the Aegean, Chios; Greece.

[k] Also at Department of Physics, California State University, Sacramento; United States of America.

[l] Also at Department of Physics, King's College London, London; United Kingdom.

[m] Also at Department of Physics, Stanford University, Stanford CA; United States of America.

[n] Also at Department of Physics, Stellenbosch University; South Africa.

[o] Also at Department of Physics, University of Fribourg, Fribourg; Switzerland.

[p] Also at Department of Physics, University of Thessaly; Greece.

[q] Also at Department of Physics, Westmont College, Santa Barbara; United States of America.

[r] Also at Faculty of Physics, Sofia University, 'St. Kliment Ohridski', Sofia; Bulgaria.

[s] Also at Hellenic Open University, Patras; Greece.

[t] Also at Institucio Catalana de Recerca i Estudis Avancats, ICREA, Barcelona; Spain.

[u] Also at Institut für Experimentalphysik, Universität Hamburg, Hamburg; Germany.

[v] Also at Institute for Nuclear Research and Nuclear Energy (INRNE) of the Bulgarian Academy of Sciences, Sofia; Bulgaria.

[w] Also at Institute of Applied Physics, Mohammed VI Polytechnic University, Ben Guerir; Morocco.

[x] Also at Institute of Particle Physics (IPP); Canada.

[y] Also at Institute of Physics and Technology, Mongolian Academy of Sciences, Ulaanbaatar; Mongolia.

[z] Also at Institute of Physics, Azerbaijan Academy of Sciences, Baku; Azerbaijan.

[aa] Also at Institute of Theoretical Physics, Ilia State University, Tbilisi; Georgia.

[ab] Also at Lawrence Livermore National Laboratory, Livermore; United States of America.

[ac] Also at National Institute of Physics, University of the Philippines Diliman (Philippines); Philippines.

[ad] Also at Technical University of Munich, Munich; Germany.

[ae] Also at The Collaborative Innovation Center of Quantum Matter (CICQM), Beijing; China.

[af] Also at TRIUMF, Vancouver BC; Canada.

[ag] Also at Università di Napoli Parthenope, Napoli; Italy.

[ah] Also at University of Colorado Boulder, Department of Physics, Colorado; United States of America.

[ai] Also at Washington College, Chestertown, MD; United States of America.

[aj] Also at Yeditepe University, Physics Department, Istanbul; Türkiye.

[*] Deceased

Search for a resonance decaying into a scalar particle and a Higgs boson in final states with leptons and two photons in proton–proton collisions at $\sqrt{s} = 13$ TeV with the ATLAS detector

The ATLAS Collaboration

A search for a hypothetical heavy scalar particle, X, decaying into a singlet scalar particle, S, and a Standard Model Higgs boson, H, using 140 fb^{-1} of proton–proton collision data at the centre-of-mass energy of 13 TeV recorded with the ATLAS detector at the LHC is presented. The explored mass range is $300 \leq m_X \leq 1000$ GeV and $170 \leq m_S \leq 500$ GeV. The signature of this search is one or two leptons (e or μ) from the decay of vector bosons originating from the S particle, $S \rightarrow W^{\pm}W^{\mp}/ZZ$, and two photons from the Higgs boson decay, $H \rightarrow \gamma\gamma$. No significant excess is observed above the expected Standard Model background. The observed (expected) upper limits at the 95% confidence level on the cross-section for $gg \rightarrow X \rightarrow SH$, assuming the same $S \rightarrow WW/ZZ$ branching ratios as for a SM-like heavy Higgs boson, are between 530 (800) fb and 120 (170) fb.

Contents

1 Introduction

The Higgs boson was discovered by the ATLAS [1] and CMS [2] Collaborations in 2012 [3, 4]. Since then, an important goal has been to determine the Higgs boson properties and to perform precision measurements using proton–proton (pp) collision data from the Large Hadron Collider (LHC). Up until now, all measured properties are consistent with the Standard Model (SM) Higgs boson predictions [5, 6]. This discovery not only demonstrates the existence of the Higgs boson, but it also opens up new frontiers in particle physics that aim to address the limitations of the SM. There are a variety of beyond-the-SM scenarios that introduce additional scalar bosons such as the Next-to-Minimal Supersymmetric Standard Model (NMSSM) [7, 8], the Two-Real-Singlet Model (TRSM) [9, 10] or two-Higgs-Doublet Models (2HDM) [11].

The 2HDM+S model [12] extends the 2HDM hypothesis by considering the production of a heavy CP-even scalar boson (X) that could decay into an SM Higgs boson (H) and a hypothetical scalar singlet (S). A representative diagram of the $X \rightarrow SH$ production via gluon–gluon fusion is shown in Figure 1. The $X \rightarrow SH$ branching ratio is assumed to be 100%.

Searches inspired by the 2HDM+S probing $X \rightarrow SS \rightarrow WW^*WW^*$ [13], $X \rightarrow SH \rightarrow bb\gamma\gamma$ [14] and $X \rightarrow SH \rightarrow VV\tau\tau$ [15], where V can be either a $W^\pm$ or Z boson, have been performed by the ATLAS Collaboration. For the latter, no significant excess is observed above the expected SM processes, and 95% confidence level (CL) upper limits are set on the signal production cross-section between 542 fb and 72 fb in the mass ranges $500 \leq m_X \leq 1500$ GeV and $200 \leq m_S \leq 500$ GeV [15]. The $X \rightarrow SH$ search in the
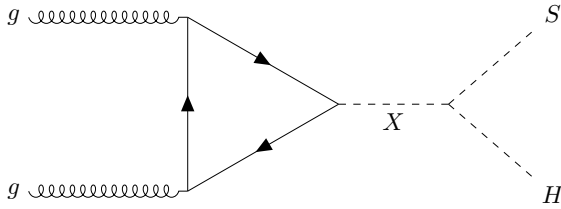
Figure 1: Illustrative Feynman diagram for $X \to SH$ production via gluon–gluon fusion.

$bb\gamma\gamma$ final state [14] set upper limits on the cross-section times the branching ratio ranging from 39 fb to 0.09 fb, over the mass ranges $170 \leq m_X \leq 1000$ GeV and $15 \leq m_S \leq 500$ GeV. The CMS Collaboration has also performed searches for $X \to SH$ in the $bb\gamma\gamma$ [16], $bb\tau\tau$ [17], and $4b$ [18] decay modes. In the diphoton plus two b-quarks search, the upper limits on the product of the production cross-section and the decay branching ratios of the signal process lie in the range of $0.9 - 0.04$ fb [**CMS:2023boe**], in the explored mass ranges $300 \leq m_X \leq 1000$ GeV and $90 \leq m_S \leq 800$ GeV. For the search with a pair of tau leptons and b-quarks in the final state, limits are set on the production cross-section ranging from 125 fb to 2.7 fb in the mass ranges $240 \leq m_X \leq 3000$ GeV and $60 \leq m_S \leq 2800$ GeV [17]. Comparable limits are found in the search involving four b-quarks in the final state, ranging from 150 to 0.1 fb in the mass ranges $0.9 \leq m_X \leq 4$ TeV and $60 \leq m_S \leq 600$ GeV [18]. All these results are obtained assuming for the S boson the same mass-dependent branching ratios as for the SM Higgs boson [19] (denoted SM-like branching ratios in the following).

This paper is focused on the search for $X \to SH \to VV\gamma\gamma$. The final state of interest is characterised by two photons from the SM Higgs boson decay ($H \to \gamma\gamma$), and one or two leptons (electrons or muons) originating from the vector bosons produced in the $S \to VV$ decays. This signature benefits from a good diphoton mass ($m_{\gamma\gamma}$) resolution [20] and the $m_{\gamma\gamma}$ distribution is used as the final discriminant. The requirement of at least one lepton rejects some SM background processes and therefore increases the signal-to-background ratio. The events are classified by the number and flavour of the leptons (electrons and muons) in the final state and multivariate analysis techniques are used to enhance the sensitivity of the search. The algorithm is trained to distinguish between the dominant SM backgrounds (multi-jet processes and vector bosons produced in association with a pair of photons) and the $X \to SH \to VV\gamma\gamma$ signal. This search is performed over the mass ranges $300 \leq m_X \leq 1000$ GeV and $170 \leq m_S \leq 500$ GeV. It allows to explore lower mass ranges than other final states with b-quarks where the signal becomes boosted at low m_S values, and suffer from low energetic b-quarks falling below the reconstructed threshold in the low m_X region. In the interpretation of the search results, the S boson is assumed to have SM-like branching ratios. Two additional scenarios wherein the S boson decays with a 100% branching ratio into a pair of $W^\pm$ or Z bosons, $S \to W^+W^-/ZZ$, are also considered.

This paper is organised as follows. A brief description of the ATLAS detector is given in Section 2. Data and simulation samples are described in Section 3. The object reconstruction and event selection are outlined in Section 4. The background estimation and the systematic uncertainties are described in Section 5 and Section 6, respectively. Section 7 presents the results of this search, which are summarised in Section 8.

2 ATLAS detector

The ATLAS detector [1] at the LHC covers nearly the entire solid angle around the collision point.[1] It consists of an inner tracking detector surrounded by a thin superconducting solenoid, electromagnetic and hadronic calorimeters, and a muon spectrometer incorporating three large superconducting air-core toroidal magnets.

The inner-detector system (ID) is immersed in a 2 T axial magnetic field and provides charged-particle tracking in the range $|\eta| < 2.5$. The high-granularity silicon pixel detector covers the vertex region and typically provides four measurements per track, the first hit generally being in the insertable B-layer (IBL) installed before Run 2 [21, 22]. It is followed by the SemiConductor Tracker (SCT), which usually provides eight measurements per track. These silicon detectors are complemented by the transition radiation tracker (TRT), which enables radially extended track reconstruction up to $|\eta| = 2.0$. The TRT also provides electron identification information based on the fraction of hits (typically 30 in total) above a higher energy-deposit threshold corresponding to transition radiation.

The calorimeter system covers the pseudorapidity range $|\eta| < 4.9$. Within the region $|\eta| < 3.2$, electromagnetic calorimetry is provided by barrel and endcap high-granularity lead/liquid-argon (LAr) calorimeters, with an additional thin LAr presampler covering $|\eta| < 1.8$ to correct for energy loss in material upstream of the calorimeters. Hadronic calorimetry is provided by the steel/scintillator-tile calorimeter, segmented into three barrel structures within $|\eta| < 1.7$, and two copper/LAr hadronic endcap calorimeters. The solid angle coverage is completed with forward copper/LAr and tungsten/LAr calorimeter modules optimised for electromagnetic and hadronic energy measurements respectively.

The muon spectrometer (MS) comprises separate trigger and high-precision tracking chambers measuring the deflection of muons in a magnetic field generated by the superconducting air-core toroidal magnets. The field integral of the toroids ranges between 2.0 and 6.0 T m across most of the detector. Three layers of precision chambers, each consisting of layers of monitored drift tubes, cover the region $|\eta| < 2.7$, complemented by cathode-strip chambers in the forward region, where the background is highest. The muon trigger system covers the range $|\eta| < 2.4$ with resistive-plate chambers in the barrel, and thin-gap chambers in the endcap regions.

The luminosity is measured mainly by the LUCID–2 [23] detector that records Cherenkov light produced in the quartz windows of photomultipliers located close to the beampipe.

Events are selected by the first-level trigger system implemented in custom hardware, followed by selections made by algorithms implemented in software in the high-level trigger [24]. The first-level trigger accepts events from the 40 MHz bunch crossings at a rate below 100 kHz, which the high-level trigger further reduces in order to record complete events to disk at about 1 kHz.

A software suite [25] is used in data simulation, in the reconstruction and analysis of real and simulated data, in detector operations, and in the trigger and data acquisition systems of the experiment.

---

[1] ATLAS uses a right-handed coordinate system with its origin at the nominal interaction point (IP) in the centre of the detector and the z-axis along the beam pipe. The x-axis points from the IP to the centre of the LHC ring, and the y-axis points upwards. Polar coordinates (r, ϕ) are used in the transverse plane, ϕ being the azimuthal angle around the z-axis. The pseudorapidity is defined in terms of the polar angle θ as $\eta = -\ln\tan(\theta/2)$ and is equal to the rapidity $y = \frac{1}{2}\ln\left(\frac{E+p_z c}{E-p_z c}\right)$ in the relativistic limit. Angular distance is measured in units of $\Delta R \equiv \sqrt{(\Delta y)^2 + (\Delta \phi)^2}$.

3 Data and simulation samples

3.1 Data Samples

The data used were collected with the ATLAS detector during 2015–2018, from pp collisions at a centre-of-mass energy $\sqrt{s}$ = 13 TeV, corresponding to an integrated luminosity of 140 fb^{-1} with an uncertainty of 0.83% [26] after data quality requirements [27]. Events were recorded using diphoton triggers that require two reconstructed photon candidates with minimum transverse energies of 35 GeV and 25 GeV [28]. During the 2015–2016 data taking period, a *Loose* identification requirement was applied for this diphoton trigger while it was replaced by the *Medium* selection criteria to keep a tolerable trigger rate in 2017–2018 due to the increased instantaneous luminosity.

3.2 Monte Carlo simulated samples

3.2.1 Signal samples

The Monte Carlo (MC) simulated signal samples were produced with the PYTHIA 8 generator [29] with the matrix element calculation at leading order (LO) accuracy in quantum chromodynamics (QCD), followed by parton showering, hadronisation and underlying event modelling using the A14 set of tuned parameters ("tune") [30] and the NNPDF2.3LO parton distribution functions (PDF) [31]. During the sample generation, both X and S were assumed to have a narrow width compared with the experimental resolution, and their widths are fixed to 10 MeV. A total of 20 signal samples for various m_X and m_S were generated. The X boson was required to decay into S and H with S only decaying into a pair of W or Z bosons and H decaying into a pair of photons. By considering leptonic decays of W or Z bosons, the following three final state samples were produced for each m_X and m_S combination: $WW(\ell\nu q\bar{q}') + \gamma\gamma$, $WW(\ell\nu\ell\nu) + \gamma\gamma$, and $ZZ(\ell\ell q\bar{q}/\ell\ell\nu\nu) + \gamma\gamma$, where $\ell = e$, μ, or τ. The $ZZ(4\ell) + \gamma\gamma$ decay sample is excluded due to its negligible contribution. To achieve a better signal generation efficiency, the samples were produced by requiring to have at least one lepton with transverse momentum (p_T) greater than 7 GeV and pseudorapidity $|\eta| < 3$ at the generator level.

3.2.2 Background samples

The main background contributions result from SM single and double-Higgs boson production, forming a resonance on the diphoton mass ($m_{\gamma\gamma}$) spectrum, and other SM processes giving a smoothly falling $m_{\gamma\gamma}$ spectrum (continuum background). The corresponding events were generated with MC simulation.

Simulated events for single Higgs boson production via gluon–gluon fusion (ggF) were produced with the POWHEG BOX v2 generator [32–36] at next-to-next-to-leading order (NNLO) accuracy in QCD and interfaced with PYTHIA 8. The NNLO accuracy for arbitrary inclusive $gg \rightarrow H$ observables was achieved by reweighting the Higgs boson rapidity spectrum in HJ-MINLO [37–39] to that of HNNLO [40]. The PDF4LHC15NNLO PDF set [41] and the AZNLO tune [42] of PYTHIA 8 were used and the decays of b- and c-hadrons were modelled by the EVTGEN 1.6.0 programme [43]. These events were normalised using the NNLO cross-section in QCD plus electroweak corrections at next-to-leading order (NLO) [19, 44–53].

Simulated single Higgs boson events produced via vector-boson fusion (VBF) were generated with POWHEG BOX v2 at NLO accuracy in QCD and interfaced with PYTHIA 8. The PDF4LHC15NLO PDF

set and AZNLO tune were used. Simulated events were normalised using an approximate-NNLO QCD cross-section with NLO electroweak corrections [54–56].

Events of single Higgs boson produced in association with a vector boson (VH, $V = W/Z$) were simulated using Powheg Box v2 and interfaced with Pythia 8. The Powheg prediction is accurate to NLO in QCD for VH+1jet distributions by using the MiNLO [57] prescription. The loop-induced $gg \rightarrow ZH$ process was generated separately at LO. The PDF4LHC15nlo PDF set and the AZNLO tune were used. Cross-sections calculated at NNLO in QCD with NLO electroweak corrections for $q\bar{q}/qg \rightarrow VH$ and at NLO and next-to-leading-logarithm accuracy in QCD for $gg \rightarrow ZH$ [58–64] were used for the normalisation of the MC samples.

Events corresponding to Higgs boson production in association with a pair of top or bottom quarks ($t\bar{t}H$ or $b\bar{b}H$) were simulated using Powheg Box v2 at NLO with the NNPDF3.0nlo PDF set [65]. The events were interfaced with Pythia 8 using the A14 tune and the NNPDF2.3lo PDF set. The decays of bottom and charm hadrons were performed with EvtGen 1.6.0.

Finally, events for single Higgs boson production in association with a single top quark were simulated with the MadGraph_ aMC@NLO 2.3.3 [66] generator at NLO with the NNPDF3.0nlo PDF set. The events were interfaced with Pythia 8 using the A14 tune and the NNPDF2.3lo PDF set.

In addition to the single Higgs boson processes, events corresponding to the SM double Higgs boson ggF and VBF production modes are also considered. Those events were generated with Powheg Box v2 at NLO accuracy in QCD using the PDF4LHC15nlo PDF set and interfaced with Pythia 8. During the sample generation, one of the Higgs bosons was required to decay into two photons and the other Higgs boson was required to decay into WW, ZZ or $\tau\tau$, giving a final state with a pair of electrons or muons, or with one electron and one muon. Leptons were required to have $p_T > 7\,\text{GeV}$ and $|\eta| < 3$ at the generator level.

The normalisation of all Higgs boson samples accounts for the decay branching ratios calculated with HDECAY [67–69] and Prophecy4f [70–72].

Continuum background from $\gamma\gamma$+jets, $V+\gamma\gamma$, and $t\bar{t}+\gamma\gamma$ processes is considered. Their contributions are described with corresponding MC simulated samples that are exclusively used for the event selection optimisation. These samples were normalised with cross-sections as predicted by their corresponding MC generators.

Events from $\gamma\gamma$+jets production were simulated using the Sherpa 2.2.4 generator [73] at NLO accuracy in QCD with up to one additional parton and at LO with up to three additional partons. The matrix elements of these events were calculated with the Comix [74] and OpenLoops [75, 76] libraries and then matched to the Sherpa parton shower [77] using the MEPS@NLO prescription [78–81]. The NNPDF3.0nnlo PDF set [65] was used to describe the parton distributions in the incoming protons. A generator-level selection was applied to these events with the requirement of the invariant mass of the two photons to be between 90 GeV and 175 GeV.

The $V + \gamma\gamma$ events were generated using Sherpa 2.2.4 at NLO accuracy in QCD with up to one additional parton and up to three extra partons at LO. The calculation procedure is the same as in $\gamma\gamma$+jets event generation. Events were generated separately according to their final states as listed: $ee+\gamma\gamma$, $\mu\mu+\gamma\gamma$, $\tau\tau+\gamma\gamma$, $e\nu+\gamma\gamma$, $\mu\nu+\gamma\gamma$, $\tau\nu+\gamma\gamma$, and $\nu\nu+\gamma\gamma$. The generator-level photon p_T was required to be greater than 17 GeV and the invariant mass of the two photons should be larger than 80 GeV for these events.

Table 1: Summary of MC simulated samples used in this analysis.

Process	Generator	PDF	Tune
Signal			
$X \rightarrow SH \rightarrow VV + \gamma\gamma$	Pythia 8	NNPDF2.3LO	A14
SM Single and double Higgs boson production			
ggF H	Powheg+Pythia 8	PDF4LHC15NNLO	AZNLO
VBF H	Powheg+Pythia 8	PDF4LHC15NLO	AZNLO
WH	Powheg+Pythia 8	PDF4LHC15NLO	AZNLO
$qq \rightarrow ZH$	Powheg+Pythia 8	PDF4LHC15NLO	AZNLO
$gg \rightarrow ZH$	Powheg+Pythia 8	PDF4LHC15NLO	AZNLO
$t\bar{t}H$	Powheg+Pythia 8	NNPDF3.0NLO	A14
$b\bar{b}H$	Powheg+Pythia 8	NNPDF3.0NLO	A14
$tHbj$	MadGraph_aMC@NLO+Pythia 8	NNPDF3.0NLO	A14
tHW	MadGraph_aMC@NLO+Pythia 8	NNPDF3.0NLO	A14
ggF $HH \rightarrow VV + \gamma\gamma$	Powheg+Pythia 8	PDF4LHC15NLO	A14
VBF $HH \rightarrow VV + \gamma\gamma$	Powheg+Pythia 8	PDF4LHC15NLO	A14
Continuum background			
$\gamma\gamma$ + jets	Sherpa	NNPDF3.0NNLO	–
$V + \gamma\gamma$	Sherpa	NNPDF3.0NNLO	–
$t\bar{t}\gamma\gamma$	MadGraph_aMC@NLO+Pythia 8	NNPDF3.0NLO	A14
Lepton-dependence samples			
$\gamma\gamma + 0\ell$ + jets	MadGraph_aMC@NLO+Pythia 8	NNPDF3.0NLO	A14
$\gamma\gamma + 1\ell$ + jets	MadGraph_aMC@NLO+Pythia 8	NNPDF3.0NLO	A14
$\gamma\gamma + 2\ell$ + jets	MadGraph_aMC@NLO+Pythia 8	NNPDF3.0NLO	A14

The $t\bar{t}+\gamma\gamma$ process is simulated with the MadGraph5_aMC@NLO generator at LO and interfaced with Pythia 8. The NNPDF2.3LO PDF set and A14 tune were used for this production. The decays of bottom and charm hadrons were performed with EvtGen 1.6.0.

In addition, dedicated samples (denoted "lepton-dependence samples") corresponding to final states of $\gamma\gamma + 0\ell$ + jets, $\gamma\gamma + 1\ell$ + jets, and $\gamma\gamma + 2\ell$ + jets are generated to study the $m_{\gamma\gamma}$ distribution difference for cases with different lepton multiplicity at the generator level. These samples were produced with MadGraph5_aMC@NLO interfaced with Pythia 8. All possible SM processes with described final states except for those with $H \rightarrow \gamma\gamma$ were included in the event generation.

All simulated events except for the signals, $\gamma\gamma$+jets and lepton-dependence samples were passed through a detailed detector simulation of the ATLAS detector implemented with Geant4 [82, 83]. The remaining samples were simulated using AtlFastII [83], which exploys Geant4 except for a parameterisation of the calorimeter response [84]. The effect of multiple interactions in the same and neighbouring bunch crossings (pile-up) was modelled by overlaying the simulated hard-scattering event with inelastic pp events generated with Pythia 8 [85] using the NNPDF2.3LO PDF set and the A3 tune [86]. A summary of MC simulated samples can be found in Table 1.

4 Object and event selection

4.1 Object selection

Vertices from pp collisions are reconstructed if they have associated at least two ID tracks with $p_T > 0.5$ GeV. The diphoton primary vertex (PV) is chosen by using a neural network algorithm that uses information about the ID tracks as well as the photon candidates [87].

Photons are reconstructed based on a dynamic, topological cell clustering-based algorithm from the energy deposits in the electromagnetic calorimeter in the region $|\eta| < 2.37$, excluding the transition region between the barrel and endcap calorimeters $1.37 < |\eta| < 1.52$ [88]. The photon identification criteria is constructed using information from the shower shapes and the primary identification criteria is labelled as $Tight$. The photon isolation criteria quantifies the activity near the photons from the tracks of nearby charged particles, or from energy deposits in the calorimeter [88]. This analysis considers events by selecting photon candidates which are required to satisfy a set of preselection criteria. The two photons with the highest transverse momentum, referred to as leading (γ_1) and subleading (γ_2) photons, must satisfy $p_T > 22$ GeV and $|\eta| < 2.37$, excluding the transition region between the barrel and endcap calorimeters $1.37 < |\eta| < 1.52$. Photon candidates are separated from multi-jet backgrounds by applying $Tight$ identification and further isolation requirements to suppress jets misidentified as photons.

Electrons are reconstructed and identified based on clusters built from energy deposits in the electromagnetic calorimeter, which are matched to a track in the inner detector [88]. The muon reconstruction is performed using information from the inner detector and muon spectrometer, as well as the electromagnetic and hadronic calorimeters [89]. In this search, electron candidates are required to have $p_T > 10$ GeV and $|\eta| < 2.47$, excluding the transition region between the barrel and endcap calorimeters $1.37 < |\eta| < 1.52$. Muon candidates should have $p_T > 10$ GeV and $|\eta| < 2.7$. Leptons must satisfy $Medium$ identification and $Loose$ isolation [88, 89], and a set of requirements based on the longitudinal and transverse impact parameters relative to the vertex and the beam axis.

Jets are reconstructed using a particle flow algorithm [90] from noise-suppressed positive-energy topological clusters [91] in the calorimeter using the anti-k_t algorithm [92, 93] with a radius parameter $R = 0.4$. The jet energy scale calibration restores the jet p_T, energy, and mass to that of jets reconstructed at particle level [94]. In this search, jets are required to have $p_T > 25$ GeV and to be in the central region of the detector, $|\eta| < 2.5$. To suppress jets from pileup, a jet-vertex-tagger multivariate discriminant [95] is applied to jets with $p_T < 60$ GeV. Jets containing b-hadrons are identified (b-tagged) using the 77% efficiency working point of the DL1r b-tagging algorithm [96].

An overlap removal procedure is performed to avoid double-counting objects. First, electrons overlapping with any of the two selected photons ($\Delta R < 0.4$) are removed. Jets overlapping with the selected photons ($\Delta R < 0.4$) or electrons ($\Delta R < 0.2$) are removed. Electrons overlapping with the remaining jets ($\Delta R < 0.4$) are removed to match the requirements imposed when measuring isolated electron efficiencies. Finally, muons overlapping with photons or jets ($\Delta R < 0.4$) are removed.

The missing transverse momentum, with magnitude E_T^{miss}, is defined as the negative vector sum of the transverse momenta of the selected photon, electron, muon, and jet objects, as well as of the transverse momenta of remaining low-p_T particles estimated by using tracks associated with the diphoton primary vertex but not assigned to any of the selected objects [97].

The above requirements constitute the event preselection of this search.

Table 2: Event selection and classification strategy.

Preselection	Two photon candidates and no b-tagged jets			
Region	1ℓ	$e\mu$	$2\ell(WW)$	$2\ell(ZZ)$
Number of leptons	1	2	2	2
Total electric charge	–	0	0	0
Same flavour leptons	–	No	Yes	Yes
$\lvert m_{\ell\ell} - m_Z \rvert$ [GeV]	–	–	> 10	< 10
Number of jets	≥ 2	–	-	≥ 2
Strategy	BDT	Cut-based	BDT	Cut-based
Number of signal regions	2	1	2	1
$m_{\gamma\gamma}$ region	[105, 160] GeV			

4.2 Event selection

This search selects events with two photons from the Higgs boson decay, and one or two leptons coming from the vector bosons originated from the $S \to VV$ process. Events are required to pass diphoton triggers as described in Section 3. Moreover, photons are required to have $p_T^{\gamma_{1(2)}}/m_{\gamma\gamma} > 0.35\ (0.25)$ [20]. Selected events must contain one or two additional leptons (e or μ) with $p_T > 10$ GeV. To suppress backgrounds with top quarks, events containing one or more b-tagged jets are rejected.

The events are classified into four different regions depending on the number and flavour of leptons originating from the vector boson decays in the $S \to W^{\pm}W^{\mp}$ and $S \to ZZ$ processes. Events in the one-lepton (1ℓ) region are required to have one lepton and at least two jets. The other regions account for events with two leptons with opposite electric charge. Events with two leptons of different flavour are targeted in the $e\mu$ region. Events having two leptons of same flavour (SF) are further split by checking the compatibility of the dilepton invariant mass with the Z-mass pole. Events with at least two jets and satisfying $\lvert m_{\ell\ell} - 91.2\,\text{GeV} \rvert < 10$ GeV are classified in the $2\ell(ZZ)$ region, which targets the $S \to ZZ \to \ell\ell+$jets process. The remaining SF events are included in the $2\ell(WW)$ region.

Two optimisation strategies are adopted. For each of the 1ℓ and $2\ell(WW)$ regions, a Boosted Decision Tree (BDT) is used to enhance the analysis sensitivity. The 1ℓ and $2\ell(WW)$ regions further split the events by dividing the BDT output distribution into the loose (low BDT score) and tight (high BDT score) signal regions. The $e\mu$ and $2\ell(ZZ)$ signal regions are limited in statistics and have higher signal-over-background ratios than the BDT-based regions. Due to this, the $e\mu$ and $2\ell(ZZ)$ signal regions follow an inclusive cut-based strategy and events are not further split into sub-regions. This analysis strategy results in six signal regions.

The final discriminant of this search is the diphoton invariant mass spectrum. To be consistent with the $H \to \gamma\gamma$ process and to exclude the region of the Z-boson resonance, the range of $m_{\gamma\gamma}$ is limited to the [105, 160] GeV region. The signal region is defined as the $m_{\gamma\gamma}$ within [120, 130] GeV. Events outside the signal region, referred to as sideband events, are used to estimate the main background processes as described in Section 5. After all selections described above are applied, the combined acceptance and selection efficiency for the signal production ranges from 11% to 25%, which increases for higher m_X hypotheses. Table 2 summarises the event selection and strategy for each of the signal regions.

4.3 Boosted Decision Tree strategy

The dominant signal process in this search is the $S \to W^+W^-$ decay given the larger branching ratio compared with the $S \to ZZ$ process for the explored m_S range. In the 1ℓ region one of the W bosons decays leptonically and the other decays hadronically. In the $e\mu$ and $2\ell(WW)$ regions both W bosons decay leptonically resulting into a pair of leptons with different and same flavour, respectively. Two BDTs are built based on the kinematic observables from the final-state objects in the 1ℓ and $2\ell(WW)$ regions. The different signal samples are grouped according to the S mass into four groups: $m_S = 170$ GeV, $m_S = 200$ GeV, $m_S = 300$ GeV and $m_S = 400, 500$ GeV. These groups contain from four to six signal samples depending on the m_X values in each group. The BDT algorithms are trained for each group against the total background from MC simulation using the parameterised BDT method [98].

Twelve and nine variables for the 1ℓ and $2\ell(WW)$ regions respectively are used to train each BDT, as listed in Table 3. The BDT input variables list excludes $m_{\gamma\gamma}$ as it is used as the main discriminant; these variables are selected to have small correlation with $m_{\gamma\gamma}$. The BDT variable with the highest separation power is the transverse momentum of the pairs of photons from the SM Higgs boson decay ($p_T^{\gamma\gamma}$). The comparison of the $p_T^{\gamma\gamma}$ distributions for data, the expected SM background processes and the $(m_X, m_S) = (1000, 300)$ GeV signal from simulation is shown in Figure 2 for the 1ℓ and $2\ell(WW)$ regions.

(a) (b)
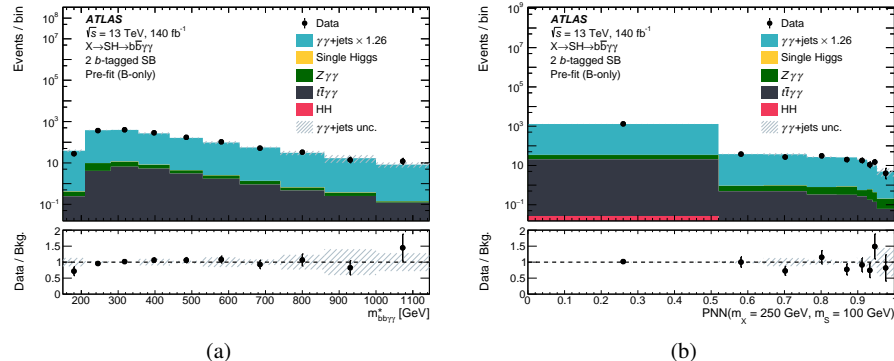
Figure 2: Transverse momentum of the diphoton system, $p_T^{\gamma\gamma}$, in the (a) 1ℓ and (b) $2\ell(WW)$ regions for data and the expected SM background from simulation after the event selection is applied. The $V\gamma\gamma$ and $\gamma\gamma$+jets simulated background is scaled to match the data yield excluding the $120 < m_{\gamma\gamma} < 130$ GeV region. The contribution from the SM single and double Higgs boson processes (denoted "SM Higgs"), which is estimated from the MC simulation, is also shown. The $(m_X, m_S) = (1000, 300)$ GeV signal prediction (open red histogram) for the scenario of SM-like $\mathcal{B}(S \to WW/ZZ)$ is also shown, normalised to a cross-section corresponding to the 95% CL upper limit shown in Figure 6. An additional normalisation factor, as indicated in the legend, is applied to scale the signal for visibility. The last bin in each distribution contains the overflow.

Figure 3 shows the BDT output distributions for data, the expected SM background processes and the $(m_X, m_S) = (1000, 300)$ GeV signal from simulation. The BDT output discriminant is used to further split events in loose and tight BDT regions: 1ℓloose and 1ℓtight regions are defined for the 1ℓ region, as well as 2ℓloose and 2ℓtight signal regions for the $2\ell(WW)$ region. The BDT score threshold values used range from -0.1 to 0.2 depending on the signal mass hypothesis, and result from a scan using the root square of the signal significance in each region added in quadrature: $Z_{\text{comb}} = \sqrt{Z_{\text{loose}}^2 + Z_{\text{tight}}^2}$, being

Table 3: Variables used as inputs to the BDT in the 1ℓ and $2\ell(WW)$ regions. The highest-p_T (leading) lepton is denoted ℓ_1, and the subleading lepton is denoted ℓ_2. The numbers indicate the ranking of each input variable, with 1 corresponding to the most highly ranked variable.

Variable	Description	BDT-based regions	
		1ℓ	$2\ell(WW)$
$\Delta R(\gamma\gamma, \ell\nu jj)$	ΔR between the diphoton system and the $\ell + E_\mathrm{T}^\mathrm{miss} jj$ system	10	
$\Delta R(\gamma\gamma, \ell\nu\ell\nu)$	ΔR between the diphoton system and the $\ell\ell + E_\mathrm{T}^\mathrm{miss}$ system		9
$\Delta R(jj, \ell\nu)$	ΔR between the dijet system and the $\ell + E_\mathrm{T}^\mathrm{miss}$ system	9	
$\Delta R(\ell_1\nu, \ell_2)$	ΔR between leading lepton $+ E_\mathrm{T}^\mathrm{miss}$ and subleading lepton		8
$p_\mathrm{T}^{\ell+E_\mathrm{T}^\mathrm{miss} jj}$	p_T of the $\ell + E_\mathrm{T}^\mathrm{miss} jj$ system	2	
$p_\mathrm{T}^{\gamma\gamma}$	p_T of the diphoton system	1	2
$\Delta\phi(\gamma\gamma, \ell_{(1)})$	$\Delta\phi$ between the diphoton system and the (leading) lepton	12	7
$\Delta R(\ell, E_\mathrm{T}^\mathrm{miss})$	ΔR between the lepton and the $E_\mathrm{T}^\mathrm{miss}$	8	
$p_\mathrm{T}^{\ell_{(1)}}$	p_T of the (leading) lepton	4	4
$p_\mathrm{T}^{\ell_1+E_\mathrm{T}^\mathrm{miss}}$	p_T of the leading lepton and $E_\mathrm{T}^\mathrm{miss}$ system		3
$m_\mathrm{T}(\ell_{(1)} E_\mathrm{T}^\mathrm{miss})$	Transverse mass of the (leading) lepton and $E_\mathrm{T}^\mathrm{miss}$	11	5
$m_{\ell\ell}$	Invariant mass of the dilepton system		6
$E_\mathrm{T}^\mathrm{miss}$	Missing transverse energy	3	1
$\Delta R(j, j)$	ΔR between the two jets with closest mass to m_W	6	
p_T^{jj}	p_T of the the two jets with closest mass to m_W	5	
m_{jj}	Invariant mass of the dijet system with closest mass to m_W	7	

$$Z_\mathrm{loose/tight} = \sqrt{2 \times \left[(s+b) \times \left(\ln\frac{s+b}{b} \right) - s \right]_\mathrm{loose/tight}}, \qquad (1)$$

where s represents the signal event yields and b is the background yield in each BDT region. Both signal and background yields are calculated by considering events in the region of $120 < m_{\gamma\gamma} < 130$ GeV. The selected threshold values are established by maximising Z_comb under the requirement of the presence of at least one sideband data event in the tight BDT regions. Table 4 shows the SM expected event yields, estimated as detailed in Section 5, and the observed data for each of the analysis regions. The expected signal yields for $(m_X, m_S) = (1000, 300)$ GeV, considering a $gg \to X \to SH$ production cross-section of 1 pb, are provided for comparison. The S scalar boson is assumed to decay into other SM particles with the same mass-dependent branching ratios of the SM Higgs boson.
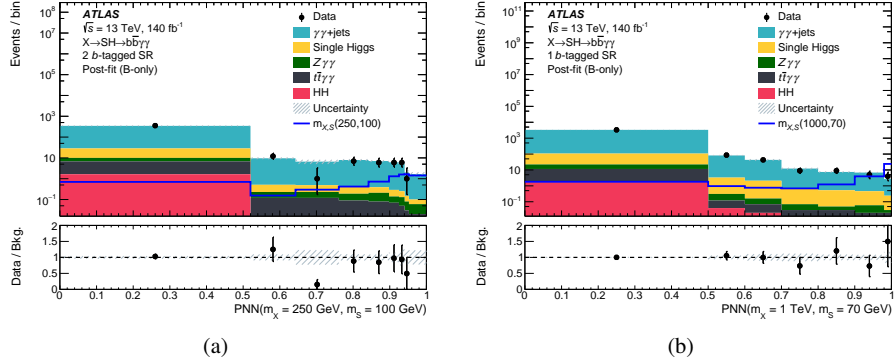
Figure 3: BDT output distributions in the (a) 1ℓ and (b) $2\ell(WW)$ regions for data and the expected SM background from simulation after the event selection is applied. The $V\gamma\gamma$ and $\gamma\gamma$+jets simulated background is scaled to match the data yield excluding the $120 < m_{\gamma\gamma} < 130$ GeV region. The contribution from the SM single and double Higgs boson processes (denoted "SM Higgs"), which is estimated from the MC simulation, is also shown. The $(m_X, m_S) = (1000, 300)$ GeV signal prediction (open red histogram) for the scenario of SM-like $\mathscr{B}(S \rightarrow WW/ZZ)$ is also shown, normalised to a cross-section corresponding to the 95% CL upper limit shown in Figure 6. An additional normalisation factor, as indicated in the legend, is applied to scale the signal for visibility. The BDT score threshold values are represented by the dashed vertical lines. The shaded band represents the statistical uncertainty on the background prediction. The last bin in each distribution contains the overflow.

Table 4: Observed data and expected event yields for the different analysis regions after the full selection from Table 2 is applied. The continuum background includes the $V\gamma\gamma$, $\gamma\gamma$+jets and $t\bar{t}\gamma\gamma$ processes estimated as described in Section 5. The contribution from the SM single and double Higgs boson processes (denoted "SM Higgs") is estimated from simulation. The uncertainties include all sources of systematic uncertainty described in Section 6. Event yields for the $(m_X, m_S) = (1000, 300)$ GeV signal are also shown assuming $\sigma(gg \rightarrow X \rightarrow SH) = 1$ pb and SM-like $\mathscr{B}(S \rightarrow WW/ZZ)$.

| | BDT-based regions | | | | | | | | Cut-based regions | | | |
	1ℓtight		1ℓloose		2ℓtight		2ℓloose		$2\ell(ZZ)$		$e\mu$	
Continuum	6.0	± 2.4	405	± 20	2.0	± 1.4	100	± 10	2.0	± 1.4	2.0	± 1.4
SM Higgs	0.55	± 0.08	6.8	± 0.9	0.46	± 0.06	3.35	± 0.46	0.52	± 0.08	0.24	± 0.03
Total background	6.6	± 2.8	412	± 23	2.46	± 1.6	103	± 11	2.52	± 1.6	2.24	± 1.5
Signal (m_X, m_S) (1000, 300) GeV	20.9	± 2.4	2.90 ±	0.34	2.96	± 0.35	0.016 ±	0.002	2.03	± 0.24	2.08	± 0.24
Data	6		405		2		100		2		2	

5 Background estimation

Background processes can be classified into "resonant" or "continuum" based on their $m_{\gamma\gamma}$ spectrum. The SM Higgs boson single and pair production events form the resonant background component. These processes are purely estimated from MC simulation.

The continuum background component arises mostly from multi-jet processes associated with two photons ($\gamma\gamma$+jets), and vector boson or top-antitop-quark production in association with a pair of photons ($V + \gamma\gamma$

and $t\bar{t}\gamma\gamma$). Contributions from these processes are checked with the MC simulated samples as described in Section 3.2.2 and used for the event selection optimisation. No dedicated MC simulated events are produced for processes with small contribution such as $VV+\gamma\gamma$ or processes with jets or leptons misidentified as photons. Their contributions are included in the data-driven background, which accounts for all possible processes. The contribution from the continuum background is estimated from a fit to the data $m_{\gamma\gamma}$ distribution in the sideband region with a template. This template is generated from an analytic function that is obtained from a fit to the $m_{\gamma\gamma}$ distribution in a dedicated data control region due to low statistics of sideband data in the signal region. These control regions are defined by requiring zero leptons and at least two photons passing looser identification and isolation criteria but failing the signal region photon selections as described in Section 4.1. Two different control samples are defined based on the number of leptons in each signal region using the selected jet to mimic the lepton behaviour. The control sample for the $\gamma\gamma + 1\ell$ region selects events with a pair of photons accompanied by one jet. For the other signal regions with a pair of leptons in the final state, the control sample requires the presence of at least two jets. A schematic diagram presenting the definitions of different regions is shown in Figure 4. The fitted $m_{\gamma\gamma}$ shape difference between the signal region and control region is considered as a systematic uncertainty in the background shape estimation. In addition, the $m_{\gamma\gamma}$ shape difference related to the number of leptons in the generator-level is also evaluated and included as a systematic uncertainty. This uncertainty is estimated by comparing the fit results to the full $m_{\gamma\gamma}$ mass range distributions in the control region and the validation region using dedicated lepton-dependence MC samples as described in Section 3.2.2, where the validation region is defined by applying almost the same event selections as the signal region but inverting identification and isolation requirements as same as in the control region.
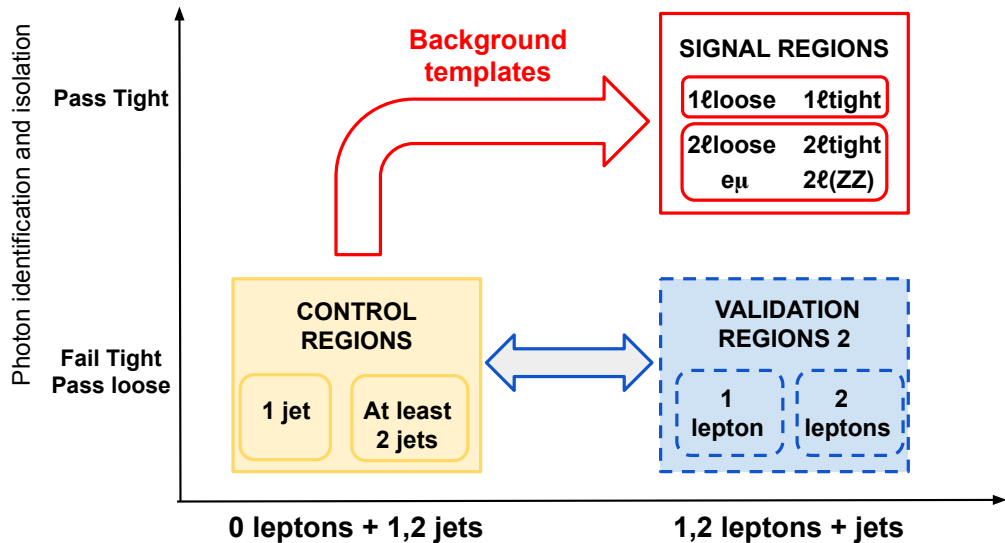
Figure 4: Definition of signal and control regions. The red arrow represents the $m_{\gamma\gamma}$ template generated in the 0-lepton control region which is applied to the signal regions. The systematic uncertainty in the background shape, obtained from differences between the control and the validation regions, is indicated by the blue arrow.

Three types of analytic functions are explored: exponential function, exponential function of a 2nd order polynomial, and a Chebyshev polynomial of order $n = 1, \dots, 5$. The functional form is chosen via a spurious signal test as described in Ref. [99]. The spurious signal is extracted by performing a

signal-plus-background fit to the data $m_{\gamma\gamma}$ distribution in the control region (denoted "background-only" template), which is assumed to only include contributions from continuum background processes. The selection criteria follow the strategy as documented in Ref. [20]. The spurious signal should be less than 20% of the background uncertainty. In addition to the spurious signal requirement, the goodness of the fit with background functional form to the background-only template is evaluated with a χ^2 test and the corresponding p-value is required to be greater than 5%. When multiple functions pass the criteria, the one with the smallest degrees of freedom is chosen. The corresponding spurious signal for the selected function is treated as the systematic uncertainty due to background modelling with the analytic function. In total 80 continuum background functions are estimated corresponding to various signal regions. Of these 80 functions, 78 are exponential functions of 2nd order polynomials and the remaining two are simple exponential functions. Due to the low statistics in the $e\mu$ and $2\ell(ZZ)$ signal regions and the fact that the $m_{\gamma\gamma}$ distribution shows a negligible dependence on the flavour of leptons, the continuum background shape estimated in the 2ℓtight region is also applied to these two regions.

6 Systematic uncertainties

Systematic uncertainties arise from the theory modelling of signal and background, the detector simulation and instrumental effects, and the estimation of the continuum background.

6.1 Theoretical uncertainties

Theoretical uncertainties are considered for signal and the SM single and double Higgs boson backgrounds. Uncertainties from six sources are considered: from PDF set and strong coupling constant α_S, from the QCD factorisation and renormalisation scales (μ_{F} and μ_{R}), and from the parton shower parameters and hadronisation models.

To evaluate the impact of varying the PDF set choice and α_S value, event weights corresponding to alternative PDF sets and α_S values are generated for each event along with the nominal weight. Effects on signal region yields are considered as systematic uncertainties. Variations on signal and SM Higgs boson yields are found to be 6% and 4% respectively.

The systematic uncertainty due to higher-order QCD effects is estimated by independently varying the QCD factorisation and renormalisation scales up and down from their nominal values by a factor of two, taking the envelope of the 7-point variation. Their impacts on signal and SM Higgs boson background yields are about 9% and 13% respectively.

The uncertainty due to the parton shower and hadronisation model is estimated by comparing the yields from the nominal MC samples using Pythia 8, with alternative samples using instead Herwig 7. The corresponding uncertainties in the signal and Higgs boson background yields are 5% and 3% respectively.

6.2 Experimental uncertainties

Systematic uncertainties arising from the luminosity determination, pileup modelling, and trigger, reconstruction and selection efficiencies, as well as energy scales and resolutions, are considered for signal,

single and double Higgs boson events. Their impacts on both the normalisation and shape are included in the statistical analysis for the final results.

The uncertainty in the integrated luminosity for 2015–2018 data taking period is 0.83% [26], obtained using the LUCID-2 detector for the primary luminosity measurement, complemented by measurements using the inner detector and calorimeters.

The uncertainty in the modelling of the pileup distribution in the simulation is estimated to have 2%–3% impacts on yields of signal, single and double Higgs boson events.

The photon reconstruction, identification and isolation efficiencies are measured using three data-driven techniques as mentioned in Ref. [100]. Their effects on yields and shapes are estimated by varying the measured efficiency scale factors between data and simulation, resulting in less than 2% variations for signal yields. Uncertainties in the photon energy scale and resolution described in Ref. [88] are considered as well. These uncertainties affect the signal yield less than 0.5%; a similar impact is found for single Higgs boson and double Higgs bosons events. The uncertainty in the photon trigger efficiency is also considered and its impact on event yields is found to be negligible.

Uncertainties in the electron reconstruction, identification and isolation efficiencies are reported in Ref. [100]. They affect the signal and SM Higgs boson yields by about 2%. Uncertainties in electron energy scale and resolution are also evaluated and found to have a negligible impact.

In addition, uncertainties in muon reconstruction, identification, isolation efficiencies as well as the muon momentum scale and resolution [89], and uncertainties in the jet energy scale and resolution [94] are also considered. Furthermore, uncertainties arising from jet property selections: jet-vertex-tagger [95] and b-jet tagging [101–103] are included. Finally, the uncertainty related to $E_{\mathrm{T}}^{\mathrm{miss}}$ resulting from tracks not associated with the selected objects [97] is considered. All these uncertainties were found to have a negligible impact on the signal and SM Higgs boson yields.

6.3 Continuum background modelling uncertainty

The continuum background estimation (see Section 5) assumes no significant shape differences between the control region (events with no leptons) and the signal region (events with at least one lepton). An uncertainty (called lepton-dependence uncertainty) associated with the background modelling is evaluated by comparing the shape of the $m_{\gamma\gamma}$ distribution in $\gamma\gamma + 0\ell$ events with that in $\gamma\gamma + \ell\nu$jj and $\gamma\gamma + \ell\nu\ell\nu$ events from dedicated MC simulated samples (see Section 3.2.2). The variations between diphoton events with and without leptons are computed using the $m_{\gamma\gamma}$ distribution in the [105, 160] GeV range. The average variation over all bins is about 2% for all signal regions. In addition to lepton-dependence uncertainty, a 2% uncertainty arises from the comparison of the shape of the $m_{\gamma\gamma}$ distribution in the control and the signal regions. The systematic uncertainty arising from a potential bias from the background shape functional form choice is accounted by the spurious signal uncertainty (see Section 5).

7 Results

The contribution of a potential signal in the data is extracted through a simultaneous fit to the $m_{\gamma\gamma}$ distributions in all six signal regions, which is implemented with the RooFit [104] and RooStats [105] frameworks. The fit is performed with a binned likelihood model built from the product of the Poisson

distribution in each bin and region, and including Gaussian distributions to describe the effect of systematic uncertainties. For each $m_{\gamma\gamma}$ distribution, 22 equal width bins in a range of 105 GeV to 160 GeV are used in the fit. The parameter-of-interest is $\sigma(gg \rightarrow X) \times \mathcal{B}(X \rightarrow SH)$ and is left unconstrained in the fit. The shape of the signal for each individual region is obtained from simulated events. Contributions from the single and double Higgs boson processes are estimated from MC simulated samples with their normalisation fixed to SM predictions. Theoretical and experimental uncertainties corresponding to both the signal and the Higgs boson backgrounds are included in the fit and controlled by the nuisance parameters. For the continuum background, the shape is estimated with the method described in Section 5 and kept fixed in the fit, while its normalisation is left unconstrained. In total four individual normalisation factors are included corresponding to 1ℓtight, 1ℓloose, 2ℓtight and 2ℓloose, respectively. The $e\mu$ and $2\ell(ZZ)$ regions share the same normalisation factor for continuum background as the 2ℓtight region. Background shape uncertainty and the spurious signal uncertainty are also considered in the fit and described by the corresponding nuisance parameters. To improve the robustness of the fit, any systematic uncertainty with less than 0.5% impact on either shape or yield is removed from the fit model. With such requirement, only uncertainties related to photon and electron, pileup reweighting, theory, and continuum background estimation are left, and others are ignored during the fit.

Three scenarios are considered for the final results corresponding to three hypotheses on the $S \rightarrow WW/ZZ$ branching ratios: SM-like $\mathcal{B}(S \rightarrow WW/ZZ)$ [19], $\mathcal{B}(S \rightarrow WW) = 100\%$, and $\mathcal{B}(S \rightarrow ZZ) = 100\%$.

Figure 5 presents the $m_{\gamma\gamma}$ distributions in the six signal regions after performing the signal-plus-background fit corresponding to a signal with $m_X = 1000\,\text{GeV}$ and $m_S = 300\,\text{GeV}$ for the SM-like $\mathcal{B}(S \rightarrow WW/ZZ)$ scenario. Other branching-ratio scenarios and signal-mass hypotheses are also tested and no deviation with respect to the SM background expectation is observed. Consequently, 95% CL upper limits are set on $\sigma(gg \rightarrow X) \times \mathcal{B}(X \rightarrow SH)$ for each branching-ratio scenario and signal-mass hypothesis using the profile likelihood ratio technique with the asymptotic approximation [106] and the CL_s [107, 108] method. The results are validated using pseudo-experiments and found to agree within 20%.

Figure 6 shows the 95% CL observed and expected limits on $\sigma(gg \rightarrow X) \times \mathcal{B}(X \rightarrow SH)$ as a function of m_X and m_S for the SM-like $\mathcal{B}(S \rightarrow WW/ZZ)$ scenario. The observed (expected) limit ranges from 530 fb (800 fb) to 120 fb (170 fb) depending on the scalar masses. The results are dominated by the 1ℓtight region, with the other regions contributing with comparably lower sensitivity. In the 1ℓtight region, a slight deficit in the data yield compared to the background expectation is observed across all mass hypotheses, which leads to a better observed limit than the expected one for every mass point.
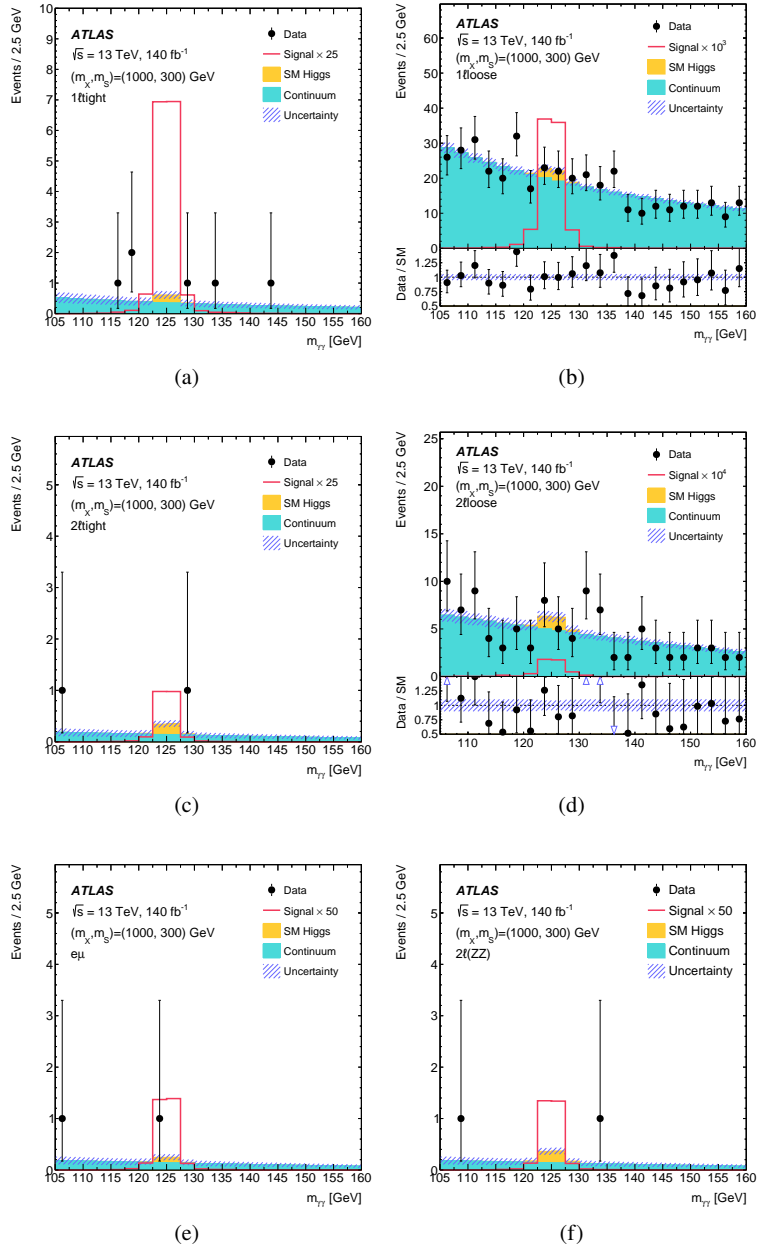
Figure 5: Distribution of $m_{\gamma\gamma}$ after the signal-plus-background fit to data in the (a) 1ℓtight, (b) 1ℓloose, (c) 2ℓtight, (d) 2ℓloose, (e) $e\mu$ and (f) 2$\ell(ZZ)$ regions. The contribution from the SM single and double Higgs boson processes (denoted "SM Higgs"), which is estimated from the MC simulation, is shown added on top of the continuum background distribution. The $(m_X, m_S) = (1000, 300)$ GeV signal prediction (open red histogram) for the scenario of SM-like $\mathscr{B}(S \rightarrow WW/ZZ)$ is also shown, normalised to a cross-section corresponding to the 95% CL upper limit shown in Figure 6. An additional normalisation factor, as indicated in the legend, is applied to scale the signal for visibility.

17
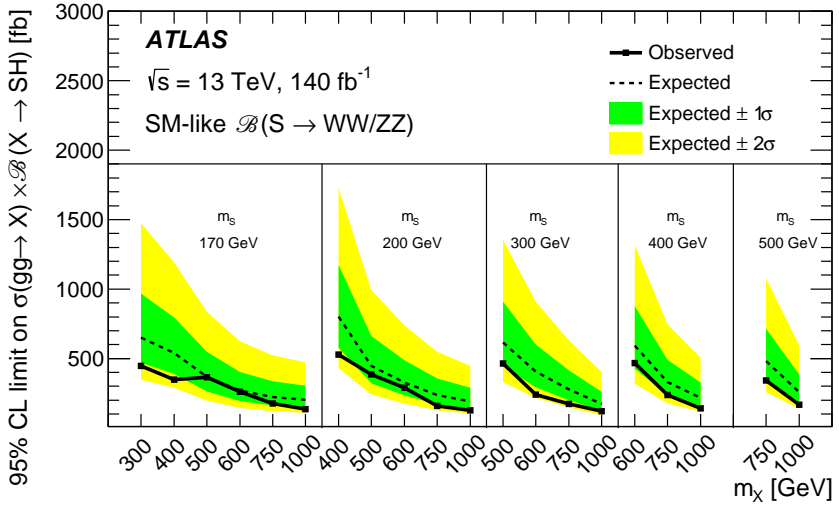
Figure 6: Observed (solid line) and expected (dashed line) 95% CL upper limits on $\sigma(gg \to X) \times \mathscr{B}(X \to SH)$ as a function of m_X and m_S, under the assumption of SM-like $\mathscr{B}(S \to WW/ZZ)$. The green and yellow shaded areas indicate the ± 1 and ± 2 standard deviations around the expected limit.

Limits corresponding to assumptions of the scalar S with a 100% decay branching ratio to WW or ZZ are derived and presented in Figures 7 and 8. Under the assumption that $\mathscr{B}(S \to WW) = 100\%$, the observed limit varies from 470 fb to 91 fb whereas the expected limit ranges from 610 fb to 120 fb. The upper limits under the scenario $\mathscr{B}(S \to ZZ) = 100\%$ are significantly higher: from 1530 fb to 360 fb for observed limits and from 2160 fb to 510 fb for expected limits. The analysis sensitivity is limited by the statistical uncertainty, with systematic uncertainties degrading the expected limits by about 2%.

These results are comparable to the $X \to SH \to VV\tau\tau$ [15] search, which observes an upper limit on the production cross-section from 540 fb to 72 fb, assuming SM-like $\mathscr{B}(S \to WW/ZZ)$. Under the $\mathscr{B}(S \to WW) = 100\%$ and $\mathscr{B}(S \to ZZ) = 100\%$ scenarios, the upper limits on the production cross-section and decay branching ratio are in the ranges $26 - 3$ fb and $33 - 6$ fb, respectively. By correcting by the $\mathscr{B}(H \to \tau\tau)$, these results can be expressed in upper limits on the $X \to SH$ production cross-section, and compared to those obtained by this analysis. These upper limits are set in the ranges $410 - 47$ fb and $520 - 95$ fb for $\mathscr{B}(S \to WW) = 100\%$ and $\mathscr{B}(S \to ZZ) = 100\%$, respectively.
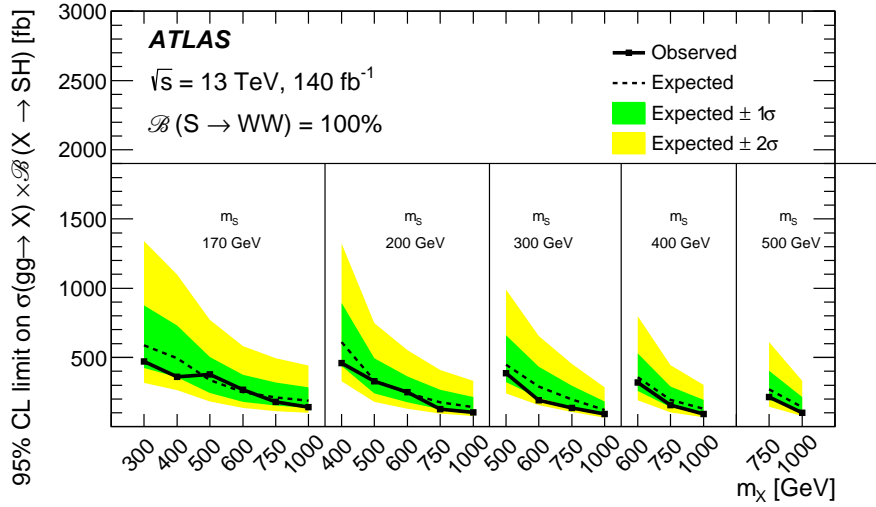
Figure 7: Observed (solid line) and expected (dashed line) 95% CL upper limits on $\sigma(gg \to X) \times \mathcal{B}(X \to SH)$ as a function of m_X and m_S, under the assumption of $\mathcal{B}(S \to WW) = 100\%$. The green and yellow shaded areas indicate the ±1 and ±2 standard deviations around the expected limit.
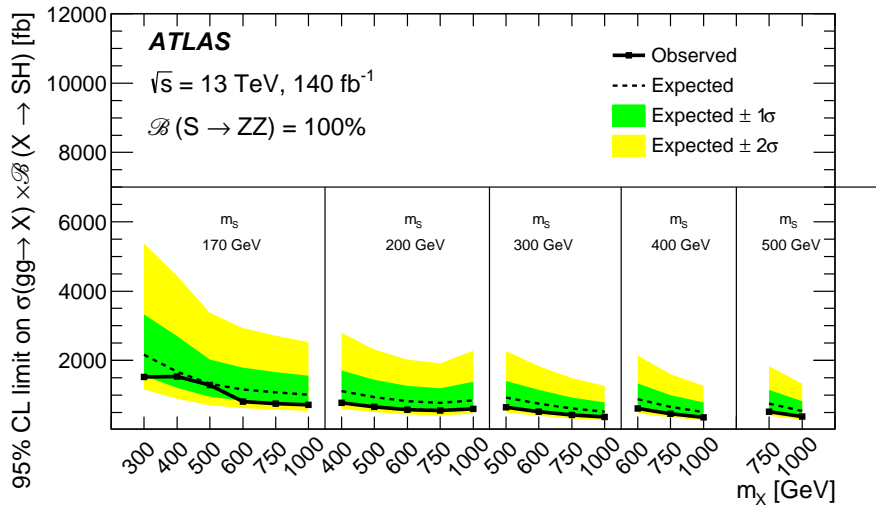
Figure 8: Observed (solid line) and expected (dashed line) 95% CL upper limits on $\sigma(gg \to X) \times \mathcal{B}(X \to SH)$ as a function of m_X and m_S, under the assumption of $\mathcal{B}(S \to ZZ) = 100\%$. The green and yellow shaded areas indicate the ±1 and ±2 standard deviations around the expected limit.

8 Conclusion

This paper presents the first search for the $X \to SH \to VV\gamma\gamma$ process by selecting events with a pair of photons accompanied by one or two leptons (electrons or muons). The analysis is based on 140 fb^{-1} of proton–proton collision data at $\sqrt{s}$ = 13 TeV recorded with the ATLAS detector at the LHC. The $X \to SH \to VV\gamma\gamma$ signal is searched for over the $300 \le m_X \le 1000$ GeV and $170 \le m_S \le 500$ GeV mass ranges, probing lower m_X values than the ATLAS $SH \to VV\tau\tau$ search, and complementing the ATLAS $X \to SH \to bb\gamma\gamma$ search by testing a different S-boson decay mode.

No excess of events above the expected SM background is observed and 95% CL upper limits are set on the cross-section times branching ratio, $\sigma(gg \to X) \times \mathscr{B}(X \to SH)$, under different assumptions for the $S \to WW/ZZ$ branching ratios. The observed (expected) upper limits lie in the range of $530 - 120$ fb $(800 - 170$ fb) under the assumption that $\mathscr{B}(S \to WW/ZZ)$ corresponding to those the SM Higgs boson would have at the mass of the S particle. The corresponding observed (expected) upper limits on the cross-section are in the range of $470 - 91$ fb $(610 - 120$ fb) under the assumption of $\mathscr{B}(S \to WW) = 100\%$. Alternatively, under the assumption of $\mathscr{B}(S \to ZZ) = 100\%$, the observed (expected) limits are in the range of $1530 - 360$ fb $(2160 - 510$ fb).

References

[1] ATLAS Collaboration, *The ATLAS Experiment at the CERN Large Hadron Collider*, JINST **3** (2008) S08003.

[2] CMS Collaboration, *The CMS Experiment at the CERN LHC*, JINST **3** (2008) S08004.

[3] ATLAS Collaboration, *Observation of a new particle in the search for the Standard Model Higgs boson with the ATLAS detector at the LHC*, Phys. Lett. B **716** (2012) 1, arXiv: `1207.7214 [hep-ex]`.

[4] CMS Collaboration, *Observation of a new boson at a mass of 125 GeV with the CMS experiment at the LHC*, Phys. Lett. B **716** (2012) 30, arXiv: `1207.7235 [hep-ex]`.

[5] ATLAS Collaboration, *A detailed map of Higgs boson interactions by the ATLAS experiment ten years after the discovery*, Nature **607** (2022) 52, arXiv: `2207.00092 [hep-ex]`, Erratum: Nature **612** (2022) E24.

[6] CMS Collaboration, *A portrait of the Higgs boson by the CMS experiment ten years after the discovery*, Nature **607** (2022) 60, arXiv: `2207.00043 [hep-ex]`, Erratum: Nature **623** (2023) E4.

[7] U. Ellwanger, C. Hugonie and A. M. Teixeira, *The Next-to-Minimal Supersymmetric Standard Model*, Phys. Rept. **496** (2010) 1, arXiv: `0910.1785 [hep-ph]`.

[8] M. Maniatis, *The Next-to-Minimal Supersymmetric extension of the Standard Model reviewed*, Int. J. Mod. Phys. A **25** (2010) 3505, arXiv: `0906.0777 [hep-ph]`.

[9] T. Robens, T. Stefaniak and J. Wittbrodt, *Two-real-scalar-singlet extension of the SM: LHC phenomenology and benchmark scenarios*, Eur. Phys. J. C **80** (2020) 151, arXiv: `1908.08554 [hep-ph]`.

[10] T. Robens, *Two-Real-Singlet-Model Benchmark Planes*, Symmetry **15** (2023) 27, arXiv: `2209.10996 [hep-ph]`.

[11] G. C. Branco et al., *Theory and phenomenology of two-Higgs-doublet models*, Phys. Rept. **516** (2012) 1, arXiv: `1106.0034 [hep-ph]`.

[12] S. Baum and N. R. Shah, *Two Higgs doublets and a complex singlet: disentangling the decay topologies and associated phenomenology*, JHEP **12** (2018) 044, arXiv: `1808.02667 [hep-ph]`.

[13] ATLAS Collaboration, *Search for Higgs boson pair production in the $WW^{(*)}WW^{(*)}$ decay channel using ATLAS data recorded at $\sqrt{s} = 13\,TeV$*, JHEP **05** (2019) 124, arXiv: `1811.11028 [hep-ex]`.

[14] ATLAS Collaboration, *Search for a resonance decaying into a scalar particle and a Higgs boson in the final state with two bottom quarks and two photons in proton-proton collisions at a center of mass energy of 13 TeV with the ATLAS detector*, (2024), arXiv: `2404.12915 [hep-ex]`.

[15] ATLAS Collaboration, *Search for a new heavy scalar particle decaying into a Higgs boson and a new scalar singlet in final states with one or two light leptons and a pair of τ-leptons with the ATLAS detector*, JHEP **10** (2023) 009, arXiv: `2307.11120 [hep-ex]`.

[16] CMS Collaboration, *Search for a new resonance decaying into two spin-0 bosons in a final state with two photons and two bottom quarks in proton–proton collisions at $\sqrt{s}$ = 13 TeV*, JHEP **05** (2023) 316, arXiv: 2310.01643 [hep-ex].

[17] CMS Collaboration, *Search for a heavy Higgs boson decaying into two lighter Higgs bosons in the $\tau\tau bb$ final state at 13 TeV*, JHEP **11** (2021) 057, arXiv: 2106.10361 [hep-ex].

[18] CMS Collaboration, *Search for a massive scalar resonance decaying to a light scalar and a Higgs boson in the four b quarks final state with boosted topology*, Phys. Lett. B **842** (2023) 137392, arXiv: 2204.12413 [hep-ex].

[19] D. de Florian et al., *Handbook of LHC Higgs Cross Sections: 4. Deciphering the Nature of the Higgs Sector*, (2017), arXiv: 1610.07922 [hep-ph].

[20] ATLAS Collaboration, *Measurements of the Higgs boson inclusive and differential fiducial cross-sections in the diphoton decay channel with pp collisions at $\sqrt{s}$ = 13 TeV with the ATLAS detector*, JHEP **08** (2022) 027, arXiv: 2202.00487 [hep-ex].

[21] ATLAS Collaboration, *ATLAS Insertable B-Layer: Technical Design Report*, ATLAS-TDR-19; CERN-LHCC-2010-013, 2010, URL: https://cds.cern.ch/record/1291633, Addendum: ATLAS-TDR-19-ADD-1; CERN-LHCC-2012-009, 2012, URL: https://cds.cern.ch/record/1451888.

[22] B. Abbott et al., *Production and integration of the ATLAS Insertable B-Layer*, JINST **13** (2018) T05008, arXiv: 1803.00844 [physics.ins-det].

[23] G. Avoni et al., *The new LUCID-2 detector for luminosity measurement and monitoring in ATLAS*, JINST **13** (2018) P07017.

[24] ATLAS Collaboration, *Performance of the ATLAS trigger system in 2015*, Eur. Phys. J. C **77** (2017) 317, arXiv: 1611.09661 [hep-ex].

[25] ATLAS Collaboration, *Software and computing for Run 3 of the ATLAS experiment at the LHC*, (2024), arXiv: 2404.06335 [hep-ex].

[26] ATLAS Collaboration, *Luminosity determination in pp collisions at $\sqrt{s}$ = 13 TeV using the ATLAS detector at the LHC*, Eur. Phys. J. C **83** (2023) 982, arXiv: 2212.09379 [hep-ex].

[27] ATLAS Collaboration, *ATLAS data quality operations and performance for 2015–2018 data-taking*, JINST **15** (2020) P04003, arXiv: 1911.04632 [physics.ins-det].

[28] ATLAS Collaboration, *Performance of electron and photon triggers in ATLAS during LHC Run 2*, Eur. Phys. J. C **80** (2020) 47, arXiv: 1909.00761 [hep-ex].

[29] T. Sjöstrand et al., *An introduction to PYTHIA 8.2*, Comput. Phys. Commun. **191** (2015) 159, arXiv: 1410.3012 [hep-ph].

[30] ATLAS Collaboration, *ATLAS Pythia 8 tunes to 7 TeV data*, ATL-PHYS-PUB-2014-021, 2014, URL: https://cds.cern.ch/record/1966419.

[31] NNPDF Collaboration, R. D. Ball et al., *Parton distributions with LHC data*, Nucl. Phys. B **867** (2013) 244, arXiv: 1207.1303 [hep-ph].

[32] K. Hamilton, P. Nason, E. Re and G. Zanderighi, *NNLOPS simulation of Higgs boson production*, JHEP **10** (2013) 222, arXiv: 1309.0017 [hep-ph].

[33] K. Hamilton, P. Nason and G. Zanderighi, *Finite quark-mass effects in the NNLOPS POWHEG+MiNLO Higgs generator*, JHEP **05** (2015) 140, arXiv: 1501.04637 [hep-ph].

[34] S. Alioli, P. Nason, C. Oleari and E. Re, *A general framework for implementing NLO calculations in shower Monte Carlo programs: the POWHEG BOX*, JHEP **06** (2010) 043, arXiv: 1002.2581 [hep-ph].

[35] P. Nason, *A new method for combining NLO QCD with shower Monte Carlo algorithms*, JHEP **11** (2004) 040, arXiv: hep-ph/0409146.

[36] S. Frixione, P. Nason and C. Oleari, *Matching NLO QCD computations with parton shower simulations: the POWHEG method*, JHEP **11** (2007) 070, arXiv: 0709.2092 [hep-ph].

[37] K. Hamilton, P. Nason and G. Zanderighi, *MINLO: multi-scale improved NLO*, JHEP **10** (2012) 155, arXiv: 1206.3572 [hep-ph].

[38] J. M. Campbell et al., *NLO Higgs boson production plus one and two jets using the POWHEG BOX, MadGraph4 and MCFM*, JHEP **07** (2012) 092, arXiv: 1202.5475 [hep-ph].

[39] K. Hamilton, P. Nason, C. Oleari and G. Zanderighi, *Merging H/W/Z + 0 and 1 jet at NLO with no merging scale: a path to parton shower + NNLO matching*, JHEP **05** (2013) 082, arXiv: 1212.4504 [hep-ph].

[40] S. Catani and M. Grazzini, *Next-to-Next-to-Leading-Order Subtraction Formalism in Hadron Collisions and its Application to Higgs-Boson Production at the Large Hadron Collider*, Phys. Rev. Lett. **98** (2007) 222002, arXiv: hep-ph/0703012 [hep-ph].

[41] J. Butterworth et al., *PDF4LHC recommendations for LHC Run II*, J. Phys. G **43** (2016) 023001, arXiv: 1510.03865 [hep-ph].

[42] ATLAS Collaboration, *Measurement of the Z/γ^* boson transverse momentum distribution in pp collisions at $\sqrt{s} = 7$ TeV with the ATLAS detector*, JHEP **09** (2014) 145, arXiv: 1406.3660 [hep-ex].

[43] D. J. Lange, *The EvtGen particle decay simulation package*, Nucl. Instrum. Meth. A **462** (2001) 152.

[44] C. Anastasiou et al., *High precision determination of the gluon fusion Higgs boson cross-section at the LHC*, JHEP **05** (2016) 058, arXiv: 1602.00695 [hep-ph].

[45] C. Anastasiou, C. Duhr, F. Dulat, F. Herzog and B. Mistlberger, *Higgs Boson Gluon-Fusion Production in QCD at Three Loops*, Phys. Rev. Lett. **114** (2015) 212001, arXiv: 1503.06056 [hep-ph].

[46] F. Dulat, A. Lazopoulos and B. Mistlberger, *iHixs 2 – Inclusive Higgs cross sections*, Comput. Phys. Commun. **233** (2018) 243, arXiv: 1802.00827 [hep-ph].

[47] R. V. Harlander and K. J. Ozeren, *Finite top mass effects for hadronic Higgs production at next-to-next-to-leading order*, JHEP **11** (2009) 088, arXiv: 0909.3420 [hep-ph].

[48] R. V. Harlander and K. J. Ozeren,
Top mass effects in Higgs production at next-to-next-to-leading order QCD: Virtual corrections,
Phys. Lett. B **679** (2009) 467, arXiv: `0907.2997 [hep-ph]`.

[49] R. V. Harlander, H. Mantler, S. Marzani and K. J. Ozeren,
Higgs production in gluon fusion at next-to-next-to-leading order QCD for finite top mass,
Eur. Phys. J. C **66** (2010) 359, arXiv: `0912.2104 [hep-ph]`.

[50] A. Pak, M. Rogal and M. Steinhauser,
Finite top quark mass effects in NNLO Higgs boson production at LHC, JHEP **02** (2010) 025,
arXiv: `0911.4662 [hep-ph]`.

[51] S. Actis, G. Passarino, C. Sturm and S. Uccirati,
NLO electroweak corrections to Higgs boson production at hadron colliders,
Phys. Lett. B **670** (2008) 12, arXiv: `0809.1301 [hep-ph]`.

[52] S. Actis, G. Passarino, C. Sturm and S. Uccirati,
NNLO computational techniques: The cases $H \rightarrow \gamma\gamma$ and $H \rightarrow gg$, Nucl. Phys. B **811** (2009) 182,
arXiv: `0809.3667 [hep-ph]`.

[53] M. Bonetti, K. Melnikov and L. Tancredi, *Higher order corrections to mixed QCD-EW
contributions to Higgs boson production in gluon fusion*, Phys. Rev. D **97** (2018) 056017,
arXiv: `1801.10403 [hep-ph]`, Erratum: Phys. Rev. D **97** (2018) 099906(E).

[54] M. Ciccolini, A. Denner and S. Dittmaier, *Strong and Electroweak Corrections to the Production
of a Higgs Boson + 2 Jets via Weak Interactions at the Large Hadron Collider*,
Phys. Rev. Lett. **99** (2007) 161803, arXiv: `0707.0381 [hep-ph]`.

[55] M. Ciccolini, A. Denner and S. Dittmaier,
Electroweak and QCD corrections to Higgs production via vector-boson fusion at the CERN LHC,
Phys. Rev. D **77** (2008) 013002, arXiv: `0710.4749 [hep-ph]`.

[56] P. Bolzoni, F. Maltoni, S.-O. Moch and M. Zaro,
Higgs Boson Production via Vector-Boson Fusion at Next-to-Next-to-Leading Order in QCD,
Phys. Rev. Lett. **105** (2010) 011801, arXiv: `1003.4451 [hep-ph]`.

[57] G. Luisoni, P. Nason, C. Oleari and F. Tramontano, *$HW^{\pm}/HZ$ + 0 and 1 jet at NLO with the
POWHEG BOX interfaced to GoSam and their merging within MiNLO*, JHEP **10** (2013) 083,
arXiv: `1306.2542 [hep-ph]`.

[58] M. L. Ciccolini, S. Dittmaier and M. Krämer,
Electroweak radiative corrections to associated WH and ZH production at hadron colliders,
Phys. Rev. D **68** (2003) 073003, arXiv: `hep-ph/0306234 [hep-ph]`.

[59] O. Brein, A. Djouadi and R. Harlander,
NNLO QCD corrections to the Higgs-strahlung processes at hadron colliders,
Phys. Lett. B **579** (2004) 149, arXiv: `hep-ph/0307206`.

[60] O. Brein, R. V. Harlander, M. Wiesemann and T. Zirke,
Top-quark mediated effects in hadronic Higgs-Strahlung, Eur. Phys. J. C **72** (2012) 1868,
arXiv: `1111.0761 [hep-ph]`.

[61] L. Altenkamp, S. Dittmaier, R. V. Harlander, H. Rzehak and T. J. E. Zirke,
Gluon-induced Higgs-strahlung at next-to-leading order QCD, JHEP **02** (2013) 078,
arXiv: `1211.5015 [hep-ph]`.

[62] A. Denner, S. Dittmaier, S. Kallweit and A. Mück, *HAWK 2.0: A Monte Carlo program for Higgs production in vector-boson fusion and Higgs strahlung at hadron colliders*, Comput. Phys. Commun. **195** (2015) 161, arXiv: 1412.5390 [hep-ph].

[63] O. Brein, R. V. Harlander and T. J. E. Zirke, *vh@nnlo – Higgs Strahlung at hadron colliders*, Comput. Phys. Commun. **184** (2013) 998, arXiv: 1210.5347 [hep-ph].

[64] R. V. Harlander, A. Kulesza, V. Theeuwes and T. Zirke, *Soft gluon resummation for gluon-induced Higgs Strahlung*, JHEP **11** (2014) 082, arXiv: 1410.0217 [hep-ph].

[65] NNPDF Collaboration, R. D. Ball et al., *Parton distributions for the LHC run II*, JHEP **04** (2015) 040, arXiv: 1410.8849 [hep-ph].

[66] J. Alwall et al., *The automated computation of tree-level and next-to-leading order differential cross sections, and their matching to parton shower simulations*, JHEP **07** (2014) 079, arXiv: 1405.0301 [hep-ph].

[67] A. Djouadi, J. Kalinowski and M. Spira, *HDECAY: a program for Higgs boson decays in the Standard Model and its supersymmetric extension*, Comput. Phys. Commun. **108** (1998) 56, arXiv: hep-ph/9704448.

[68] M. Spira, *QCD effects in Higgs physics*, Fortsch. Phys. **46** (1999) 203, arXiv: hep-ph/9705337.

[69] A. Djouadi, M. M. Mühlleitner and M. Spira, *Decays of Supersymmetric Particles: the Program SUSY-HIT (SUspect-SdecaY-Hdecay-InTerface)*, Acta Phys. Polon. B **38** (2007) 635, arXiv: hep-ph/0609292.

[70] A. Bredenstein, A. Denner, S. Dittmaier and M. M. Weber, *Radiative corrections to the semileptonic and hadronic Higgs-boson decays H → WW/ZZ → 4 fermions*, JHEP **02** (2007) 080, arXiv: hep-ph/0611234.

[71] A. Bredenstein, A. Denner, S. Dittmaier and M. M. Weber, *Precise predictions for the Higgs-boson decay H → WW/ZZ → 4 leptons*, Phys. Rev. D **74** (2006) 013004, arXiv: hep-ph/0604011 [hep-ph].

[72] A. Bredenstein, A. Denner, S. Dittmaier and M. M. Weber, *Precision calculations for the Higgs decays H —> ZZ/WW —> 4 leptons*, Nucl. Phys. B Proc. Suppl. **160** (2006) 131, ed. by J. Blumlein, S. Moch and T. Riemann, arXiv: hep-ph/0607060.

[73] E. Bothmann et al., *Event generation with Sherpa 2.2*, SciPost Phys. **7** (2019) 034, arXiv: 1905.09127 [hep-ph].

[74] T. Gleisberg and S. Höche, *Comix, a new matrix element generator*, JHEP **12** (2008) 039, arXiv: 0808.3674 [hep-ph].

[75] F. Cascioli, P. Maierhöfer and S. Pozzorini, *Scattering Amplitudes with Open Loops*, Phys. Rev. Lett. **108** (2012) 111601, arXiv: 1111.5206 [hep-ph].

[76] A. Denner, S. Dittmaier and L. Hofer, *Collier: A fortran-based complex one-loop library in extended regularizations*, Comput. Phys. Commun. **212** (2017) 220, arXiv: 1604.06792 [hep-ph].

[77] S. Schumann and F. Krauss, *A parton shower algorithm based on Catani-Seymour dipole factorisation*, JHEP **03** (2008) 038, arXiv: 0709.1027 [hep-ph].

[78] S. Catani, F. Krauss, B. R. Webber and R. Kuhn, *QCD Matrix Elements + Parton Showers*, JHEP **11** (2001) 063, arXiv: `hep-ph/0109231`.

[79] S. Höche, F. Krauss, S. Schumann and F. Siegert, *QCD matrix elements and truncated showers*, JHEP **05** (2009) 053, arXiv: `0903.1219 [hep-ph]`.

[80] S. Höche, F. Krauss, M. Schönherr and F. Siegert, *A critical appraisal of NLO+PS matching methods*, JHEP **09** (2012) 049, arXiv: `1111.1220 [hep-ph]`.

[81] S. Höche, F. Krauss, M. Schönherr and F. Siegert, *QCD matrix elements + parton showers. The NLO case*, JHEP **04** (2013) 027, arXiv: `1207.5030 [hep-ph]`.

[82] S. Agostinelli et al., *Geant4 – a simulation toolkit*, Nucl. Instrum. Meth. A **506** (2003) 250.

[83] ATLAS Collaboration, *The ATLAS Simulation Infrastructure*, Eur. Phys. J. C **70** (2010) 823, arXiv: `1005.4568 [physics.ins-det]`.

[84] ATLAS Collaboration, *The simulation principle and performance of the ATLAS fast calorimeter simulation FastCaloSim*, ATL-PHYS-PUB-2010-013, 2010, URL: `https://cds.cern.ch/record/1300517`.

[85] T. Sjöstrand, S. Mrenna and P. Skands, *A brief introduction to PYTHIA 8.1*, Comput. Phys. Commun. **178** (2008) 852, arXiv: `0710.3820 [hep-ph]`.

[86] ATLAS Collaboration, *The Pythia 8 A3 tune description of ATLAS minimum bias and inelastic measurements incorporating the Donnachie–Landshoff diffractive model*, ATL-PHYS-PUB-2016-017, 2016, URL: `https://cds.cern.ch/record/2206965`.

[87] ATLAS Collaboration, *Measurement of Higgs boson production in the diphoton decay channel in pp collisions at center-of-mass energies of 7 and 8 TeV with the ATLAS detector*, Phys. Rev. D **90** (2014) 112015, arXiv: `1408.7084 [hep-ex]`.

[88] ATLAS Collaboration, *Electron and photon performance measurements with the ATLAS detector using the 2015–2017 LHC proton–proton collision data*, JINST **14** (2019) P12006, arXiv: `1908.00005 [hep-ex]`.

[89] ATLAS Collaboration, *Muon reconstruction and identification efficiency in ATLAS using the full Run 2 pp collision data set at $\sqrt{s} = 13$ TeV*, Eur. Phys. J. C **81** (2021) 578, arXiv: `2012.00578 [hep-ex]`.

[90] ATLAS Collaboration, *Jet reconstruction and performance using particle flow with the ATLAS Detector*, Eur. Phys. J. C **77** (2017) 466, arXiv: `1703.10485 [hep-ex]`.

[91] ATLAS Collaboration, *Topological cell clustering in the ATLAS calorimeters and its performance in LHC Run 1*, Eur. Phys. J. C **77** (2017) 490, arXiv: `1603.02934 [hep-ex]`.

[92] M. Cacciari, G. P. Salam and G. Soyez, *FastJet user manual*, Eur. Phys. J. C **72** (2012) 1896, arXiv: `1111.6097 [hep-ph]`.

[93] M. Cacciari, G. P. Salam and G. Soyez, *The anti-k_t jet clustering algorithm*, JHEP **04** (2008) 063, arXiv: `0802.1189 [hep-ph]`.

[94]   ATLAS Collaboration, *Jet energy scale and resolution measured in proton–proton collisions at* $\sqrt{s} = 13\,TeV$ *with the ATLAS detector*, Eur. Phys. J. C **81** (2021) 689, arXiv: 2007.02645 [hep-ex].

[95]   ATLAS Collaboration, *Performance of pile-up mitigation techniques for jets in pp collisions at* $\sqrt{s} = 8\,TeV$ *using the ATLAS detector*, Eur. Phys. J. C **76** (2016) 581, arXiv: 1510.03823 [hep-ex].

[96]   ATLAS Collaboration, *ATLAS flavour-tagging algorithms for the LHC Run 2 pp collision dataset*, Eur. Phys. J. C **83** (2023) 681, arXiv: 2211.16345 [physics.data-an].

[97]   ATLAS Collaboration, *The performance of missing transverse momentum reconstruction and its significance with the ATLAS detector using* $140\,fb^{-1}$ *of* $\sqrt{s} = 13\,TeV\,pp$ *collisions*, (2024), arXiv: 2402.05858 [hep-ex].

[98]   P. Baldi, K. Cranmer, T. Faucett, P. Sadowski and D. Whiteson, *Parameterized neural networks for high-energy physics*, Eur. Phys. J. C **76** (2016) 235, arXiv: 1601.07913 [hep-ex].

[99]   ATLAS Collaboration, *Recommendations for the Modeling of Smooth Backgrounds*, ATL-PHYS-PUB-2020-028, 2020, URL: https://cds.cern.ch/record/2743717.

[100] ATLAS Collaboration, *Electron and photon efficiencies in LHC Run 2 with the ATLAS experiment*, JHEP **05** (2023) 162, arXiv: 2308.13362 [hep-ex].

[101] ATLAS Collaboration, *ATLAS b-jet identification performance and efficiency measurement with* $t\bar{t}$ *events in pp collisions at* $\sqrt{s} = 13\,TeV$, Eur. Phys. J. C **79** (2019) 970, arXiv: 1907.05120 [hep-ex].

[102] ATLAS Collaboration, *Measurement of the c-jet mistagging efficiency in* $t\bar{t}$ *events using pp collision data at* $\sqrt{s} = 13\,TeV$ *collected with the ATLAS detector*, Eur. Phys. J. C **82** (2022) 95, arXiv: 2109.10627 [hep-ex].

[103] ATLAS Collaboration, *Calibration of the light-flavour jet mistagging efficiency of the b-tagging algorithms with Z+jets events using* $139\,fb^{-1}$ *of ATLAS proton–proton collision data at* $\sqrt{s} = 13\,TeV$, Eur. Phys. J. C **83** (2023) 728, arXiv: 2301.06319 [hep-ex].

[104] W. Verkerke and D. Kirkby, *The RooFit toolkit for data modeling*, 2003, arXiv: physics/0306116 [physics.data-an].

[105] L. Moneta et al., *The RooStats Project*, PoS **ACAT2010** (2010) 057, ed. by T. Speer et al., arXiv: 1009.1003 [physics.data-an].

[106] G. Cowan, K. Cranmer, E. Gross and O. Vitells, *Asymptotic formulae for likelihood-based tests of new physics*, Eur. Phys. J. C **71** (2011) 1554, arXiv: 1007.1727 [physics.data-an], Erratum: Eur. Phys. J. C 73, 2501 (2013).

[107] A. L. Read, *Presentation of search results: the* CL_s *technique*, J. Phys. G **28** (2002) 2693, ed. by M. R. Whalley and L. Lyons.

[108] T. Junk, *Confidence level computation for combining searches with small statistics*, Nucl. Instrum. Meth. A **434** (1999) 435, arXiv: hep-ex/9902006.

[109] ATLAS Collaboration, *ATLAS Computing Acknowledgements*, ATL-SOFT-PUB-2023-001, 2023, URL: https://cds.cern.ch/record/2869272.

The ATLAS Collaboration

G. Aad [103], E. Aakvaag [16], B. Abbott [121], K. Abeling [55], N.J. Abicht [49], S.H. Abidi [29],
M. Aboelela [44], A. Aboulhorma [35e], H. Abramowicz [152], H. Abreu [151], Y. Abulaiti [118],
B.S. Acharya [69a,69b,l], A. Ackermann [63a], C. Adam Bourdarios [4], L. Adamczyk [86a],
S.V. Addepalli [26], M.J. Addison [102], J. Adelman [116], A. Adiguzel [21c], T. Adye [135],
A.A. Affolder [137], Y. Afik [39], M.N. Agaras [13], J. Agarwala [73a,73b], A. Aggarwal [101],
C. Agheorghiesei [27c], A. Ahmad [36], F. Ahmadov [38,z], W.S. Ahmed [105], S. Ahuja [96], X. Ai [62e],
G. Aielli [76a,76b], A. Aikot [164], M. Ait Tamlihat [35e], B. Aitbenchikh [35a], I. Aizenberg [170],
M. Akbiyik [101], T.P.A. Åkesson [99], A.V. Akimov [37], D. Akiyama [169], N.N. Akolkar [24],
S. Aktas [21a], K. Al Khoury [41], G.L. Alberghi [23b], J. Albert [166], P. Albicocco [53], G.L. Albouy [60],
S. Alderweireldt [52], Z.L. Alegria [122], M. Aleksa [36], I.N. Aleksandrov [38], C. Alexa [27b],
T. Alexopoulos [10], F. Alfonsi [23b], M. Algren [56], M. Alhroob [142], B. Ali [133], H.M.J. Ali [92],
S. Ali [149], S.W. Alibocus [93], M. Aliev [33c], G. Alimonti [71a], W. Alkakhi [55], C. Allaire [66],
B.M.M. Allbrooke [147], J.F. Allen [52], C.A. Allendes Flores [138f], P.P. Allport [20], A. Aloisio [72a,72b],
F. Alonso [91], C. Alpigiani [139], M. Alvarez Estevez [100], A. Alvarez Fernandez [101],
M. Alves Cardoso [56], M.G. Alviggi [72a,72b], M. Aly [102], Y. Amaral Coutinho [83b], A. Ambler [105],
C. Amelung[36], M. Amerl [102], C.G. Ames [110], D. Amidei [107], K.J. Amirie [156],
S.P. Amor Dos Santos [131a], K.R. Amos [164], V. Ananiev [126], C. Anastopoulos [140], T. Andeen [11],
J.K. Anders [36], S.Y. Andrean [47a,47b], A. Andreazza [71a,71b], S. Angelidakis [9], A. Angerami [41,ab],
A.V. Anisenkov [37], A. Annovi [74a], C. Antel [56], M.T. Anthony [140], E. Antipov [146],
M. Antonelli [53], F. Anulli [75a], M. Aoki [84], T. Aoki [154], J.A. Aparisi Pozo [164], M.A. Aparo [147],
L. Aperio Bella [48], C. Appelt [18], A. Apyan [26], S.J. Arbiol Val [87], C. Arcangeletti [53],
A.T.H. Arce [51], E. Arena [93], J-F. Arguin [109], S. Argyropoulos [54], J.-H. Arling [48], O. Arnaez [4],
H. Arnold [115], G. Artoni [75a,75b], H. Asada [112], K. Asai [119], S. Asai [154], N.A. Asbah [36],
K. Assamagan [29], R. Astalos [28a], S. Atashi [160], R.J. Atkin [33a], M. Atkinson[163], H. Atmani[35f],
P.A. Atmasiddha [129], K. Augsten [133], S. Auricchio [72a,72b], A.D. Auriol [20], V.A. Austrup [102],
G. Avolio [36], K. Axiotis [56], G. Azuelos [109,af], D. Babal [28b], H. Bachacou [136], K. Bachas [153,p],
A. Bachiu [34], F. Backman [47a,47b], A. Badea [39], T.M. Baer [107], P. Bagnaia [75a,75b],
M. Bahmani [18], D. Bahner [54], K. Bai [124], A.J. Bailey [164], J.T. Baines [135], L. Baines [95],
O.K. Baker [173], E. Bakos [15], D. Bakshi Gupta [8], V. Balakrishnan [121], R. Balasubramanian [115],
E.M. Baldin [37], P. Balek [86a], E. Ballabene [23b,23a], F. Balli [136], L.M. Baltes [63a], W.K. Balunas [32],
J. Balz [101], E. Banas [87], M. Bandieramonte [130], A. Bandyopadhyay [24], S. Bansal [24],
L. Barak [152], M. Barakat [48], E.L. Barberio [106], D. Barberis [57b,57a], M. Barbero [103],
M.Z. Barel [115], K.N. Barends [33a], T. Barillari [111], M-S. Barisits [36], T. Barklow [144], P. Baron [123],
D.A. Baron Moreno [102], A. Baroncelli [62a], G. Barone [29], A.J. Barr [127], J.D. Barr [97],
F. Barreiro [100], J. Barreiro Guimarães da Costa [14a], U. Barron [152], M.G. Barros Teixeira [131a],
S. Barsov [37], F. Bartels [63a], R. Bartoldus [144], A.E. Barton [92], P. Bartos [28a], A. Basan [101],
M. Baselga [49], A. Bassalat [66,b], M.J. Basso [157a], R.L. Bates [59], S. Batlamous[35e], B. Batool [142],
M. Battaglia [137], D. Battulga [18], M. Bauce [75a,75b], M. Bauer [36], P. Bauer [24],
L.T. Bazzano Hurrell [30], J.B. Beacham [51], T. Beau [128], J.Y. Beaucamp [91], P.H. Beauchemin [159],
P. Bechtle [24], H.P. Beck [19,o], K. Becker [168], A.J. Beddall [82], V.A. Bednyakov [38], C.P. Bee [146],
L.J. Beemster [15], T.A. Beermann [36], M. Begalli [83d], M. Begel [29], A. Behera [146], J.K. Behr [48],
J.F. Beirer [36], F. Beisiegel [24], M. Belfkir [117b], G. Bella [152], L. Bellagamba [23b], A. Bellerive [34],
P. Bellos [20], K. Beloborodov [37], D. Benchekroun [35a], F. Bendebba [35a], Y. Benhammou [152],
K.C. Benkendorfer [61], L. Beresford [48], M. Beretta [53], E. Bergeaas Kuutmann [162], N. Berger [4],

B. Bergmann [133], J. Beringer [17a], G. Bernardi [5], C. Bernius [144], F.U. Bernlochner [24],
F. Bernon [36,103], A. Berrocal Guardia [13], T. Berry [96], P. Berta [134], A. Berthold [50], S. Bethke [111],
A. Betti [75a,75b], A.J. Bevan [95], N.K. Bhalla [54], M. Bhamjee [33c], S. Bhatta [146],
D.S. Bhattacharya [167], P. Bhattarai [144], K.D. Bhide [54], V.S. Bhopatkar [122], R.M. Bianchi [130],
G. Bianco [23b,23a], O. Biebel [110], R. Bielski [124], M. Biglietti [77a], C.S. Billingsley[44], M. Bindi [55],
A. Bingul [21b], C. Bini [75a,75b], A. Biondini [93], C.J. Birch-sykes [102], G.A. Bird [32], M. Birman [170],
M. Biros [134], S. Biryukov [147], T. Bisanz [49], E. Bisceglie [43b,43a], J.P. Biswal [135], D. Biswas [142],
K. Bjørke [126], I. Bloch [48], A. Blue [59], U. Blumenschein [95], J. Blumenthal [101],
V.S. Bobrovnikov [37], M. Boehler [54], B. Boehm [167], D. Bogavac [36], A.G. Bogdanchikov [37],
C. Bohm [47a], V. Boisvert [96], P. Bokan [36], T. Bold [86a], M. Bomben [5], M. Bona [95],
M. Boonekamp [136], C.D. Booth [96], A.G. Borbély [59], I.S. Bordulev [37], H.M. Borecka-Bielska [109],
G. Borissov [92], D. Bortoletto [127], D. Boscherini [23b], M. Bosman [13], J.D. Bossio Sola [36],
K. Bouaouda [35a], N. Bouchhar [164], J. Boudreau [130], E.V. Bouhova-Thacker [92], D. Boumediene [40],
R. Bouquet [57b,57a], A. Boveia [120], J. Boyd [36], D. Boye [29], I.R. Boyko [38], J. Bracinik [20],
N. Brahimi [4], G. Brandt [172], O. Brandt [32], F. Braren [48], B. Brau [104], J.E. Brau [124],
R. Brener [170], L. Brenner [115], R. Brenner [162], S. Bressler [170], D. Britton [59], D. Britzger [111],
I. Brock [24], R. Brock [108], G. Brooijmans [41], E. Brost [29], L.M. Brown [166], L.E. Bruce [61],
T.L. Bruckler [127], P.A. Bruckman de Renstrom [87], B. Brüers [48], A. Bruni [23b], G. Bruni [23b],
D. Brunner [47b], M. Bruschi [23b], N. Bruscino [75a,75b], T. Buanes [16], Q. Buat [139], D. Buchin [111],
A.G. Buckley [59], O. Bulekov [37], B.A. Bullard [144], S. Burdin [93], C.D. Burgard [49],
A.M. Burger [36], B. Burghgrave [8], O. Burlayenko [54], J.T.P. Burr [32], C.D. Burton [11],
J.C. Burzynski [143], E.L. Busch [41], V. Büscher [101], P.J. Bussey [59], J.M. Butler [25], C.M. Buttar [59],
J.M. Butterworth [97], W. Buttinger [135], C.J. Buxo Vazquez [108], A.R. Buzykaev [37],
S. Cabrera Urbán [164], L. Cadamuro [66], D. Caforio [58], H. Cai [130], Y. Cai [14a,14e], Y. Cai [14c],
V.M.M. Cairo [36], O. Cakir [3a], N. Calace [36], P. Calafiura [17a], G. Calderini [128], P. Calfayan [68],
G. Callea [59], L.P. Caloba[83b], D. Calvet [40], S. Calvet [40], M. Calvetti [74a,74b], R. Camacho Toro [128],
S. Camarda [36], D. Camarero Munoz [26], P. Camarri [76a,76b], M.T. Camerlingo [72a,72b],
D. Cameron [36], C. Camincher [166], M. Campanelli [97], A. Camplani [42], V. Canale [72a,72b],
A.C. Canbay [3a], J. Cantero [164], Y. Cao [163], F. Capocasa [26], M. Capua [43b,43a], A. Carbone [71a,71b],
R. Cardarelli [76a], J.C.J. Cardenas [8], F. Cardillo [164], G. Carducci [43b,43a], T. Carli [36],
G. Carlino [72a], J.I. Carlotto [13], B.T. Carlson [130,q], E.M. Carlson [166,157a], L. Carminati [71a,71b],
A. Carnelli [136], M. Carnesale [75a,75b], S. Caron [114], E. Carquin [138f], S. Carrá [71a],
G. Carratta [23b,23a], A.M. Carroll [124], T.M. Carter [52], M.P. Casado [13,i], M. Caspar [48],
F.L. Castillo [4], L. Castillo Garcia [13], V. Castillo Gimenez [164], N.F. Castro [131a,131e],
A. Catinaccio [36], J.R. Catmore [126], T. Cavaliere [4], V. Cavaliere [29], N. Cavalli [23b,23a],
Y.C. Cekmecelioglu [48], E. Celebi [21a], S. Cella [36], F. Celli [127], M.S. Centonze [70a,70b],
V. Cepaitis [56], K. Cerny [123], A.S. Cerqueira [83a], A. Cerri [147], L. Cerrito [76a,76b], F. Cerutti [17a],
B. Cervato [142], A. Cervelli [23b], G. Cesarini [53], S.A. Cetin [82], D. Chakraborty [116], J. Chan [17a],
W.Y. Chan [154], J.D. Chapman [32], E. Chapon [136], B. Chargeishvili [150b], D.G. Charlton [20],
M. Chatterjee [19], C. Chauhan [134], Y. Che [14c], S. Chekanov [6], S.V. Chekulaev [157a],
G.A. Chelkov [38,a], A. Chen [107], B. Chen [152], B. Chen [166], H. Chen [14c], H. Chen [29],
J. Chen [62c], J. Chen [143], M. Chen [127], S. Chen [154], S.J. Chen [14c], X. Chen [62c,136],
X. Chen [14b,ae], Y. Chen [62a], C.L. Cheng [171], H.C. Cheng [64a], S. Cheong [144], A. Cheplakov [38],
E. Cheremushkina [48], E. Cherepanova [115], R. Cherkaoui El Moursli [35e], E. Cheu [7], K. Cheung [65],
L. Chevalier [136], V. Chiarella [53], G. Chiarelli [74a], N. Chiedde [103], G. Chiodini [70a],
A.S. Chisholm [20], A. Chitan [27b], M. Chitishvili [164], M.V. Chizhov [38,r], K. Choi [11], Y. Chou [139],
E.Y.S. Chow [114], K.L. Chu [170], M.C. Chu [64a], X. Chu [14a,14e], J. Chudoba [132],

J.J. Chwastowski [87], D. Cieri [111], K.M. Ciesla [86a], V. Cindro [94], A. Ciocio [17a], F. Cirotto [72a,72b],
Z.H. Citron [170], M. Citterio [71a], D.A. Ciubotaru [27b], A. Clark [56], P.J. Clark [52], C. Clarry [156],
J.M. Clavijo Columbie [48], S.E. Clawson [48], C. Clement [47a,47b], J. Clercx [48], Y. Coadou [103],
M. Cobal [69a,69c], A. Coccaro [57b], R.F. Coelho Barrue [131a], R. Coelho Lopes De Sa [104],
S. Coelli [71a], B. Cole [41], J. Collot [60], P. Conde Muiño [131a,131g], M.P. Connell [33c],
S.H. Connell [33c], E.I. Conroy [127], F. Conventi [72a,ag], H.G. Cooke [20], A.M. Cooper-Sarkar [127],
A. Cordeiro Oudot Choi [128], L.D. Corpe [40], M. Corradi [75a,75b], F. Corriveau [105,x],
A. Cortes-Gonzalez [18], M.J. Costa [164], F. Costanza [4], D. Costanzo [140], B.M. Cote [120],
G. Cowan [96], K. Cranmer [171], D. Cremonini [23b,23a], S. Crépé-Renaudin [60], F. Crescioli [128],
M. Cristinziani [142], M. Cristoforetti [78a,78b], V. Croft [115], J.E. Crosby [122], G. Crosetti [43b,43a],
A. Cueto [100], T. Cuhadar Donszelmann [160], H. Cui [14a,14e], Z. Cui [7], W.R. Cunningham [59],
F. Curcio [164], J.R. Curran [52], P. Czodrowski [36], M.M. Czurylo [36],
M.J. Da Cunha Sargedas De Sousa [57b,57a], J.V. Da Fonseca Pinto [83b], C. Da Via [102],
W. Dabrowski [86a], T. Dado [49], S. Dahbi [149], T. Dai [107], D. Dal Santo [19], C. Dallapiccola [104],
M. Dam [42], G. D'amen [29], V. D'Amico [110], J. Damp [101], J.R. Dandoy [34], M. Danninger [143],
V. Dao [36], G. Darbo [57b], S. Darmora [6], S.J. Das [29,ah], S. D'Auria [71a,71b], A. D'Avanzo [131a],
C. David [33a], T. Davidek [134], B. Davis-Purcell [34], I. Dawson [95], H.A. Day-hall [133], K. De [8],
R. De Asmundis [72a], N. De Biase [48], S. De Castro [23b,23a], N. De Groot [114], P. de Jong [115],
H. De la Torre [116], A. De Maria [14c], A. De Salvo [75a], U. De Sanctis [76a,76b], F. De Santis [70a,70b],
A. De Santo [147], J.B. De Vivie De Regie [60], D.V. Dedovich [38], J. Degens [115], A.M. Deiana [44],
F. Del Corso [23b,23a], J. Del Peso [100], F. Del Rio [63a], L. Delagrange [128], F. Deliot [136],
C.M. Delitzsch [49], M. Della Pietra [72a,72b], D. Della Volpe [56], A. Dell'Acqua [36],
L. Dell'Asta [71a,71b], M. Delmastro [4], P.A. Delsart [60], S. Demers [173], M. Demichev [38],
S.P. Denisov [37], L. D'Eramo [40], D. Derendarz [87], F. Derue [128], P. Dervan [93], K. Desch [24],
C. Deutsch [24], F.A. Di Bello [57b,57a], A. Di Ciaccio [76a,76b], L. Di Ciaccio [4],
A. Di Domenico [75a,75b], C. Di Donato [72a,72b], A. Di Girolamo [36], G. Di Gregorio [36],
A. Di Luca [78a,78b], B. Di Micco [77a,77b], R. Di Nardo [77a,77b], M. Diamantopoulou [34], F.A. Dias [115],
T. Dias Do Vale [143], M.A. Diaz [138a,138b], F.G. Diaz Capriles [24], M. Didenko [164], E.B. Diehl [107],
S. Díez Cornell [48], C. Diez Pardos [142], C. Dimitriadi [162,24], A. Dimitrievska [17a], J. Dingfelder [24],
I-M. Dinu [27b], S.J. Dittmeier [63b], F. Dittus [36], M. Divisek [134], F. Djama [103], T. Djobava [150b],
C. Doglioni [102,99], A. Dohnalova [28a], J. Dolejsi [134], Z. Dolezal [134], K.M. Dona [39],
M. Donadelli [83c], B. Dong [108], J. Donini [40], A. D'Onofrio [72a,72b], M. D'Onofrio [93],
J. Dopke [135], A. Doria [72a], N. Dos Santos Fernandes [131a], P. Dougan [102], M.T. Dova [91],
A.T. Doyle [59], M.A. Draguet [127], E. Dreyer [170], I. Drivas-koulouris [10], M. Drnevich [118],
M. Drozdova [56], D. Du [62a], T.A. du Pree [115], F. Dubinin [37], M. Dubovsky [28a], E. Duchovni [170],
G. Duckeck [110], O.A. Ducu [27b], D. Duda [52], A. Dudarev [36], E.R. Duden [26], M. D'uffizi [102],
L. Duflot [66], M. Dührssen [36], A.E. Dumitriu [27b], M. Dunford [63a], S. Dungs [49], K. Dunne [47a,47b],
A. Duperrin [103], H. Duran Yildiz [3a], M. Düren [58], A. Durglishvili [150b], B.L. Dwyer [116],
G.I. Dyckes [17a], M. Dyndal [86a], B.S. Dziedzic [87], Z.O. Earnshaw [147], G.H. Eberwein [127],
B. Eckerova [28a], S. Eggebrecht [55], E. Egidio Purcino De Souza [128], L.F. Ehrke [56], G. Eigen [16],
K. Einsweiler [17a], T. Ekelof [162], P.A. Ekman [99], S. El Farkh [35b], Y. El Ghazali [35b],
H. El Jarrari [36], A. El Moussaouy [109], V. Ellajosyula [162], M. Ellert [162], F. Ellinghaus [172],
N. Ellis [36], J. Elmsheuser [29], M. Elsing [36], D. Emeliyanov [135], Y. Enari [154], I. Ene [17a],
S. Epari [13], P.A. Erland [87], M. Errenst [172], M. Escalier [66], C. Escobar [164], E. Etzion [152],
G. Evans [131a], H. Evans [68], L.S. Evans [96], A. Ezhilov [37], S. Ezzarqtouni [35a], F. Fabbri [23b,23a],
L. Fabbri [23b,23a], G. Facini [97], V. Fadeyev [137], R.M. Fakhrutdinov [37], D. Fakoudis [101],
S. Falciano [75a], L.F. Falda Ulhoa Coelho [36], P.J. Falke [24], J. Faltova [134], C. Fan [163], Y. Fan [14a],

Y. Fang [14a,14e], M. Fanti [71a,71b], M. Faraj [69a,69b], Z. Farazpay [98], A. Farbin [8], A. Farilla [77a],
T. Farooque [108], S.M. Farrington [52], F. Fassi [35e], D. Fassouliotis [9], M. Faucci Giannelli [76a,76b],
W.J. Fawcett [32], L. Fayard [66], P. Federic [134], P. Federicova [132], O.L. Fedin [37,a], M. Feickert [171],
L. Feligioni [103], D.E. Fellers [124], C. Feng [62b], M. Feng [14b], Z. Feng [115], M.J. Fenton [160],
L. Ferencz [48], R.A.M. Ferguson [92], S.I. Fernandez Luengo [138f], P. Fernandez Martinez [13],
M.J.V. Fernoux [103], J. Ferrando [92], A. Ferrari [162], P. Ferrari [115,114], R. Ferrari [73a], D. Ferrere [56],
C. Ferretti [107], F. Fiedler [101], P. Fiedler [133], A. Filipčič [94], E.K. Filmer [1], F. Filthaut [114],
M.C.N. Fiolhais [131a,131c,c], L. Fiorini [164], W.C. Fisher [108], T. Fitschen [102], P.M. Fitzhugh[136],
I. Fleck [142], P. Fleischmann [107], T. Flick [172], M. Flores [33d,ac], L.R. Flores Castillo [64a],
L. Flores Sanz De Acedo [36], F.M. Follega [78a,78b], N. Fomin [16], J.H. Foo [156], A. Formica [136],
A.C. Forti [102], E. Fortin [36], A.W. Fortman [17a], M.G. Foti [17a], L. Fountas [9,j], D. Fournier [66],
H. Fox [92], P. Francavilla [74a,74b], S. Francescato [61], S. Franchellucci [56], M. Franchini [23b,23a],
S. Franchino [63a], D. Francis[36], L. Franco [114], V. Franco Lima [36], L. Franconi [48], M. Franklin [61],
G. Frattari [26], W.S. Freund [83b], Y.Y. Frid [152], J. Friend [59], N. Fritzsche [50], A. Froch [54],
D. Froidevaux [36], J.A. Frost [127], Y. Fu [62a], S. Fuenzalida Garrido [138f], M. Fujimoto [103],
K.Y. Fung [64a], E. Furtado De Simas Filho [83e], M. Furukawa [154], J. Fuster [164], A. Gabrielli [23b,23a],
A. Gabrielli [156], P. Gadow [36], G. Gagliardi [57b,57a], L.G. Gagnon [17a], S. Galantzan [152],
E.J. Gallas [127], B.J. Gallop [135], K.K. Gan [120], S. Ganguly [154], Y. Gao [52],
F.M. Garay Walls [138a,138b], B. Garcia[29], C. García [164], A. Garcia Alonso [115],
A.G. Garcia Caffaro [173], J.E. García Navarro [164], M. Garcia-Sciveres [17a], G.L. Gardner [129],
R.W. Gardner [39], N. Garelli [159], D. Garg [80], R.B. Garg [144,m], J.M. Gargan [52], C.A. Garner[156],
C.M. Garvey [33a], P. Gaspar [83b], V.K. Gassmann[159], G. Gaudio [73a], V. Gautam[13], P. Gauzzi [75a,75b],
I.L. Gavrilenko [37], A. Gavrilyuk [37], C. Gay [165], G. Gaycken [48], E.N. Gazis [10], A.A. Geanta [27b],
C.M. Gee [137], A. Gekow[120], C. Gemme [57b], M.H. Genest [60], A.D. Gentry [113], S. George [96],
W.F. George [20], T. Geralis [46], P. Gessinger-Befurt [36], M.E. Geyik [172], M. Ghani [168],
M. Ghneimat [142], K. Ghorbanian [95], A. Ghosal [142], A. Ghosh [160], A. Ghosh [7], B. Giacobbe [23b],
S. Giagu [75a,75b], T. Giani [115], P. Giannetti [74a], A. Giannini [62a], S.M. Gibson [96], M. Gignac [137],
D.T. Gil [86b], A.K. Gilbert [86a], B.J. Gilbert [41], D. Gillberg [34], G. Gilles [115], L. Ginabat [128],
D.M. Gingrich [2,af], M.P. Giordani [69a,69c], P.F. Giraud [136], G. Giugliarelli [69a,69c], D. Giugni [71a],
F. Giuli [36], I. Gkialas [9,j], L.K. Gladilin [37], C. Glasman [100], G.R. Gledhill [124], G. Glemža [48],
M. Glisic[124], I. Gnesi [43b,f], Y. Go [29], M. Goblirsch-Kolb [36], B. Gocke [49], D. Godin[109],
B. Gokturk [21a], S. Goldfarb [106], T. Golling [56], M.G.D. Gololo [33g], D. Golubkov [37],
J.P. Gombas [108], A. Gomes [131a,131b], G. Gomes Da Silva [142], A.J. Gomez Delegido [164],
R. Gonçalo [131a,131c], L. Gonella [20], A. Gongadze [150c], F. Gonnella [20], J.L. Gonski [144],
R.Y. González Andana [52], S. González de la Hoz [164], R. Gonzalez Lopez [93],
C. Gonzalez Renteria [17a], M.V. Gonzalez Rodrigues [48], R. Gonzalez Suarez [162],
S. Gonzalez-Sevilla [56], L. Goossens [36], B. Gorini [36], E. Gorini [70a,70b], A. Gorišek [94],
T.C. Gosart [129], A.T. Goshaw [51], M.I. Gostkin [38], S. Goswami [122], C.A. Gottardo [36],
S.A. Gotz [110], M. Gouighri [35b], V. Goumarre [48], A.G. Goussiou [139], N. Govender [33c],
I. Grabowska-Bold [86a], K. Graham [34], E. Gramstad [126], S. Grancagnolo [70a,70b], C.M. Grant[1,136],
P.M. Gravila [27f], F.G. Gravili [70a,70b], H.M. Gray [17a], M. Greco [70a,70b], C. Grefe [24],
I.M. Gregor [48], P. Grenier [144], S.G. Grewe[111], A.A. Grillo [137], K. Grimm [31], S. Grinstein [13,t],
J.-F. Grivaz [66], E. Gross [170], J. Grosse-Knetter [55], J.C. Grundy [127], L. Guan [107], C. Gubbels [165],
J.G.R. Guerrero Rojas [164], G. Guerrieri [69a,69c], F. Guescini [111], R. Gugel [101], J.A.M. Guhit [107],
A. Guida [18], E. Guilloton [168], S. Guindon [36], F. Guo [14a,14e], J. Guo [62c], L. Guo [48], Y. Guo [107],
R. Gupta [48], R. Gupta [130], S. Gurbuz [24], S.S. Gurdasani [54], G. Gustavino [36], M. Guth [56],
P. Gutierrez [121], L.F. Gutierrez Zagazeta [129], M. Gutsche [50], C. Gutschow [97], C. Gwenlan [127],

C.B. Gwilliam [93], E.S. Haaland [126], A. Haas [118], M. Habedank [48], C. Haber [17a],
H.K. Hadavand [8], A. Hadef [50], S. Hadzic [111], A.I. Hagan [92], J.J. Hahn [142], E.H. Haines [97],
M. Haleem [167], J. Haley [122], J.J. Hall [140], G.D. Hallewell [103], L. Halser [19], K. Hamano [166],
M. Hamer [24], G.N. Hamity [52], E.J. Hampshire [96], J. Han [62b], K. Han [62a], L. Han [14c],
L. Han [62a], S. Han [17a], Y.F. Han [156], K. Hanagaki [84], M. Hance [137], D.A. Hangal [41],
H. Hanif [143], M.D. Hank [129], J.B. Hansen [42], P.H. Hansen [42], K. Hara [158], D. Harada [56],
T. Harenberg [172], S. Harkusha [37], M.L. Harris [104], Y.T. Harris [127], J. Harrison [13],
N.M. Harrison [120], P.F. Harrison [168], N.M. Hartman [111], N.M. Hartmann [110], Y. Hasegawa [141],
R. Hauser [108], C.M. Hawkes [20], R.J. Hawkings [36], Y. Hayashi [154], S. Hayashida [112],
D. Hayden [108], C. Hayes [107], R.L. Hayes [115], C.P. Hays [127], J.M. Hays [95], H.S. Hayward [93],
F. He [62a], M. He [14a,14e], Y. He [155], Y. He [48], Y. He [97], N.B. Heatley [95], V. Hedberg [99],
A.L. Heggelund [126], N.D. Hehir [95,*], C. Heidegger [54], K.K. Heidegger [54], W.D. Heidorn [81],
J. Heilman [34], S. Heim [48], T. Heim [17a], J.G. Heinlein [129], J.J. Heinrich [124], L. Heinrich [111,ad],
J. Hejbal [132], A. Held [171], S. Hellesund [16], C.M. Helling [165], S. Hellman [47a,47b],
R.C.W. Henderson [92], L. Henkelmann [32], A.M. Henriques Correia [36], H. Herde [99],
Y. Hernández Jiménez [146], L.M. Herrmann [24], T. Herrmann [50], G. Herten [54], R. Hertenberger [110],
L. Hervas [36], M.E. Hesping [101], N.P. Hessey [157a], E. Hill [156], S.J. Hillier [20], J.R. Hinds [108],
F. Hinterkeuser [24], M. Hirose [125], S. Hirose [158], D. Hirschbuehl [172], T.G. Hitchings [102],
B. Hiti [94], J. Hobbs [146], R. Hobincu [27e], N. Hod [170], M.C. Hodgkinson [140],
B.H. Hodkinson [127], A. Hoecker [36], D.D. Hofer [107], J. Hofer [48], T. Holm [24], M. Holzbock [111],
L.B.A.H. Hommels [32], B.P. Honan [102], J. Hong [62c], T.M. Hong [130], B.H. Hooberman [163],
W.H. Hopkins [6], Y. Horii [112], S. Hou [149], A.S. Howard [94], J. Howarth [59], J. Hoya [6],
M. Hrabovsky [123], A. Hrynevich [48], T. Hryn'ova [4], P.J. Hsu [65], S.-C. Hsu [139], Q. Hu [62a],
S. Huang [64b], X. Huang [14a,14e], Y. Huang [140], Y. Huang [14a], Z. Huang [102], Z. Hubacek [133],
M. Huebner [24], F. Huegging [24], T.B. Huffman [127], C.A. Hugli [48], M. Huhtinen [36],
S.K. Huiberts [16], R. Hulsken [105], N. Huseynov [12], J. Huston [108], J. Huth [61], R. Hyneman [144],
G. Iacobucci [56], G. Iakovidis [29], I. Ibragimov [142], L. Iconomidou-Fayard [66], J.P. Iddon [36],
P. Iengo [72a,72b], R. Iguchi [154], T. Iizawa [127], Y. Ikegami [84], N. Ilic [156], H. Imam [35a],
M. Ince Lezki [56], T. Ingebretsen Carlson [47a,47b], G. Introzzi [73a,73b], M. Iodice [77a],
V. Ippolito [75a,75b], R.K. Irwin [93], M. Ishino [154], W. Islam [171], C. Issever [18,48], S. Istin [21a,aj],
H. Ito [169], R. Iuppa [78a,78b], A. Ivina [170], J.M. Izen [45], V. Izzo [72a], P. Jacka [132,133], P. Jackson [1],
B.P. Jaeger [143], C.S. Jagfeld [110], G. Jain [157a], P. Jain [54], K. Jakobs [54], T. Jakoubek [170],
J. Jamieson [59], K.W. Janas [86a], M. Javurkova [104], L. Jeanty [124], J. Jejelava [150a,aa], P. Jenni [54,g],
C.E. Jessiman [34], C. Jia [62b], J. Jia [146], X. Jia [61], X. Jia [14a,14e], Z. Jia [14c], S. Jiggins [48],
J. Jimenez Pena [13], S. Jin [14c], A. Jinaru [27b], O. Jinnouchi [155], P. Johansson [140], K.A. Johns [7],
J.W. Johnson [137], D.M. Jones [32], E. Jones [48], P. Jones [32], R.W.L. Jones [92], T.J. Jones [93],
H.L. Joos [55,36], R. Joshi [120], J. Jovicevic [15], X. Ju [17a], J.J. Junggeburth [104], T. Junkermann [63a],
A. Juste Rozas [13,t], M.K. Juzek [87], S. Kabana [138e], A. Kaczmarska [87], M. Kado [111],
H. Kagan [120], M. Kagan [144], A. Kahn [41], A. Kahn [129], C. Kahra [101], T. Kaji [154],
E. Kajomovitz [151], N. Kakati [170], I. Kalaitzidou [54], C.W. Kalderon [29], N.J. Kang [137],
D. Kar [33g], K. Karava [127], M.J. Kareem [157b], E. Karentzos [54], I. Karkanias [153], O. Karkout [115],
S.N. Karpov [38], Z.M. Karpova [38], V. Kartvelishvili [92], A.N. Karyukhin [37], E. Kasimi [153],
J. Katzy [48], S. Kaur [34], K. Kawade [141], M.P. Kawale [121], C. Kawamoto [88], T. Kawamoto [62a],
E.F. Kay [36], F.I. Kaya [159], S. Kazakos [108], V.F. Kazanin [37], Y. Ke [146], J.M. Keaveney [33a],
R. Keeler [166], G.V. Kehris [61], J.S. Keller [34], A.S. Kelly [97], J.J. Kempster [147], P.D. Kennedy [101],
O. Kepka [132], B.P. Kerridge [135], S. Kersten [172], B.P. Kerševan [94], L. Keszeghova [28a],
S. Ketabchi Haghighat [156], R.A. Khan [130], A. Khanov [122], A.G. Kharlamov [37], T. Kharlamova [37],

E.E. Khoda [139], M. Kholodenko [37], T.J. Khoo [18], G. Khoriauli [167], J. Khubua [150b,*],
Y.A.R. Khwaira [66], B. Kibirige[33g], A. Kilgallon [124], D.W. Kim [47a,47b], Y.K. Kim [39],
N. Kimura [97], M.K. Kingston [55], A. Kirchhoff [55], C. Kirfel [24], F. Kirfel [24], J. Kirk [135],
A.E. Kiryunin [111], C. Kitsaki [10], O. Kivernyk [24], M. Klassen [63a], C. Klein [34], L. Klein [167],
M.H. Klein [44], S.B. Klein [56], U. Klein [93], P. Klimek [36], A. Klimentov [29], T. Klioutchnikova [36],
P. Kluit [115], S. Kluth [111], E. Kneringer [79], T.M. Knight [156], A. Knue [49], R. Kobayashi [88],
D. Kobylianskii [170], S.F. Koch [127], M. Kocian [144], P. Kodyš [134], D.M. Koeck [124],
P.T. Koenig [24], T. Koffas [34], O. Kolay [50], I. Koletsou [4], T. Komarek [123], K. Köneke [54],
A.X.Y. Kong [1], T. Kono [119], N. Konstantinidis [97], P. Kontaxakis [56], B. Konya [99],
R. Kopeliansky [41], S. Koperny [86a], K. Korcyl [87], K. Kordas [153,e], A. Korn [97], S. Korn [55],
I. Korolkov [13], N. Korotkova [37], B. Kortman [115], O. Kortner [111], S. Kortner [111],
W.H. Kostecka [116], V.V. Kostyukhin [142], A. Kotsokechagia [136], A. Kotwal [51], A. Koulouris [36],
A. Kourkoumeli-Charalampidi [73a,73b], C. Kourkoumelis [9], E. Kourlitis [111,ad], O. Kovanda [124],
R. Kowalewski [166], W. Kozanecki [136], A.S. Kozhin [37], V.A. Kramarenko [37], G. Kramberger [94],
P. Kramer [101], M.W. Krasny [128], A. Krasznahorkay [36], J.W. Kraus [172], J.A. Kremer [48],
T. Kresse [50], J. Kretzschmar [93], K. Kreul [18], P. Krieger [156], S. Krishnamurthy [104],
M. Krivos [134], K. Krizka [20], K. Kroeninger [49], H. Kroha [111], J. Kroll [132], J. Kroll [129],
K.S. Krowpman [108], U. Kruchonak [38], H. Krüger [24], N. Krumnack[81], M.C. Kruse [51],
O. Kuchinskaia [37], S. Kuday [3a], S. Kuehn [36], R. Kuesters [54], T. Kuhl [48], V. Kukhtin [38],
Y. Kulchitsky [37,a], S. Kuleshov [138d,138b], M. Kumar [33g], N. Kumari [48], P. Kumari [157b],
A. Kupco [132], T. Kupfer[49], A. Kupich [37], O. Kuprash [54], H. Kurashige [85], L.L. Kurchaninov [157a],
O. Kurdysh [66], Y.A. Kurochkin [37], A. Kurova [37], M. Kuze [155], A.K. Kvam [104], J. Kvita [123],
T. Kwan [105], N.G. Kyriacou [107], L.A.O. Laatu [103], C. Lacasta [164], F. Lacava [75a,75b],
H. Lacker [18], D. Lacour [128], N.N. Lad [97], E. Ladygin [38], A. Lafarge [40], B. Laforge [128],
T. Lagouri [173], F.Z. Lahbabi [35a], S. Lai [55], I.K. Lakomiec [86a], N. Lalloue [60], J.E. Lambert [166],
S. Lammers [68], W. Lampl [7], C. Lampoudis [153,e], G. Lamprinoudis[101], A.N. Lancaster [116],
E. Lançon [29], U. Landgraf [54], M.P.J. Landon [95], V.S. Lang [54], O.K.B. Langrekken [126],
A.J. Lankford [160], F. Lanni [36], K. Lantzsch [24], A. Lanza [73a], A. Lapertosa [57b,57a],
J.F. Laporte [136], T. Lari [71a], F. Lasagni Manghi [23b], M. Lassnig [36], V. Latonova [132],
A. Laudrain [101], A. Laurier [151], S.D. Lawlor [140], Z. Lawrence [102], R. Lazaridou[168],
M. Lazzaroni [71a,71b], B. Le [102], E.M. Le Boulicaut [51], B. Leban [23b,23a], A. Lebedev [81],
M. LeBlanc [102], F. Ledroit-Guillon [60], A.C.A. Lee[97], S.C. Lee [149], S. Lee [47a,47b], T.F. Lee [93],
L.L. Leeuw [33c], H.P. Lefebvre [96], M. Lefebvre [166], C. Leggett [17a], G. Lehmann Miotto [36],
M. Leigh [56], W.A. Leight [104], W. Leinonen [114], A. Leisos [153,s], M.A.L. Leite [83c],
C.E. Leitgeb [18], R. Leitner [134], K.J.C. Leney [44], T. Lenz [24], S. Leone [74a], C. Leonidopoulos [52],
A. Leopold [145], C. Leroy [109], R. Les [108], C.G. Lester [32], M. Levchenko [37], J. Levêque [4],
L.J. Levinson [170], G. Levrini [23b,23a], M.P. Lewicki [87], D.J. Lewis [4], A. Li [5], B. Li [62b], C. Li[62a],
C-Q. Li [111], H. Li [62a], H. Li [62b], H. Li [14c], H. Li [14b], H. Li [62b], J. Li [62c], K. Li [139],
L. Li [62c], M. Li [14a,14e], Q.Y. Li [62a], S. Li [14a,14e], S. Li [62d,62c,d], T. Li [5], X. Li [105], Z. Li [127],
Z. Li [154], Z. Li [14a,14e], S. Liang [14a,14e], Z. Liang [14a], M. Liberatore [136], B. Liberti [76a],
K. Lie [64c], J. Lieber Marin [83b], H. Lien [68], K. Lin [108], R.E. Lindley [7], J.H. Lindon [2],
E. Lipeles [129], A. Lipniacka [16], A. Lister [165], J.D. Little [4], B. Liu [14a], B.X. Liu [143],
D. Liu [62d,62c], E.H.L. Liu [20], J.B. Liu [62a], J.K.K. Liu [32], K. Liu [62d], K. Liu [62d,62c], M. Liu [62a],
M.Y. Liu [62a], P. Liu [14a], Q. Liu [62d,139,62c], X. Liu [62a], X. Liu [62b], Y. Liu [14d,14e], Y.L. Liu [62b],
Y.W. Liu [62a], J. Llorente Merino [143], S.L. Lloyd [95], E.M. Lobodzinska [48], P. Loch [7],
T. Lohse [18], K. Lohwasser [140], E. Loiacono [48], M. Lokajicek [132,*], J.D. Lomas [20],
J.D. Long [163], I. Longarini [160], L. Longo [70a,70b], R. Longo [163], I. Lopez Paz [67],

A. Lopez Solis [48], N. Lorenzo Martinez [4], A.M. Lory [110], G. Löschcke Centeno [147], O. Loseva [37], X. Lou [47a,47b], X. Lou [14a,14e], A. Lounis [66], P.A. Love [92], G. Lu [14a,14e], M. Lu [80], S. Lu [129], Y.J. Lu [65], H.J. Lubatti [139], C. Luci [75a,75b], F.L. Lucio Alves [14c], F. Luehring [68], I. Luise [146], O. Lukianchuk [66], O. Lundberg [145], B. Lund-Jensen [145,*], N.A. Luongo [6], M.S. Lutz [36], A.B. Lux [25], D. Lynn [29], R. Lysak [132], E. Lytken [99], V. Lyubushkin [38], T. Lyubushkina [38], M.M. Lyukova [146], H. Ma [29], K. Ma [62a], L.L. Ma [62b], W. Ma [62a], Y. Ma [122], D.M. Mac Donell [166], G. Maccarrone [53], J.C. MacDonald [101], P.C. Machado De Abreu Farias [83b], R. Madar [40], T. Madula [97], J. Maeda [85], T. Maeno [29], H. Maguire [140], V. Maiboroda [136], A. Maio [131a,131b,131d], K. Maj [86a], O. Majersky [48], S. Majewski [124], N. Makovec [66], V. Maksimovic [15], B. Malaescu [128], Pa. Malecki [87], V.P. Maleev [37], F. Malek [60,n], M. Mali [94], D. Malito [96], U. Mallik [80,*], S. Maltezos [10], S. Malyukov [38], J. Mamuzic [13], G. Mancini [53], M.N. Mancini [26], G. Manco [73a,73b], J.P. Mandalia [95], I. Mandić [94], L. Manhaes de Andrade Filho [83a], I.M. Maniatis [170], J. Manjarres Ramos [90], D.C. Mankad [170], A. Mann [110], S. Manzoni [36], L. Mao [62c], X. Mapekula [33c], A. Marantis [153,s], G. Marchiori [5], M. Marcisovsky [132], C. Marcon [71a], M. Marinescu [20], S. Marium [48], M. Marjanovic [121], M. Markovitch [66], E.J. Marshall [92], Z. Marshall [17a], S. Marti-Garcia [164], T.A. Martin [168], V.J. Martin [52], B. Martin dit Latour [16], L. Martinelli [75a,75b], M. Martinez [13,t], P. Martinez Agullo [164], V.I. Martinez Outschoorn [104], P. Martinez Suarez [13], S. Martin-Haugh [135], G. Martinovicova [134], V.S. Martoiu [27b], A.C. Martyniuk [97], A. Marzin [36], D. Mascione [78a,78b], L. Masetti [101], T. Mashimo [154], J. Masik [102], A.L. Maslennikov [37], P. Massarotti [72a,72b], P. Mastrandrea [74a,74b], A. Mastroberardino [43b,43a], T. Masubuchi [154], T. Mathisen [162], J. Matousek [134], N. Matsuzawa [154], J. Maurer [27b], A.J. Maury [66], B. Maček [94], D.A. Maximov [37], R. Mazini [149], I. Maznas [116], M. Mazza [108], S.M. Mazza [137], E. Mazzeo [71a,71b], C. Mc Ginn [29], J.P. Mc Gowan [166], S.P. Mc Kee [107], C.C. McCracken [165], E.F. McDonald [106], A.E. McDougall [115], J.A. Mcfayden [147], R.P. McGovern [129], G. Mchedlidze [150b], R.P. Mckenzie [33g], T.C. Mclachlan [48], D.J. Mclaughlin [97], S.J. McMahon [135], C.M. Mcpartland [93], R.A. McPherson [166,x], S. Mehlhase [110], A. Mehta [93], D. Melini [164], B.R. Mellado Garcia [33g], A.H. Melo [55], F. Meloni [48], A.M. Mendes Jacques Da Costa [102], H.Y. Meng [156], L. Meng [92], S. Menke [111], M. Mentink [36], E. Meoni [43b,43a], G. Mercado [116], C. Merlassino [69a,69c], L. Merola [72a,72b], C. Meroni [71a,71b], J. Metcalfe [6], A.S. Mete [6], C. Meyer [68], J-P. Meyer [136], R.P. Middleton [135], L. Mijović [52], G. Mikenberg [170], M. Mikestikova [132], M. Mikuž [94], H. Mildner [101], A. Milic [36], D.W. Miller [39], E.H. Miller [144], L.S. Miller [34], A. Milov [170], D.A. Milstead [47a,47b], T. Min [14c], A.A. Minaenko [37], I.A. Minashvili [150b], L. Mince [59], A.I. Mincer [118], B. Mindur [86a], M. Mineev [38], Y. Mino [88], L.M. Mir [13], M. Miralles Lopez [59], M. Mironova [17a], A. Mishima [154], M.C. Missio [114], A. Mitra [168], V.A. Mitsou [164], Y. Mitsumori [112], O. Miu [156], P.S. Miyagawa [95], T. Mkrtchyan [63a], M. Mlinarevic [97], T. Mlinarevic [97], M. Mlynarikova [36], S. Mobius [19], P. Mogg [110], M.H. Mohamed Farook [113], A.F. Mohammed [14a,14e], S. Mohapatra [41], G. Mokgatitswane [33g], L. Moleri [170], B. Mondal [142], S. Mondal [133], K. Mönig [48], E. Monnier [103], L. Monsonis Romero [164], J. Montejo Berlingen [13], M. Montella [120], F. Montereali [77a,77b], F. Monticelli [91], S. Monzani [69a,69c], N. Morange [66], A.L. Moreira De Carvalho [131a], M. Moreno Llácer [164], C. Moreno Martinez [56], P. Morettini [57b], S. Morgenstern [36], M. Morii [61], M. Morinaga [154], F. Morodei [75a,75b], L. Morvaj [36], P. Moschovakos [36], B. Moser [36], M. Mosidze [150b], T. Moskalets [54], P. Moskvitina [114], J. Moss [31,k], A. Moussa [35d], E.J.W. Moyse [104], O. Mtintsilana [33g], S. Muanza [103], J. Mueller [130], D. Muenstermann [92], R. Müller [19], G.A. Mullier [162], A.J. Mullin [32], J.J. Mullin [129], D.P. Mungo [156], D. Munoz Perez [164], F.J. Munoz Sanchez [102], M. Murin [102], W.J. Murray [168,135],

M. Muškinja [94], C. Mwewa [29], A.G. Myagkov [37,a], A.J. Myers [8], G. Myers [107], M. Myska [133],
B.P. Nachman [17a], O. Nackenhorst [49], K. Nagai [127], K. Nagano [84], J.L. Nagle [29,ah], E. Nagy [103],
A.M. Nairz [36], Y. Nakahama [84], K. Nakamura [84], K. Nakkalil [5], H. Nanjo [125], R. Narayan [44],
E.A. Narayanan [113], I. Naryshkin [37], M. Naseri [34], S. Nasri [117b], C. Nass [24], G. Navarro [22a],
J. Navarro-Gonzalez [164], R. Nayak [152], A. Nayaz [18], P.Y. Nechaeva [37], F. Nechansky [48],
L. Nedic [127], T.J. Neep [20], A. Negri [73a,73b], M. Negrini [23b], C. Nellist [115], C. Nelson [105],
K. Nelson [107], S. Nemecek [132], M. Nessi [36,h], M.S. Neubauer [163], F. Neuhaus [101],
J. Neundorf [48], R. Newhouse [165], P.R. Newman [20], C.W. Ng [130], Y.W.Y. Ng [48], B. Ngair [117a],
H.D.N. Nguyen [109], R.B. Nickerson [127], R. Nicolaidou [136], J. Nielsen [137], M. Niemeyer [55],
J. Niermann [55], N. Nikiforou [36], V. Nikolaenko [37,a], I. Nikolic-Audit [128], K. Nikolopoulos [20],
P. Nilsson [29], I. Ninca [48], H.R. Nindhito [56], G. Ninio [152], A. Nisati [75a], N. Nishu [2],
R. Nisius [111], J-E. Nitschke [50], E.K. Nkadimeng [33g], T. Nobe [154], D.L. Noel [32],
T. Nommensen [148], M.B. Norfolk [140], R.R.B. Norisam [97], B.J. Norman [34], M. Noury [35a],
J. Novak [94], T. Novak [48], L. Novotny [133], R. Novotny [113], L. Nozka [123], K. Ntekas [160],
N.M.J. Nunes De Moura Junior [83b], J. Ocariz [128], A. Ochi [85], I. Ochoa [131a], S. Oerdek [48,u],
J.T. Offermann [39], A. Ogrodnik [134], A. Oh [102], C.C. Ohm [145], H. Oide [84], R. Oishi [154],
M.L. Ojeda [48], Y. Okumura [154], L.F. Oleiro Seabra [131a], S.A. Olivares Pino [138d],
D. Oliveira Damazio [29], D. Oliveira Goncalves [83a], J.L. Oliver [160], Ö.O. Öncel [54],
A.P. O'Neill [19], A. Onofre [131a,131e], P.U.E. Onyisi [11], M.J. Oreglia [39], G.E. Orellana [91],
D. Orestano [77a,77b], N. Orlando [13], R.S. Orr [156], V. O'Shea [59], L.M. Osojnak [129],
R. Ospanov [62a], G. Otero y Garzon [30], H. Otono [89], P.S. Ott [63a], G.J. Ottino [17a], M. Ouchrif [35d],
F. Ould-Saada [126], T. Ovsiannikova [139], M. Owen [59], R.E. Owen [135], K.Y. Oyulmaz [21a],
V.E. Ozcan [21a], F. Ozturk [87], N. Ozturk [8], S. Ozturk [82], H.A. Pacey [127], A. Pacheco Pages [13],
C. Padilla Aranda [13], G. Padovano [75a,75b], S. Pagan Griso [17a], G. Palacino [68], A. Palazzo [70a,70b],
J. Pampel [24], J. Pan [173], T. Pan [64a], D.K. Panchal [11], C.E. Pandini [115], J.G. Panduro Vazquez [96],
H.D. Pandya [1], H. Pang [14b], P. Pani [48], G. Panizzo [69a,69c], L. Panwar [128], L. Paolozzi [56],
S. Parajuli [163], A. Paramonov [6], C. Paraskevopoulos [53], D. Paredes Hernandez [64b],
A. Pareti [73a,73b], K.R. Park [41], T.H. Park [156], M.A. Parker [32], F. Parodi [57b,57a], E.W. Parrish [116],
V.A. Parrish [52], J.A. Parsons [41], U. Parzefall [54], B. Pascual Dias [109], L. Pascual Dominguez [152],
E. Pasqualucci [75a], S. Passaggio [57b], F. Pastore [96], P. Patel [87], U.M. Patel [51], J.R. Pater [102],
T. Pauly [36], C.I. Pazos [159], J. Pearkes [144], M. Pedersen [126], R. Pedro [131a], S.V. Peleganchuk [37],
O. Penc [36], E.A. Pender [52], G.D. Penn [173], K.E. Penski [110], M. Penzin [37], B.S. Peralva [83d],
A.P. Pereira Peixoto [139], L. Pereira Sanchez [144], D.V. Perepelitsa [29,ah], E. Perez Codina [157a],
M. Perganti [10], H. Pernegger [36], O. Perrin [40], K. Peters [48], R.F.Y. Peters [102], B.A. Petersen [36],
T.C. Petersen [42], E. Petit [103], V. Petousis [133], C. Petridou [153,e], T. Petru [134], A. Petrukhin [142],
M. Pettee [17a], N.E. Pettersson [36], A. Petukhov [37], K. Petukhova [134], R. Pezoa [138f],
L. Pezzotti [36], G. Pezzullo [173], T.M. Pham [171], T. Pham [106], P.W. Phillips [135], G. Piacquadio [146],
E. Pianori [17a], F. Piazza [124], R. Piegaia [30], D. Pietreanu [27b], A.D. Pilkington [102],
M. Pinamonti [69a,69c], J.L. Pinfold [2], B.C. Pinheiro Pereira [131a], A.E. Pinto Pinoargote [101,136],
L. Pintucci [69a,69c], K.M. Piper [147], A. Pirttikoski [56], D.A. Pizzi [34], L. Pizzimento [64b],
A. Pizzini [115], M.-A. Pleier [29], V. Plesanovs [54], V. Pleskot [134], E. Plotnikova [38], G. Poddar [95],
R. Poettgen [99], L. Poggioli [128], I. Pokharel [55], S. Polacek [134], G. Polesello [73a], A. Poley [143,157a],
A. Polini [23b], C.S. Pollard [168], Z.B. Pollock [120], E. Pompa Pacchi [75a,75b], D. Ponomarenko [114],
L. Pontecorvo [36], S. Popa [27a], G.A. Popeneciu [27d], A. Poreba [36], D.M. Portillo Quintero [157a],
S. Pospisil [133], M.A. Postill [140], P. Postolache [27c], K. Potamianos [168], P.A. Potepa [86a],
I.N. Potrap [38], C.J. Potter [32], H. Potti [1], J. Poveda [164], M.E. Pozo Astigarraga [36],
A. Prades Ibanez [164], J. Pretel [54], D. Price [102], M. Primavera [70a], M.A. Principe Martin [100],

R. Privara [ID][123], T. Procter [ID][59], M.L. Proffitt [ID][139], N. Proklova [ID][129], K. Prokofiev [ID][64c], G. Proto [ID][111],
J. Proudfoot [ID][6], M. Przybycien [ID][86a], W.W. Przygoda [ID][86b], A. Psallidas [ID][46], J.E. Puddefoot [ID][140],
D. Pudzha [ID][37], D. Pyatiizbyantseva [ID][37], J. Qian [ID][107], D. Qichen [ID][102], Y. Qin [ID][13], T. Qiu [ID][52],
A. Quadt [ID][55], M. Queitsch-Maitland [ID][102], G. Quetant [ID][56], R.P. Quinn [ID][165], G. Rabanal Bolanos [ID][61],
D. Rafanoharana [ID][54], F. Ragusa [ID][71a,71b], J.L. Rainbolt [ID][39], J.A. Raine [ID][56], S. Rajagopalan [ID][29],
E. Ramakoti [ID][37], I.A. Ramirez-Berend [ID][34], K. Ran [ID][48,14e], N.P. Rapheeha [ID][33g], H. Rasheed [ID][27b],
V. Raskina [ID][128], D.F. Rassloff [ID][63a], A. Rastogi [ID][17a], S. Rave [ID][101], B. Ravina [ID][55], I. Ravinovich [ID][170],
M. Raymond [ID][36], A.L. Read [ID][126], N.P. Readioff [ID][140], D.M. Rebuzzi [ID][73a,73b], G. Redlinger [ID][29],
A.S. Reed [ID][111], K. Reeves [ID][26], J.A. Reidelsturz [ID][172], D. Reikher [ID][152], A. Rej [ID][49], C. Rembser [ID][36],
M. Renda [ID][27b], M.B. Rendel[111], F. Renner [ID][48], A.G. Rennie [ID][160], A.L. Rescia [ID][48], S. Resconi [ID][71a],
M. Ressegotti [ID][57b,57a], S. Rettie [ID][36], J.G. Reyes Rivera [ID][108], E. Reynolds [ID][17a], O.L. Rezanova [ID][37],
P. Reznicek [ID][134], H. Riani [ID][35d], N. Ribaric [ID][92], E. Ricci [ID][78a,78b], R. Richter [ID][111], S. Richter [ID][47a,47b],
E. Richter-Was [ID][86b], M. Ridel [ID][128], S. Ridouani [ID][35d], P. Rieck [ID][118], P. Riedler [ID][36], E.M. Riefel [ID][47a,47b],
J.O. Rieger [ID][115], M. Rijssenbeek [ID][146], M. Rimoldi [ID][36], L. Rinaldi [ID][23b,23a], T.T. Rinn [ID][29],
M.P. Rinnagel [ID][110], G. Ripellino [ID][162], I. Riu [ID][13], J.C. Rivera Vergara [ID][166], F. Rizatdinova [ID][122],
E. Rizvi [ID][95], B.R. Roberts [ID][17a], S.H. Robertson [ID][105,x], D. Robinson [ID][32], C.M. Robles Gajardo [ID][138f],
M. Robles Manzano [ID][101], A. Robson [ID][59], A. Rocchi [ID][76a,76b], C. Roda [ID][74a,74b], S. Rodriguez Bosca [ID][36],
Y. Rodriguez Garcia [ID][22a], A. Rodriguez Rodriguez [ID][54], A.M. Rodríguez Vera [ID][116], S. Roe[36],
J.T. Roemer [ID][160], A.R. Roepe-Gier [ID][137], J. Roggel [ID][172], O. Røhne [ID][126], R.A. Rojas [ID][104],
C.P.A. Roland [ID][128], J. Roloff [ID][29], A. Romaniouk [ID][37], E. Romano [ID][73a,73b], M. Romano [ID][23b],
A.C. Romero Hernandez [ID][163], N. Rompotis [ID][93], L. Roos [ID][128], S. Rosati [ID][75a], B.J. Rosser [ID][39],
E. Rossi [ID][127], E. Rossi [ID][72a,72b], L.P. Rossi [ID][61], L. Rossini [ID][54], R. Rosten [ID][120], M. Rotaru [ID][27b],
B. Rottler [ID][54], C. Rougier [ID][90], D. Rousseau [ID][66], D. Rousso [ID][32], A. Roy [ID][163], S. Roy-Garand [ID][156],
A. Rozanov [ID][103], Z.M.A. Rozario [ID][59], Y. Rozen [ID][151], A. Rubio Jimenez [ID][164], A.J. Ruby [ID][93],
V.H. Ruelas Rivera [ID][18], T.A. Ruggeri [ID][1], A. Ruggiero [ID][127], A. Ruiz-Martinez [ID][164], A. Rummler [ID][36],
Z. Rurikova [ID][54], N.A. Rusakovich [ID][38], H.L. Russell [ID][166], G. Russo [ID][75a,75b], J.P. Rutherfoord [ID][7],
S. Rutherford Colmenares [ID][32], K. Rybacki[92], M. Rybar [ID][134], E.B. Rye [ID][126], A. Ryzhov [ID][44],
J.A. Sabater Iglesias [ID][56], P. Sabatini [ID][164], H.F-W. Sadrozinski [ID][137], F. Safai Tehrani [ID][75a],
B. Safarzadeh Samani [ID][135], M. Safdari [ID][144], S. Saha [ID][1], M. Sahinsoy [ID][111], A. Saibel [ID][164],
M. Saimpert [ID][136], M. Saito [ID][154], T. Saito [ID][154], D. Salamani [ID][36], A. Salnikov [ID][144], J. Salt [ID][164],
A. Salvador Salas [ID][152], D. Salvatore [ID][43b,43a], F. Salvatore [ID][147], A. Salzburger [ID][36], D. Sammel [ID][54],
E. Sampson [ID][92], D. Sampsonidis [ID][153,e], D. Sampsonidou [ID][124], J. Sánchez [ID][164],
V. Sanchez Sebastian [ID][164], H. Sandaker [ID][126], C.O. Sander [ID][48], J.A. Sandesara [ID][104], M. Sandhoff [ID][172],
C. Sandoval [ID][22b], D.P.C. Sankey [ID][135], T. Sano [ID][88], A. Sansoni [ID][53], L. Santi [ID][75a,75b], C. Santoni [ID][40],
H. Santos [ID][131a,131b], A. Santra [ID][170], K.A. Saoucha [ID][161], J.G. Saraiva [ID][131a,131d], J. Sardain [ID][7],
O. Sasaki [ID][84], K. Sato [ID][158], C. Sauer[63b], F. Sauerburger [ID][54], E. Sauvan [ID][4], P. Savard [ID][156,af],
R. Sawada [ID][154], C. Sawyer [ID][135], L. Sawyer [ID][98], I. Sayago Galvan[164], C. Sbarra [ID][23b], A. Sbrizzi [ID][23b,23a],
T. Scanlon [ID][97], J. Schaarschmidt [ID][139], U. Schäfer [ID][101], A.C. Schaffer [ID][66,44], D. Schaile [ID][110],
R.D. Schamberger [ID][146], C. Scharf [ID][18], M.M. Schefer [ID][19], V.A. Schegelsky [ID][37], D. Scheirich [ID][134],
F. Schenck [ID][18], M. Schernau [ID][160], C. Scheulen [ID][55], C. Schiavi [ID][57b,57a], M. Schioppa [ID][43b,43a],
B. Schlag [ID][144,m], K.E. Schleicher [ID][54], S. Schlenker [ID][36], J. Schmeing [ID][172], M.A. Schmidt [ID][172],
K. Schmieden [ID][101], C. Schmitt [ID][101], N. Schmitt [ID][101], S. Schmitt [ID][48], L. Schoeffel [ID][136],
A. Schoening [ID][63b], P.G. Scholer [ID][34], E. Schopf [ID][127], M. Schott [ID][101], J. Schovancova [ID][36],
S. Schramm [ID][56], T. Schroer [ID][56], H-C. Schultz-Coulon [ID][63a], M. Schumacher [ID][54], B.A. Schumm [ID][137],
Ph. Schune [ID][136], A.J. Schuy [ID][139], H.R. Schwartz [ID][137], A. Schwartzman [ID][144], T.A. Schwarz [ID][107],
Ph. Schwemling [ID][136], R. Schwienhorst [ID][108], A. Sciandra [ID][137], G. Sciolla [ID][26], F. Scuri [ID][74a],
C.D. Sebastiani [ID][93], K. Sedlaczek [ID][116], P. Seema [ID][18], S.C. Seidel [ID][113], A. Seiden [ID][137],

B.D. Seidlitz [41], C. Seitz [48], J.M. Seixas [83b], G. Sekhniaidze [72a], L. Selem [60],
N. Semprini-Cesari [23b,23a], D. Sengupta [56], V. Senthilkumar [164], L. Serin [66], L. Serkin [69a,69b],
M. Sessa [76a,76b], H. Severini [121], F. Sforza [57b,57a], A. Sfyrla [56], Q. Sha [14a], E. Shabalina [55],
R. Shaheen [145], J.D. Shahinian [129], D. Shaked Renous [170], L.Y. Shan [14a], M. Shapiro [17a],
A. Sharma [36], A.S. Sharma [165], P. Sharma [80], P.B. Shatalov [37], K. Shaw [147], S.M. Shaw [102],
A. Shcherbakova [37], Q. Shen [62c,5], D.J. Sheppard [143], P. Sherwood [97], L. Shi [97], X. Shi [14a],
C.O. Shimmin [173], J.D. Shinner [96], I.P.J. Shipsey [127], S. Shirabe [89], M. Shiyakova [38,v],
J. Shlomi [170], M.J. Shochet [39], J. Shojaii [106], D.R. Shope [126], B. Shrestha [121], S. Shrestha [120,ai],
E.M. Shrif [33g], M.J. Shroff [166], P. Sicho [132], A.M. Sickles [163], E. Sideras Haddad [33g],
A. Sidoti [23b], F. Siegert [50], Dj. Sijacki [15], F. Sili [91], J.M. Silva [52], M.V. Silva Oliveira [29],
S.B. Silverstein [47a], S. Simion [66], R. Simoniello [36], E.L. Simpson [59], H. Simpson [147],
L.R. Simpson [107], N.D. Simpson [99], S. Simsek [82], S. Sindhu [55], P. Sinervo [156], S. Singh [156],
S. Sinha [48], S. Sinha [102], M. Sioli [23b,23a], I. Siral [36], E. Sitnikova [48], J. Sjölin [47a,47b],
A. Skaf [55], E. Skorda [20], P. Skubic [121], M. Slawinska [87], V. Smakhtin [170], B.H. Smart [135],
S.Yu. Smirnov [37], Y. Smirnov [37], L.N. Smirnova [37,a], O. Smirnova [99], A.C. Smith [41],
E.A. Smith [39], H.A. Smith [127], J.L. Smith [102], R. Smith [144], M. Smizanska [92], K. Smolek [133],
A.A. Snesarev [37], S.R. Snider [156], H.L. Snoek [115], S. Snyder [29], R. Sobie [166,x], A. Soffer [152],
C.A. Solans Sanchez [36], E.Yu. Soldatov [37], U. Soldevila [164], A.A. Solodkov [37], S. Solomon [26],
A. Soloshenko [38], K. Solovieva [54], O.V. Solovyanov [40], V. Solovyev [37], P. Sommer [36],
A. Sonay [13], W.Y. Song [157b], A. Sopczak [133], A.L. Sopio [97], F. Sopkova [28b], J.D. Sorenson [113],
I.R. Sotarriva Alvarez [155], V. Sothilingam [63a], O.J. Soto Sandoval [138c,138b], S. Sottocornola [68],
R. Soualah [161], Z. Soumaimi [35e], D. South [48], N. Soybelman [170], S. Spagnolo [70a,70b],
M. Spalla [111], D. Sperlich [54], G. Spigo [36], S. Spinali [92], D.P. Spiteri [59], M. Spousta [134],
E.J. Staats [34], R. Stamen [63a], A. Stampekis [20], M. Standke [24], E. Stanecka [87], M.V. Stange [50],
B. Stanislaus [17a], M.M. Stanitzki [48], B. Stapf [48], E.A. Starchenko [37], G.H. Stark [137], J. Stark [90],
P. Staroba [132], P. Starovoitov [63a], S. Stärz [105], R. Staszewski [87], G. Stavropoulos [46],
J. Steentoft [162], P. Steinberg [29], B. Stelzer [143,157a], H.J. Stelzer [130], O. Stelzer-Chilton [157a],
H. Stenzel [58], T.J. Stevenson [147], G.A. Stewart [36], J.R. Stewart [122], M.C. Stockton [36],
G. Stoicea [27b], M. Stolarski [131a], S. Stonjek [111], A. Straessner [50], J. Strandberg [145],
S. Strandberg [47a,47b], M. Stratmann [172], M. Strauss [121], T. Strebler [103], P. Strizenec [28b],
R. Ströhmer [167], D.M. Strom [124], R. Stroynowski [44], A. Strubig [47a,47b], S.A. Stucci [29],
B. Stugu [16], J. Stupak [121], N.A. Styles [48], D. Su [144], S. Su [62a], W. Su [62d], X. Su [62a],
D. Suchy [28a], K. Sugizaki [154], V.V. Sulin [37], M.J. Sullivan [93], D.M.S. Sultan [127],
L. Sultanaliyeva [37], S. Sultansoy [3b], T. Sumida [88], S. Sun [107], S. Sun [171],
O. Sunneborn Gudnadottir [162], N. Sur [103], M.R. Sutton [147], H. Suzuki [158], M. Svatos [132],
M. Swiatlowski [157a], T. Swirski [167], I. Sykora [28a], M. Sykora [134], T. Sykora [134], D. Ta [101],
K. Tackmann [48,u], A. Taffard [160], R. Tafirout [157a], J.S. Tafoya Vargas [66], Y. Takubo [84],
M. Talby [103], A.A. Talyshev [37], K.C. Tam [64b], N.M. Tamir [152], A. Tanaka [154], J. Tanaka [154],
R. Tanaka [66], M. Tanasini [57b,57a], Z. Tao [165], S. Tapia Araya [138f], S. Tapprogge [101],
A. Tarek Abouelfadl Mohamed [108], S. Tarem [151], K. Tariq [14a], G. Tarna [103,27b], G.F. Tartarelli [71a],
P. Tas [134], M. Tasevsky [132], E. Tassi [43b,43a], A.C. Tate [163], G. Tateno [154], Y. Tayalati [35e,w],
G.N. Taylor [106], W. Taylor [157b], A.S. Tee [171], R. Teixeira De Lima [144], P. Teixeira-Dias [96],
J.J. Teoh [156], K. Terashi [154], J. Terron [100], S. Terzo [13], M. Testa [53], R.J. Teuscher [156,x],
A. Thaler [79], O. Theiner [56], N. Themistokleous [52], T. Theveneaux-Pelzer [103], O. Thielmann [172],
D.W. Thomas [96], J.P. Thomas [20], E.A. Thompson [17a], P.D. Thompson [20], E. Thomson [129],
R.E. Thornberry [44], Y. Tian [55], V. Tikhomirov [37,a], Yu.A. Tikhonov [37], S. Timoshenko [37],
D. Timoshyn [134], E.X.L. Ting [1], P. Tipton [173], S.H. Tlou [33g], K. Todome [155],

S. Todorova-Nova [134], S. Todt[50], M. Togawa [84], J. Tojo [89], S. Tokár [28a], K. Tokushuku [84],
O. Toldaiev [68], R. Tombs [32], M. Tomoto [84,112], L. Tompkins [144,m], K.W. Topolnicki [86b],
E. Torrence [124], H. Torres [90], E. Torró Pastor [164], M. Toscani [30], C. Tosciri [39], M. Tost [11],
D.R. Tovey [140], A. Traet[16], I.S. Trandafir [27b], T. Trefzger [167], A. Tricoli [29], I.M. Trigger [157a],
S. Trincaz-Duvoid [128], D.A. Trischuk [26], B. Trocmé [60], L. Truong [33c], M. Trzebinski [87],
A. Trzupek [87], F. Tsai [146], M. Tsai [107], A. Tsiamis [153,e], P.V. Tsiareshka[37], S. Tsigaridas [157a],
A. Tsirigotis [153,s], V. Tsiskaridze [156], E.G. Tskhadadze [150a], M. Tsopoulou [153], Y. Tsujikawa [88],
I.I. Tsukerman [37], V. Tsulaia [17a], S. Tsuno [84], K. Tsuri [119], D. Tsybychev [146], Y. Tu [64b],
A. Tudorache [27b], V. Tudorache [27b], A.N. Tuna [61], S. Turchikhin [57b,57a], I. Turk Cakir [3a],
R. Turra [71a], T. Turtuvshin [38,y], P.M. Tuts [41], S. Tzamarias [153,e], E. Tzovara [101], F. Ukegawa [158],
P.A. Ulloa Poblete [138c,138b], E.N. Umaka [29], G. Unal [36], A. Undrus [29], G. Unel [160], J. Urban [28b],
P. Urquijo [106], P. Urrejola [138a], G. Usai [8], R. Ushioda [155], M. Usman [109], Z. Uysal [82],
V. Vacek [133], B. Vachon [105], K.O.H. Vadla [126], T. Vafeiadis [36], A. Vaitkus [97], C. Valderanis [110],
E. Valdes Santurio [47a,47b], M. Valente [157a], S. Valentinetti [23b,23a], A. Valero [164],
E. Valiente Moreno [164], A. Vallier [90], J.A. Valls Ferrer [164], D.R. Van Arneman [115],
T.R. Van Daalen [139], A. Van Der Graaf [49], P. Van Gemmeren [6], M. Van Rijnbach [126],
S. Van Stroud [97], I. Van Vulpen [115], P. Vana [134], M. Vanadia [76a,76b], W. Vandelli [36],
E.R. Vandewall [122], D. Vannicola [152], L. Vannoli [53], R. Vari [75a], E.W. Varnes [7], C. Varni [17b],
T. Varol [149], D. Varouchas [66], L. Varriale [164], K.E. Varvell [148], M.E. Vasile [27b], L. Vaslin[84],
G.A. Vasquez [166], A. Vasyukov [38], R. Vavricka[101], F. Vazeille [40], T. Vazquez Schroeder [36],
J. Veatch [31], V. Vecchio [102], M.J. Veen [104], I. Veliscek [29], L.M. Veloce [156], F. Veloso [131a,131c],
S. Veneziano [75a], A. Ventura [70a,70b], S. Ventura Gonzalez [136], A. Verbytskyi [111],
M. Verducci [74a,74b], C. Vergis [24], M. Verissimo De Araujo [83b], W. Verkerke [115],
J.C. Vermeulen [115], C. Vernieri [144], M. Vessella [104], M.C. Vetterli [143,af], A. Vgenopoulos [153,e],
N. Viaux Maira [138f], T. Vickey [140], O.E. Vickey Boeriu [140], G.H.A. Viehhauser [127], L. Vigani [63b],
M. Villa [23b,23a], M. Villaplana Perez [164], E.M. Villhauer[52], E. Vilucchi [53], M.G. Vincter [34],
G.S. Virdee [20], A. Vishwakarma [52], A. Visibile[115], C. Vittori [36], I. Vivarelli [23b,23a],
E. Voevodina [111], F. Vogel [110], J.C. Voigt [50], P. Vokac [133], Yu. Volkotrub [86b], J. Von Ahnen [48],
E. Von Toerne [24], B. Vormwald [36], V. Vorobel [134], K. Vorobev [37], M. Vos [164], K. Voss [142],
M. Vozak [115], L. Vozdecky [121], N. Vranjes [15], M. Vranjes Milosavljevic [15], M. Vreeswijk [115],
N.K. Vu [62d,62c], R. Vuillermet [36], O. Vujinovic [101], I. Vukotic [39], S. Wada [158], C. Wagner[104],
J.M. Wagner [17a], W. Wagner [172], S. Wahdan [172], H. Wahlberg [91], M. Wakida [112], J. Walder [135],
R. Walker [110], W. Walkowiak [142], A. Wall [129], E.J. Wallin [99], T. Wamorkar [6], A.Z. Wang [137],
C. Wang [101], C. Wang [11], H. Wang [17a], J. Wang [64c], R.-J. Wang [101], R. Wang [61], R. Wang [6],
S.M. Wang [149], S. Wang [62b], T. Wang [62a], W.T. Wang [80], W. Wang [14a], X. Wang [14c],
X. Wang [163], X. Wang [62c], Y. Wang [62d], Y. Wang [14c], Z. Wang [107], Z. Wang [62d,51,62c],
Z. Wang [107], A. Warburton [105], R.J. Ward [20], N. Warrack [59], S. Waterhouse [96], A.T. Watson [20],
H. Watson [59], M.F. Watson [20], E. Watton [59,135], G. Watts [139], B.M. Waugh [97], C. Weber [29],
H.A. Weber [18], M.S. Weber [19], S.M. Weber [63a], C. Wei [62a], Y. Wei [127], A.R. Weidberg [127],
E.J. Weik [118], J. Weingarten [49], M. Weirich [101], C. Weiser [54], C.J. Wells [48], T. Wenaus [29],
B. Wendland [49], T. Wengler [36], N.S. Wenke[111], N. Wermes [24], M. Wessels [63a], A.M. Wharton [92],
A.S. White [61], A. White [8], M.J. White [1], D. Whiteson [160], L. Wickremasinghe [125],
W. Wiedenmann [171], M. Wielers [135], C. Wiglesworth [42], D.J. Wilbern[121], H.G. Wilkens [36],
D.M. Williams [41], H.H. Williams[129], S. Williams [32], S. Willocq [104], B.J. Wilson [102],
P.J. Windischhofer [39], F.I. Winkel [30], F. Winklmeier [124], B.T. Winter [54], J.K. Winter [102],
M. Wittgen[144], M. Wobisch [98], Z. Wolffs [115], J. Wollrath[160], M.W. Wolter [87], H. Wolters [131a,131c],
M.C. Wong[137], E.L. Woodward [41], S.D. Worm [48], B.K. Wosiek [87], K.W. Woźniak [87],

S. Wozniewski [55], K. Wraight [59], C. Wu [20], M. Wu [14d], M. Wu [114], S.L. Wu [171], X. Wu [56],
Y. Wu [62a], Z. Wu [4], J. Wuerzinger [111,ad], T.R. Wyatt [102], B.M. Wynne [52], S. Xella [42],
L. Xia [14c], M. Xia [14b], J. Xiang [64c], M. Xie [62a], X. Xie [62a], S. Xin [14a,14e], A. Xiong [124],
J. Xiong [17a], D. Xu [14a], H. Xu [62a], L. Xu [62a], R. Xu [129], T. Xu [107], Y. Xu [14b], Z. Xu [52],
Z. Xu [14c], B. Yabsley [148], S. Yacoob [33a], Y. Yamaguchi [155], E. Yamashita [154], H. Yamauchi [158],
T. Yamazaki [17a], Y. Yamazaki [85], J. Yan [62c], S. Yan [59], Z. Yan [104], H.J. Yang [62c,62d],
H.T. Yang [62a], S. Yang [62a], T. Yang [64c], X. Yang [36], X. Yang [14a], Y. Yang [44], Y. Yang [62a],
Z. Yang [62a], W-M. Yao [17a], H. Ye [14c], H. Ye [55], J. Ye [14a], S. Ye [29], X. Ye [62a], Y. Yeh [97],
I. Yeletskikh [38], B. Yeo [17b], M.R. Yexley [97], P. Yin [41], K. Yorita [169], S. Younas [27b],
C.J.S. Young [36], C. Young [144], C. Yu [14a,14e], Y. Yu [62a], M. Yuan [107], R. Yuan [62b], L. Yue [97],
M. Zaazoua [62a], B. Zabinski [87], E. Zaid [52], Z.K. Zak [87], T. Zakareishvili [164], N. Zakharchuk [34],
S. Zambito [56], J.A. Zamora Saa [138d,138b], J. Zang [154], D. Zanzi [54], O. Zaplatilek [133],
C. Zeitnitz [172], H. Zeng [14a], J.C. Zeng [163], D.T. Zenger Jr [26], O. Zenin [37], T. Ženiš [28a],
S. Zenz [95], S. Zerradi [35a], D. Zerwas [66], M. Zhai [14a,14e], D.F. Zhang [140], J. Zhang [62b],
J. Zhang [6], K. Zhang [14a,14e], L. Zhang [14c], P. Zhang [14a,14e], R. Zhang [171], S. Zhang [107],
S. Zhang [44], T. Zhang [154], X. Zhang [62c], X. Zhang [62b], Y. Zhang [62c,5], Y. Zhang [97],
Y. Zhang [14c], Z. Zhang [17a], Z. Zhang [66], H. Zhao [139], T. Zhao [62b], Y. Zhao [137], Z. Zhao [62a],
A. Zhemchugov [38], J. Zheng [14c], K. Zheng [163], X. Zheng [62a], Z. Zheng [144], D. Zhong [163],
B. Zhou [107], H. Zhou [7], N. Zhou [62c], Y. Zhou [14c], Y. Zhou [7], C.G. Zhu [62b], J. Zhu [107],
Y. Zhu [62c], Y. Zhu [62a], X. Zhuang [14a], K. Zhukov [37], N.I. Zimine [38], J. Zinsser [63b],
M. Ziolkowski [142], L. Živković [15], A. Zoccoli [23b,23a], K. Zoch [61], T.G. Zorbas [140],
O. Zormpa [46], W. Zou [41], L. Zwalinski [36].

[1]Department of Physics, University of Adelaide, Adelaide; Australia.

[2]Department of Physics, University of Alberta, Edmonton AB; Canada.

[3](a)Department of Physics, Ankara University, Ankara;(b)Division of Physics, TOBB University of Economics and Technology, Ankara; Türkiye.

[4]LAPP, Université Savoie Mont Blanc, CNRS/IN2P3, Annecy; France.

[5]APC, Université Paris Cité, CNRS/IN2P3, Paris; France.

[6]High Energy Physics Division, Argonne National Laboratory, Argonne IL; United States of America.

[7]Department of Physics, University of Arizona, Tucson AZ; United States of America.

[8]Department of Physics, University of Texas at Arlington, Arlington TX; United States of America.

[9]Physics Department, National and Kapodistrian University of Athens, Athens; Greece.

[10]Physics Department, National Technical University of Athens, Zografou; Greece.

[11]Department of Physics, University of Texas at Austin, Austin TX; United States of America.

[12]Institute of Physics, Azerbaijan Academy of Sciences, Baku; Azerbaijan.

[13]Institut de Física d'Altes Energies (IFAE), Barcelona Institute of Science and Technology, Barcelona; Spain.

[14](a)Institute of High Energy Physics, Chinese Academy of Sciences, Beijing;(b)Physics Department, Tsinghua University, Beijing;(c)Department of Physics, Nanjing University, Nanjing;(d)School of Science, Shenzhen Campus of Sun Yat-sen University;(e)University of Chinese Academy of Science (UCAS), Beijing; China.

[15]Institute of Physics, University of Belgrade, Belgrade; Serbia.

[16]Department for Physics and Technology, University of Bergen, Bergen; Norway.

[17](a)Physics Division, Lawrence Berkeley National Laboratory, Berkeley CA;(b)University of California, Berkeley CA; United States of America.

[18]Institut für Physik, Humboldt Universität zu Berlin, Berlin; Germany.

[19]Albert Einstein Center for Fundamental Physics and Laboratory for High Energy Physics, University of Bern, Bern; Switzerland.

[20]School of Physics and Astronomy, University of Birmingham, Birmingham; United Kingdom.

[21][a]Department of Physics, Bogazici University, Istanbul;[b]Department of Physics Engineering, Gaziantep University, Gaziantep;[c]Department of Physics, Istanbul University, Istanbul; Türkiye.

[22][a]Facultad de Ciencias y Centro de Investigaciónes, Universidad Antonio Nariño, Bogotá;[b]Departamento de Física, Universidad Nacional de Colombia, Bogotá; Colombia.

[23][a]Dipartimento di Fisica e Astronomia A. Righi, Università di Bologna, Bologna;[b]INFN Sezione di Bologna; Italy.

[24]Physikalisches Institut, Universität Bonn, Bonn; Germany.

[25]Department of Physics, Boston University, Boston MA; United States of America.

[26]Department of Physics, Brandeis University, Waltham MA; United States of America.

[27][a]Transilvania University of Brasov, Brasov;[b]Horia Hulubei National Institute of Physics and Nuclear Engineering, Bucharest;[c]Department of Physics, Alexandru Ioan Cuza University of Iasi, Iasi;[d]National Institute for Research and Development of Isotopic and Molecular Technologies, Physics Department, Cluj-Napoca;[e]National University of Science and Technology Politechnica, Bucharest;[f]West University in Timisoara, Timisoara;[g]Faculty of Physics, University of Bucharest, Bucharest; Romania.

[28][a]Faculty of Mathematics, Physics and Informatics, Comenius University, Bratislava;[b]Department of Subnuclear Physics, Institute of Experimental Physics of the Slovak Academy of Sciences, Kosice; Slovak Republic.

[29]Physics Department, Brookhaven National Laboratory, Upton NY; United States of America.

[30]Universidad de Buenos Aires, Facultad de Ciencias Exactas y Naturales, Departamento de Física, y CONICET, Instituto de Física de Buenos Aires (IFIBA), Buenos Aires; Argentina.

[31]California State University, CA; United States of America.

[32]Cavendish Laboratory, University of Cambridge, Cambridge; United Kingdom.

[33][a]Department of Physics, University of Cape Town, Cape Town;[b]iThemba Labs, Western Cape;[c]Department of Mechanical Engineering Science, University of Johannesburg, Johannesburg;[d]National Institute of Physics, University of the Philippines Diliman (Philippines);[e]University of South Africa, Department of Physics, Pretoria;[f]University of Zululand, KwaDlangezwa;[g]School of Physics, University of the Witwatersrand, Johannesburg; South Africa.

[34]Department of Physics, Carleton University, Ottawa ON; Canada.

[35][a]Faculté des Sciences Ain Chock, Université Hassan II de Casablanca;[b]Faculté des Sciences, Université Ibn-Tofail, Kénitra;[c]Faculté des Sciences Semlalia, Université Cadi Ayyad, LPHEA-Marrakech;[d]LPMR, Faculté des Sciences, Université Mohamed Premier, Oujda;[e]Faculté des sciences, Université Mohammed V, Rabat;[f]Institute of Applied Physics, Mohammed VI Polytechnic University, Ben Guerir; Morocco.

[36]CERN, Geneva; Switzerland.

[37]Affiliated with an institute covered by a cooperation agreement with CERN.

[38]Affiliated with an international laboratory covered by a cooperation agreement with CERN.

[39]Enrico Fermi Institute, University of Chicago, Chicago IL; United States of America.

[40]LPC, Université Clermont Auvergne, CNRS/IN2P3, Clermont-Ferrand; France.

[41]Nevis Laboratory, Columbia University, Irvington NY; United States of America.

[42]Niels Bohr Institute, University of Copenhagen, Copenhagen; Denmark.

[43][a]Dipartimento di Fisica, Università della Calabria, Rende;[b]INFN Gruppo Collegato di Cosenza, Laboratori Nazionali di Frascati; Italy.

[44]Physics Department, Southern Methodist University, Dallas TX; United States of America.

[45]Physics Department, University of Texas at Dallas, Richardson TX; United States of America.

[46]National Centre for Scientific Research "Demokritos", Agia Paraskevi; Greece.

[47][(a)]Department of Physics, Stockholm University;[(b)]Oskar Klein Centre, Stockholm; Sweden.

[48]Deutsches Elektronen-Synchrotron DESY, Hamburg and Zeuthen; Germany.

[49]Fakultät Physik , Technische Universität Dortmund, Dortmund; Germany.

[50]Institut für Kern- und Teilchenphysik, Technische Universität Dresden, Dresden; Germany.

[51]Department of Physics, Duke University, Durham NC; United States of America.

[52]SUPA - School of Physics and Astronomy, University of Edinburgh, Edinburgh; United Kingdom.

[53]INFN e Laboratori Nazionali di Frascati, Frascati; Italy.

[54]Physikalisches Institut, Albert-Ludwigs-Universität Freiburg, Freiburg; Germany.

[55]II. Physikalisches Institut, Georg-August-Universität Göttingen, Göttingen; Germany.

[56]Département de Physique Nucléaire et Corpusculaire, Université de Genève, Genève; Switzerland.

[57][(a)]Dipartimento di Fisica, Università di Genova, Genova;[(b)]INFN Sezione di Genova; Italy.

[58]II. Physikalisches Institut, Justus-Liebig-Universität Giessen, Giessen; Germany.

[59]SUPA - School of Physics and Astronomy, University of Glasgow, Glasgow; United Kingdom.

[60]LPSC, Université Grenoble Alpes, CNRS/IN2P3, Grenoble INP, Grenoble; France.

[61]Laboratory for Particle Physics and Cosmology, Harvard University, Cambridge MA; United States of America.

[62][(a)]Department of Modern Physics and State Key Laboratory of Particle Detection and Electronics, University of Science and Technology of China, Hefei;[(b)]Institute of Frontier and Interdisciplinary Science and Key Laboratory of Particle Physics and Particle Irradiation (MOE), Shandong University, Qingdao;[(c)]School of Physics and Astronomy, Shanghai Jiao Tong University, Key Laboratory for Particle Astrophysics and Cosmology (MOE), SKLPPC, Shanghai;[(d)]Tsung-Dao Lee Institute, Shanghai;[(e)]School of Physics and Microelectronics, Zhengzhou University; China.

[63][(a)]Kirchhoff-Institut für Physik, Ruprecht-Karls-Universität Heidelberg, Heidelberg;[(b)]Physikalisches Institut, Ruprecht-Karls-Universität Heidelberg, Heidelberg; Germany.

[64][(a)]Department of Physics, Chinese University of Hong Kong, Shatin, N.T., Hong Kong;[(b)]Department of Physics, University of Hong Kong, Hong Kong;[(c)]Department of Physics and Institute for Advanced Study, Hong Kong University of Science and Technology, Clear Water Bay, Kowloon, Hong Kong; China.

[65]Department of Physics, National Tsing Hua University, Hsinchu; Taiwan.

[66]IJCLab, Université Paris-Saclay, CNRS/IN2P3, 91405, Orsay; France.

[67]Centro Nacional de Microelectrónica (IMB-CNM-CSIC), Barcelona; Spain.

[68]Department of Physics, Indiana University, Bloomington IN; United States of America.

[69][(a)]INFN Gruppo Collegato di Udine, Sezione di Trieste, Udine;[(b)]ICTP, Trieste;[(c)]Dipartimento Politecnico di Ingegneria e Architettura, Università di Udine, Udine; Italy.

[70][(a)]INFN Sezione di Lecce;[(b)]Dipartimento di Matematica e Fisica, Università del Salento, Lecce; Italy.

[71][(a)]INFN Sezione di Milano;[(b)]Dipartimento di Fisica, Università di Milano, Milano; Italy.

[72][(a)]INFN Sezione di Napoli;[(b)]Dipartimento di Fisica, Università di Napoli, Napoli; Italy.

[73][(a)]INFN Sezione di Pavia;[(b)]Dipartimento di Fisica, Università di Pavia, Pavia; Italy.

[74][(a)]INFN Sezione di Pisa;[(b)]Dipartimento di Fisica E. Fermi, Università di Pisa, Pisa; Italy.

[75][(a)]INFN Sezione di Roma;[(b)]Dipartimento di Fisica, Sapienza Università di Roma, Roma; Italy.

[76][(a)]INFN Sezione di Roma Tor Vergata;[(b)]Dipartimento di Fisica, Università di Roma Tor Vergata, Roma; Italy.

[77][(a)]INFN Sezione di Roma Tre;[(b)]Dipartimento di Matematica e Fisica, Università Roma Tre, Roma; Italy.

[78][(a)]INFN-TIFPA;[(b)]Università degli Studi di Trento, Trento; Italy.

[79]Universität Innsbruck, Department of Astro and Particle Physics, Innsbruck; Austria.

[80]University of Iowa, Iowa City IA; United States of America.

[81]Department of Physics and Astronomy, Iowa State University, Ames IA; United States of America.

[82]Istinye University, Sariyer, Istanbul; Türkiye.

[83][a]Departamento de Engenharia Elétrica, Universidade Federal de Juiz de Fora (UFJF), Juiz de Fora;[b]Universidade Federal do Rio De Janeiro COPPE/EE/IF, Rio de Janeiro;[c]Instituto de Física, Universidade de São Paulo, São Paulo;[d]Rio de Janeiro State University, Rio de Janeiro;[e]Federal University of Bahia, Bahia; Brazil.

[84]KEK, High Energy Accelerator Research Organization, Tsukuba; Japan.

[85]Graduate School of Science, Kobe University, Kobe; Japan.

[86][a]AGH University of Krakow, Faculty of Physics and Applied Computer Science, Krakow;[b]Marian Smoluchowski Institute of Physics, Jagiellonian University, Krakow; Poland.

[87]Institute of Nuclear Physics Polish Academy of Sciences, Krakow; Poland.

[88]Faculty of Science, Kyoto University, Kyoto; Japan.

[89]Research Center for Advanced Particle Physics and Department of Physics, Kyushu University, Fukuoka ; Japan.

[90]L2IT, Université de Toulouse, CNRS/IN2P3, UPS, Toulouse; France.

[91]Instituto de Física La Plata, Universidad Nacional de La Plata and CONICET, La Plata; Argentina.

[92]Physics Department, Lancaster University, Lancaster; United Kingdom.

[93]Oliver Lodge Laboratory, University of Liverpool, Liverpool; United Kingdom.

[94]Department of Experimental Particle Physics, Jožef Stefan Institute and Department of Physics, University of Ljubljana, Ljubljana; Slovenia.

[95]School of Physics and Astronomy, Queen Mary University of London, London; United Kingdom.

[96]Department of Physics, Royal Holloway University of London, Egham; United Kingdom.

[97]Department of Physics and Astronomy, University College London, London; United Kingdom.

[98]Louisiana Tech University, Ruston LA; United States of America.

[99]Fysiska institutionen, Lunds universitet, Lund; Sweden.

[100]Departamento de Física Teorica C-15 and CIAFF, Universidad Autónoma de Madrid, Madrid; Spain.

[101]Institut für Physik, Universität Mainz, Mainz; Germany.

[102]School of Physics and Astronomy, University of Manchester, Manchester; United Kingdom.

[103]CPPM, Aix-Marseille Université, CNRS/IN2P3, Marseille; France.

[104]Department of Physics, University of Massachusetts, Amherst MA; United States of America.

[105]Department of Physics, McGill University, Montreal QC; Canada.

[106]School of Physics, University of Melbourne, Victoria; Australia.

[107]Department of Physics, University of Michigan, Ann Arbor MI; United States of America.

[108]Department of Physics and Astronomy, Michigan State University, East Lansing MI; United States of America.

[109]Group of Particle Physics, University of Montreal, Montreal QC; Canada.

[110]Fakultät für Physik, Ludwig-Maximilians-Universität München, München; Germany.

[111]Max-Planck-Institut für Physik (Werner-Heisenberg-Institut), München; Germany.

[112]Graduate School of Science and Kobayashi-Maskawa Institute, Nagoya University, Nagoya; Japan.

[113]Department of Physics and Astronomy, University of New Mexico, Albuquerque NM; United States of America.

[114]Institute for Mathematics, Astrophysics and Particle Physics, Radboud University/Nikhef, Nijmegen; Netherlands.

[115]Nikhef National Institute for Subatomic Physics and University of Amsterdam, Amsterdam; Netherlands.

[116]Department of Physics, Northern Illinois University, DeKalb IL; United States of America.

[117][a]New York University Abu Dhabi, Abu Dhabi;[b]United Arab Emirates University, Al Ain; United

Arab Emirates.

[118]Department of Physics, New York University, New York NY; United States of America.

[119]Ochanomizu University, Otsuka, Bunkyo-ku, Tokyo; Japan.

[120]Ohio State University, Columbus OH; United States of America.

[121]Homer L. Dodge Department of Physics and Astronomy, University of Oklahoma, Norman OK; United States of America.

[122]Department of Physics, Oklahoma State University, Stillwater OK; United States of America.

[123]Palacký University, Joint Laboratory of Optics, Olomouc; Czech Republic.

[124]Institute for Fundamental Science, University of Oregon, Eugene, OR; United States of America.

[125]Graduate School of Science, Osaka University, Osaka; Japan.

[126]Department of Physics, University of Oslo, Oslo; Norway.

[127]Department of Physics, Oxford University, Oxford; United Kingdom.

[128]LPNHE, Sorbonne Université, Université Paris Cité, CNRS/IN2P3, Paris; France.

[129]Department of Physics, University of Pennsylvania, Philadelphia PA; United States of America.

[130]Department of Physics and Astronomy, University of Pittsburgh, Pittsburgh PA; United States of America.

[131][a]Laboratório de Instrumentação e Física Experimental de Partículas - LIP, Lisboa;[b]Departamento de Física, Faculdade de Ciências, Universidade de Lisboa, Lisboa;[c]Departamento de Física, Universidade de Coimbra, Coimbra;[d]Centro de Física Nuclear da Universidade de Lisboa, Lisboa;[e]Departamento de Física, Universidade do Minho, Braga;[f]Departamento de Física Teórica y del Cosmos, Universidad de Granada, Granada (Spain);[g]Departamento de Física, Instituto Superior Técnico, Universidade de Lisboa, Lisboa; Portugal.

[132]Institute of Physics of the Czech Academy of Sciences, Prague; Czech Republic.

[133]Czech Technical University in Prague, Prague; Czech Republic.

[134]Charles University, Faculty of Mathematics and Physics, Prague; Czech Republic.

[135]Particle Physics Department, Rutherford Appleton Laboratory, Didcot; United Kingdom.

[136]IRFU, CEA, Université Paris-Saclay, Gif-sur-Yvette; France.

[137]Santa Cruz Institute for Particle Physics, University of California Santa Cruz, Santa Cruz CA; United States of America.

[138][a]Departamento de Física, Pontificia Universidad Católica de Chile, Santiago;[b]Millennium Institute for Subatomic physics at high energy frontier (SAPHIR), Santiago;[c]Instituto de Investigación Multidisciplinario en Ciencia y Tecnología, y Departamento de Física, Universidad de La Serena;[d]Universidad Andres Bello, Department of Physics, Santiago;[e]Instituto de Alta Investigación, Universidad de Tarapacá, Arica;[f]Departamento de Física, Universidad Técnica Federico Santa María, Valparaíso; Chile.

[139]Department of Physics, University of Washington, Seattle WA; United States of America.

[140]Department of Physics and Astronomy, University of Sheffield, Sheffield; United Kingdom.

[141]Department of Physics, Shinshu University, Nagano; Japan.

[142]Department Physik, Universität Siegen, Siegen; Germany.

[143]Department of Physics, Simon Fraser University, Burnaby BC; Canada.

[144]SLAC National Accelerator Laboratory, Stanford CA; United States of America.

[145]Department of Physics, Royal Institute of Technology, Stockholm; Sweden.

[146]Departments of Physics and Astronomy, Stony Brook University, Stony Brook NY; United States of America.

[147]Department of Physics and Astronomy, University of Sussex, Brighton; United Kingdom.

[148]School of Physics, University of Sydney, Sydney; Australia.

[149]Institute of Physics, Academia Sinica, Taipei; Taiwan.

[150][(a)]E. Andronikashvili Institute of Physics, Iv. Javakhishvili Tbilisi State University, Tbilisi;[(b)]High Energy Physics Institute, Tbilisi State University, Tbilisi;[(c)]University of Georgia, Tbilisi; Georgia.

[151]Department of Physics, Technion, Israel Institute of Technology, Haifa; Israel.

[152]Raymond and Beverly Sackler School of Physics and Astronomy, Tel Aviv University, Tel Aviv; Israel.

[153]Department of Physics, Aristotle University of Thessaloniki, Thessaloniki; Greece.

[154]International Center for Elementary Particle Physics and Department of Physics, University of Tokyo, Tokyo; Japan.

[155]Department of Physics, Tokyo Institute of Technology, Tokyo; Japan.

[156]Department of Physics, University of Toronto, Toronto ON; Canada.

[157][(a)]TRIUMF, Vancouver BC;[(b)]Department of Physics and Astronomy, York University, Toronto ON; Canada.

[158]Division of Physics and Tomonaga Center for the History of the Universe, Faculty of Pure and Applied Sciences, University of Tsukuba, Tsukuba; Japan.

[159]Department of Physics and Astronomy, Tufts University, Medford MA; United States of America.

[160]Department of Physics and Astronomy, University of California Irvine, Irvine CA; United States of America.

[161]University of Sharjah, Sharjah; United Arab Emirates.

[162]Department of Physics and Astronomy, University of Uppsala, Uppsala; Sweden.

[163]Department of Physics, University of Illinois, Urbana IL; United States of America.

[164]Instituto de Física Corpuscular (IFIC), Centro Mixto Universidad de Valencia - CSIC, Valencia; Spain.

[165]Department of Physics, University of British Columbia, Vancouver BC; Canada.

[166]Department of Physics and Astronomy, University of Victoria, Victoria BC; Canada.

[167]Fakultät für Physik und Astronomie, Julius-Maximilians-Universität Würzburg, Würzburg; Germany.

[168]Department of Physics, University of Warwick, Coventry; United Kingdom.

[169]Waseda University, Tokyo; Japan.

[170]Department of Particle Physics and Astrophysics, Weizmann Institute of Science, Rehovot; Israel.

[171]Department of Physics, University of Wisconsin, Madison WI; United States of America.

[172]Fakultät für Mathematik und Naturwissenschaften, Fachgruppe Physik, Bergische Universität Wuppertal, Wuppertal; Germany.

[173]Department of Physics, Yale University, New Haven CT; United States of America.

[a] Also Affiliated with an institute covered by a cooperation agreement with CERN.

[b] Also at An-Najah National University, Nablus; Palestine.

[c] Also at Borough of Manhattan Community College, City University of New York, New York NY; United States of America.

[d] Also at Center for High Energy Physics, Peking University; China.

[e] Also at Center for Interdisciplinary Research and Innovation (CIRI-AUTH), Thessaloniki; Greece.

[f] Also at Centro Studi e Ricerche Enrico Fermi; Italy.

[g] Also at CERN, Geneva; Switzerland.

[h] Also at Département de Physique Nucléaire et Corpusculaire, Université de Genève, Genève; Switzerland.

[i] Also at Departament de Fisica de la Universitat Autonoma de Barcelona, Barcelona; Spain.

[j] Also at Department of Financial and Management Engineering, University of the Aegean, Chios; Greece.

[k] Also at Department of Physics, California State University, Sacramento; United States of America.

[l] Also at Department of Physics, King's College London, London; United Kingdom.

[m] Also at Department of Physics, Stanford University, Stanford CA; United States of America.

[n] Also at Department of Physics, Stellenbosch University; South Africa.

[o] Also at Department of Physics, University of Fribourg, Fribourg; Switzerland.

[p] Also at Department of Physics, University of Thessaly; Greece.

[q] Also at Department of Physics, Westmont College, Santa Barbara; United States of America.

[r] Also at Faculty of Physics, Sofia University, 'St. Kliment Ohridski', Sofia; Bulgaria.

[s] Also at Hellenic Open University, Patras; Greece.

[t] Also at Institucio Catalana de Recerca i Estudis Avancats, ICREA, Barcelona; Spain.

[u] Also at Institut für Experimentalphysik, Universität Hamburg, Hamburg; Germany.

[v] Also at Institute for Nuclear Research and Nuclear Energy (INRNE) of the Bulgarian Academy of Sciences, Sofia; Bulgaria.

[w] Also at Institute of Applied Physics, Mohammed VI Polytechnic University, Ben Guerir; Morocco.

[x] Also at Institute of Particle Physics (IPP); Canada.

[y] Also at Institute of Physics and Technology, Mongolian Academy of Sciences, Ulaanbaatar; Mongolia.

[z] Also at Institute of Physics, Azerbaijan Academy of Sciences, Baku; Azerbaijan.

[aa] Also at Institute of Theoretical Physics, Ilia State University, Tbilisi; Georgia.

[ab] Also at Lawrence Livermore National Laboratory, Livermore; United States of America.

[ac] Also at National Institute of Physics, University of the Philippines Diliman (Philippines); Philippines.

[ad] Also at Technical University of Munich, Munich; Germany.

[ae] Also at The Collaborative Innovation Center of Quantum Matter (CICQM), Beijing; China.

[af] Also at TRIUMF, Vancouver BC; Canada.

[ag] Also at Università di Napoli Parthenope, Napoli; Italy.

[ah] Also at University of Colorado Boulder, Department of Physics, Colorado; United States of America.

[ai] Also at Washington College, Chestertown, MD; United States of America.

[aj] Also at Yeditepe University, Physics Department, Istanbul; Türkiye.

[*] Deceased